THE SIMULATION OF RANDOM VIBRATIONS

J. W. ROBERTS

Thesis submitted for the degree of
Doctor of Philosophy
University of Edinburgh
October 1969

A C K N O W L E D G E M E N T S

The author wishes to acknowledge the valuable guidance given by his supervisors; Professor J. D. Robson, Rankine Professor of Mechanical Engineering at the University of Glasgow, who suggested the research project and whose constant and critical interest in its development was much appreciated, and Dr. A. D. S. Barr of the Department of Mechanical Engineering, who made many helpful criticisms and suggestions.

The author also wishes to record his gratitude to Mr. George Smith for his advice and skill in the construction of the apparatus and to Mrs. Sally Tulley and Miss Avril Myles who jointly typed the thesis.

S Y N O P S I S

The investigation is concerned with the simulation of random vibration environments. It is relevant to the problems of environmental testing of aero-space structures and components where there is a need to replace the primary service environment by a substituted form of excitation, such as electrodynamic vibration generators. It is assumed that the structures are linear and elastic, and that the environments are well represented as stationary and gaussian.

The question of the equivalence of the service and simulated responses of a general structure is examined from a general standpoint. It is shown that simulation in probability is a meaningful basis, and that simulation in spectral density of every structure response implies this. The latter represents the more useful basis from a practical viewpoint, since spectral densities may be controlled directly by selective filtering of white noise sources.

By considering the responses of a general elastic structure to random excitation it is shown that simulation in spectral density of every response of the structure at every frequency is not possible in general. However, by considering only resonant response to be significant, a finite degree of freedom representation of the response relations is justified and the possibility of achieving accurate simulation in spectral density, using only a few vibrators, is deduced. The minimum number of force generators required is shown to be equal to the number of modes of vibration having resonant

frequencies within or near any particular frequency interval of significant response, the forces being programmed to reproduce the spectral densities of and the cross spectral densities between a set of the same number of reference responses. The procedure is particularly simple if the structure has widely spaced natural frequencies. The possibility of simulating the motions of the whole structure using a single vibrator and a single reference response then arises.

An experimental demonstration of one and two vibrator simulation is presented to illustrate the theoretical results. Simulation of the responses of a beam is attempted using one or two vibrators. For the purpose of these tests a harmonic analogue of the random vibrations response relations is devised. In this approach, random forces are represented by sets of harmonic forces and equivalent measures of spectral density and cross-spectral density are obtained from measurements of amplitude and phase of harmonic responses.

A further development of the theory shows that simulation may be based upon reproducing broad-band averages of the reference spectral densities. This is supported by further experimental results.

Finally, the prospects for an approximate form of simulation, based upon the simulation of broad-band spectral densities are examined. Each response band is assumed to contain a number of modal contributions of indeterminate magnitude and the approach is a possible one for treating the high frequency responses of complex structures. Analytical studies and related computer studies show that the approach can lead to a useful degree of simulation, but that the number of modal contributions in each response band is required to be large before a reasonable accuracy is obtained. Experimental results from a rectangular plate model show a reasonable agreement with predictions from the theory.

CONTENTS

C H A P T E R 1

INTRODUCTION

1.1 Random Vibration and the Simulation Problem

Many of the current spheres of engineering activity involve considerations of vibration. A particular class of these problems is concerned with situations where the excitation pressures and forces vary in such an irregular and complicated fashion that the traditional methods of vibration analysis and response prediction are found to be inadequate for various reasons. A particular example of this is the excitation and response of a rocket structure to its turbulent boundary layer, and to the intense acoustic pressures of its jet. Indeed, the main impetus for the study of this class of problem has come from the recent developments in aero-space structures and systems, with the associated demands for efficient design and component reliability in the presence of arduous and novel environments.

In principle, at least for linear systems, if the precise form of the excitation is specified, then the response quantities of interest may be computed from a knowledge of the system frequency or impulse response functions. While such methods are the basis of vibration analysis, their use in the present situation is limited for the following reason. A general feature of excitations of this type is that the fluctuations of the exciting pressures or forces are not reproduced in successive tests or trials even if the controllable parameters of the trials are exactly reproduced. For example, the detailed variations of a turbulent boundary layer pressure on the skin of a missile would not be exactly reproduced even if the overall parameters of the turbulence, such as mean velocities and temperatures were reproduced in a further trial. Only a general similarity will be maintained in successive trials and as a result, a

set of records from a single trial cannot completely characterize the excitation and if these are used to predict response by means of the deterministic methods outlined above, can only give a limited picture of the range of possible responses in future trials.

Such excitations are classed as 'Random' and these shortcomings have led to the development of the theory of 'Random Vibrations'. The mathematical model predicated by the phenomena is the random or stochastic process. Probabilistic terms are used to describe the excitation and as a result, predictions of responses can only be made in probabilistic and related terms. Experimental records are processed to obtain estimates of the parameters of the excitation or response processes. By this approach the indeterminacy present in the phenomena is represented in the analysis and the mathematical model, whose parameters may be based on measurements from a few sample records, represents the whole range of possible responses albeit in indeterminate terms.

This investigation is concerned with the simulation of random motions. The aim of simulation is to reproduce, in some sense, the service motions of the structure under laboratory conditions, so that the reliability of operation under service conditions can be assessed, component malfunctions and structural fatigue problems investigated, and design proving tests carried out. Simulation procedures generally consist of testing the structures or component parts according to some test specification using one or more vibration generator. The central role played by vibration simulation in the developments of aero-space systems has been emphasized by Morrow * (1963). This is a consequence of the fact that the theoretical methods of random vibrations cannot be reduced to feasible design

* the references are listed in alphabetical order in the Bibliography.

calculations for all but the simplest cases. The methods require complete description of the dynamical properties of the structure, together with a complete probabilistic description of the service environment. Such information is not in general available, so that equipment development is almost entirely dependent upon repeated environmental test and re-design. In this way the vibration test specification supplants the actual environment as the design specification. It is clear that if the crucial balance is to be struck between over conservatism with associated weight penalties on the one hand, and the prospect of serious structural failure or malfunction on the other, then accurate test specifications and test methods are essential.

1.2 Review of Previous Work

The earliest application of probabilistic methods to dynamical systems on other than a molecular scale can be traced to extensions of the work of Einstein, Langevin and Smoluchowski on the Brownian movement of particles. Ornstein (1917) studied the random motion of an elastically restrained particle and in 1927 applied the same ideas to a finite string. The elastically bound particle was considered further by Uhlenbeck and Ornstein (1930) and Chandrasekhar (1943). The method used by these authors required that the excitation be temporally uncorrelated (white noise). The response process could be regarded as a Markoff process. For prescribed initial conditions, solution of a differential equation of the diffusion type yielded the conditional density function of the response of the phase space variables of the system. This function could be integrated to obtain the moments of the responses as a function of time, or corresponding asymptotic values. This method has been superseded for linear systems by the frequency

domain approach, but has found recent application in the study of non-linear system response.

In 1920, G. I. Taylor, in a study of turbulence, introduced the autocovariance function, or autocorrelation function. N. Weiner, in 1930, while extending the ideas of harmonic analysis to arbitrary functions, introduced the power spectral density function and showed that this was the fourier transform of the autocorrelation function. This important relation was discovered independently by Khintchine (1934), and these related functions played a central role in the application of the theory to problems in communications, control and vibrations

A paper by Lin (1943) seems to be the first application of correlation functions to a vibration problem. Lin studied the response of a pendulum immersed in a turbulent flow. The classic work of Rice (1944) which followed, did much to popularize the application of correlation functions and spectral densities to linear problems and presented important results concerning the response of non-linear systems and the statistical properties of sample functions. Wang and Uhlenbeck (1948) reviewed both the classical approach through the diffusion or Fokker-Planck equation and the spectral density approach. The comparative simplicity of the latter approach, and its ability to treat non-white excitations was demonstrated by application to (a) a simple oscillator and (b) a system of coupled oscillators.

Over this period, papers, principally by Kolmogorov (1933), Khintchine (1934), Cramér (1940) and Doob (1942), were concerned with the rigorous development of the theory of stochastic processes. These works considered problems of existence and uniqueness, and did not contribute directly to the practical applications of the theory.

The next decade witnessed a wide range of papers dealing with applications of the theory to structural vibrations problems. These are reported in detail in the review by Crandall (1959) and included the buffeting of aircraft (Liepmann, 1952), landing impacts (Fung, 1955), the response to turbulent boundary layers of strings, (Lyon, 1956), beams and plates (Eringen 1957; Dyer, 1959). Thomson and Barton (1957) examined the response of a general system to a simple form of general loading, and showed that important approximations could be introduced to simplify the mean square response expression if the system had low damping and separated natural frequencies. Lyon and Dyer demonstrated the important coincidence effect in finite strings and plates respectively. This takes place when the coherent patterns in the turbulence convect over the surface at speeds near to the phase velocities of the structural modes, and can lead to enhanced amplitudes of vibration. The problem of fatigue failure prediction under random vibration was considered by Miles (1954) and Powell (1958). Miles treated a single degree of freedom system and used Rice's results for peak distribution of a normal process, together with a cumulative damage criterion. Powell took several modes into account and emphasized the role of the excitation space-time correlations and the correlations between the motions in the different modes.

In 1958 Blackman and Tukey investigated the problem of estimation of the autocorrelation function and spectral density from finite records. Methods were discussed for the analysis of signals by analogue and digital means, and the basic difficulty of reconciling spectral resolution, record length and standard error of the estimate was emphasized.

By 1959, solutions had been presented for the response of continuous linear elastic structures to general random excitation. The solution required that space-time correlations of the excitation over the whole

structure be completely specified and that the normal modes, natural frequencies and corresponding damping ratios be known. Responses could then be obtained in terms of spectral densities, and these implied complete probablistic description of the response, subject to the assumption of a Gaussian excitation process. The paper by Powell (Crandall, 1958, Chapter 8) illustrates the method.

It was clear that the method would have a limited usefulness for application to real structures. Notwithstanding the sheer weight of numbers of participating modes in a complex missile structure, it was unlikely that the detailed information about mode shapes and excitation fields would be available. This practical difficulty has led to the subsequent development of the statistical energy method of response prediction. The method asserts that the response spectral density, averaged over a frequency band, is fairly homogeneous over the structure provided a reasonable number of modes contribute their energies in the band.

Simple expressions for the average structural response for each frequency band can be obtained on the basis of a statistical treatment of the structure modes and an approximate treatment of the excitation. Dyer (Crandall, 1963, Chapter 7) describes the method and illustrates its application to the response of a Titan missile. Further considerations are presented by Lyon and Maidanik (1964) and by Eichler (1965). This method holds interesting promise for the solution of practical problems, but further work must seek to establish how representative these average responses are when considering for example, fatigue life at critical locations.

1.3 Review of the Simulation Problem

In 1955 Morrow and Muchmore emphasized the importance of introducing random vibration testing, drew attention to the basic differences between sine wave and random signals and pointed out the features of a continuous spectrum of random vibrations and the associated measurement difficulties. Papers by Metzgar and by Priest in Random Vibrations Vol.I. (Crandall 1959) explain the philosophy and practicalities of random vibrations testing at that time, and similar papers by Vigness, Booth and Morrow in Random Vibrations Vol.II (Crandall 1963) contain a subsequent review of the same area. The papers by Metzgar, Priest and Booth discuss in detail the uses and limitations of vibration test equipment, while Vigness and Morrow discuss in more general terms, the aims and means of vibration testing as currently practised. The central type of simulation discussed by these authors is the simulation of the random motions at the points of support of equipment according to a prescribed acceleration spectral density spectrum. The test specification is derived somewhat unprecisely by envelopping field measurements, or by extrapolation from previous specifications. The final form of the test specification usually consists of straight line segments for ease of application. Figure 1.3.1 shows a typical test specification. More recently Piersol (1966) has reviewed the problem of vibration testing. He considers the test method outlined above to be the most feasible, and attempts to develop a standardized approach to the implementation of the test. The paper contains an extensive bibliography.

This type of simulation may be termed "direct" simulation since one attempts to replace the equipment environment, namely the spectral density of the mounting point motions, by a probabilistically similar environment. While this is a straightforward approach to use, it is clearly only relevant to the testing of equipment with distinct points

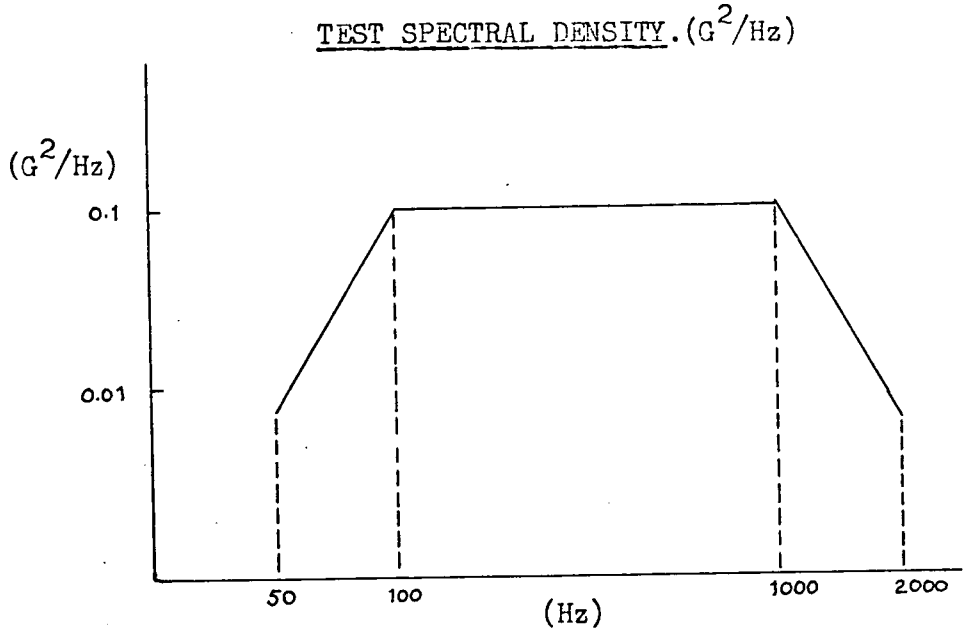

FIG. 1.3.1

Typical Random Vibration Test Envelope.

(Vigness, 1963.)

of attachment to a superstructure, and where the only service excitation is via the mounting point. Substantial errors can still occur due to (a) the test specification not reflecting the finely scaled spectral variations of the actual environment over critical intervals of frequency and (b) incorrect compensation for the effects of equipment motion on the motion of the support points.

Such tests generally required equipment with a high power rating, and extensive capital investment. It was natural that there would be a search for equivalent tests based on the idea of cycling a sine wave input or a narrow band of random noise over the test frequency range. Such methods have been reported by Booth (1963), Booth and Broch (1965) and Broch (1966). Some degree of equivalence can be arranged in these tests, based on the accumulated number of stress peaks in a range of stress intervals, but it is subject to severe assumptions about the nature of cumulative fatigue damage. The general feature of wide band random excitation, that many modes are excited at resonance simultaneously, is not reproduced in such a test. Consequently they have not gained general acceptance. (Piersol, 1966).

The monograph by Lyon (1967) contains a comprehensive review of the intensive efforts and methods currently being applied in environmental test programs in the United States. Lyon describes a wider range of test methods than previous authors, including the substitution of an acoustic excitation for a turbulence environment and the replacement of either by mechanical vibrators. This type of simulation may be termed simulation by substitution, and has wide application in environmental testing. Lyon discusses the problems of simulation in general terms, and refers to the work of Noiseux (1964) as the most comprehensive investigation to date of the simulation of an acoustic environment by force generators.

Noiseux, in fact, used a single vibrator to reproduce the response of a missile computer to reverberant acoustic excitation. The basis of the method was that the input power transmitted by the vibrator to the test structure was adjusted to predicted levels in each third octave band, the predictions being based upon the root mean square pressure of the acoustic field and the estimated radiation resistance of the structure in each band. This is a most promising approach because of its inherent simplicity. Only a single parameter of the service environment is required, namely the r.m.s. pressure in (say) third octave bands. However the approach is based on the assumptions of the statistical energy method and hence is valid only for wide band average responses of structures where the modal frequencies in any band are sufficiently dense. This is borne out by Noiseux's results, in that poor simulation is obtained at low frequencies where there are only a few modal frequencies in each band. At high frequencies, good simulation is implied, but the results presented by Noiseux are not extensive enough to determine this with any great accuracy.

An investigation of the substitution of a sound field for a turbulence field is reported by Lyon (1965). Lyon considers the similarities between the response of a structural panel to each type of excitation and concludes that, if the damping of the panel is low enough, such that the reflected energy from the boundaries is significant, then the response will be insensitive to the precise spatial distribution of the excitation, and simulation will be realistic if the required modal energy levels in the various frequency bands can be reproduced. The calculations are based on the statistical energy approach.

In summary, the techniques of direct simulation, relevant to the testing of equipment modules, excited through their supports only, are

soundly based but as currently practised, must make many concessions of accuracy to the limitations of testing facilities. When equipment and structures are excited by acoustic or turbulent, or support excitation, or combinations of these, simulation by substitution may be the only practicable approach. With such an approach the question of equivalence of the substituted environment is a basic one, but investigations of this approach so far have been restricted to a few particular cases, and have been based on the statistical energy method.

1.4 Scope of the Present Investigation

It is clear from the papers reviewed in the previous section, that at the present time, approaches to simulation are severely constrained by economic factors, time limitations, equipment limitations, and the necessity for dealing with only the simplest form of test specification. One must take the view, however, that in a matter of some years more comprehensive approaches to the simulation will be entirely possible, as a result of advances in transducers, data recording and processing, and in test equipment technology. For this reason it is desirable to establis something of the nature of theoretical and practical limits to what can be achieved in simulation of environments by substitution.

The present investigation examines the problem of simulation of the motions of a general elastic structure, starting from the general respons relation in terms of probability distributions. Subject to some assumptions about the nature of the service environment, it is shown that simulation can be reasonably achieved, but in general multi-force excitation is required, and cross-correlations play a significant role. Some simple results, of practical importance emerge in particular circumstance

however. Some idealizations are made in the theoretical model. For example it is assumed that electro-magnetic vibration generators are ideal force generators, having negligible output impedance, and that any relevant response of the structure to the service environment can be recorded for use in the simulation experiment. These assumptions are justified because they enable the analysis to circumvent current practical difficulties.

A preliminary publication of the theoretical work of the present investigation was made in 1965 (Robson and Roberts, 1965), and contains some of the results of Chapter 3 of the present thesis.

CHAPTER 2

THE RESPONSE OF AN ELASTIC STRUCTURE TO RANDOM EXCITATION

2.1 Introduction

In this preliminary chapter, the description of a stationary multi-dimensional random process is reviewed, and the response of a general structure to random excitation is summarized as a prelude to the discussion of simulation in chapter 3. The treatment of response uses standard methods. (Robson, 1963).

2.2 Probabilistic Description of a Random Process

Let $q_j(t)$, $j = 1, 2 \ldots n$ be a set of continuous simultaneous records of physical parameters of interest. When deterministic descriptions of $q_j(t)$ are not feasible, then $q_j(t)$ may be considered as a stochastic process of real continuous type and the set constitutes an n dimensional process. This implies that for any $t = t_k$, $q_j(t_k)$ is considered as a random or chance variable of continuous type, and further, for any m and for distinct times $t_1, t_2 \ldots t_m$, then $q_j(t_1), \ldots q_j(t_m)$ constitute a set of joint random variables or a random vector of continuous type. It is useful to think of each $q_j(t)$ as representing a set of possible sample functions, designated an ensemble. Figure 2.2.1 represents some typical sample functions of the $q_i(t)$ and $q_j(t)$ processes. A set of joint random variables may also be chosen from the component processes in the following way. Let $t_1, t_2 \ldots t_m$ be a set of times, not necessarily distinct. Then $q_1(t_1), q_2(t_2) \ldots q_m(t_m)$ constitute a set of joint random variables. In Figure 2.2.1, $q_i(t_1)$, $q_i(t_2)$, $q_j(t_3)$ $q_j(t_4)$ are each random variables, and any combination of these constitutes a set of joint random variables. Such joint random variables are described by their probability distribution function or probability density

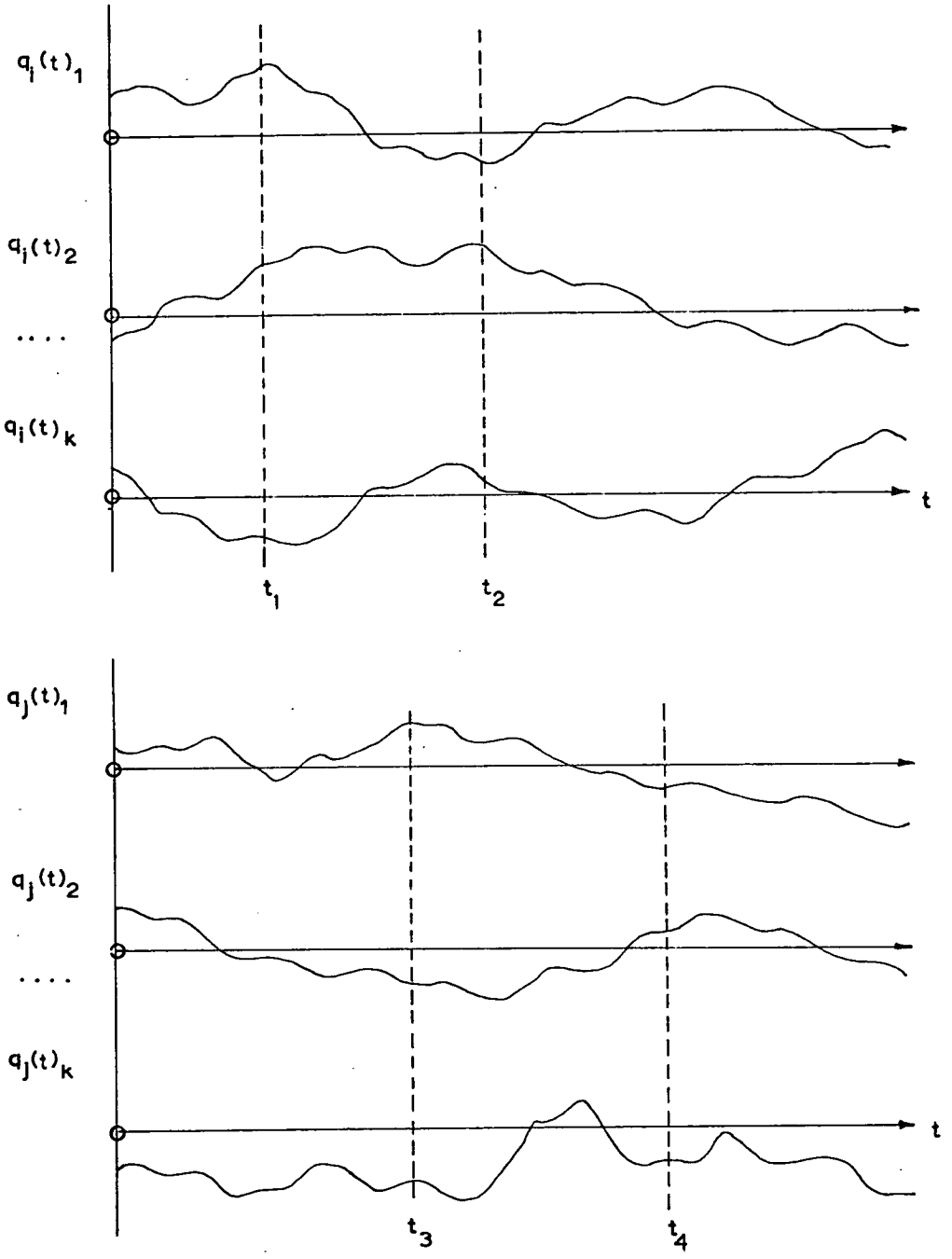

Fig. 2.2.1

Sample Functions of Random Processes.

function. For example, let $F_m(x_1, x_2 \ldots x_m; t_1, t_2 \ldots t_m)$ be the joint distribution function of the random variables $q_1(t_1) \ldots q_m(t_m)$. Then:

$$F_m(x_1, x_2 \ldots x_m; t_1, t_2 \ldots t_m) \equiv \text{Prob}\left\{-\infty < q_1(t_1) \leq x_1 \text{ and} \ldots \text{and } -\infty < q_m(t_m) \leq x_m\right\} \qquad 2.2.1$$

Similarly, let $f_m(x_1, x_2 \ldots x_m; t_1, t_2 \ldots t_m)$ be the joint density function of the random variables $q_1(t_1) \ldots q_m(t_m)$. Then:

$$f_m(x_1, x_2, \ldots x_m; t_1, t_2 \ldots t_m)\, dx_1\, dx_2 \ldots dx_m \equiv$$

$$\text{Prob}\left\{x_1 < q_1(t_1) \leq x_1 + dx_1 \text{ and} \ldots \text{and } x_m < q_m(t_m) \leq x_m + dx_m\right\} \qquad 2.2.2$$

Complete probabilistic description of the joint random variables is obtained if either F_m or f_m is specified at all points in the m dimensional sample space of the variables.

Complete probabilistic description of the n dimensional process requires that the distributions or density functions of all such joint random variables of any finite order, generated by the process, be specified at all points in the relevant sample space. These are termed the finite dimensional distributions of the process. In general it is impracticable to determine these by measurement from sample functions. The usual practice is to infer the form of these distributions from a priori considerations of the processes, and then to determine the parameters of the distributions from certain averages.

Denote the expectation or ensemble average of a function g ( ) of random variables $q_1(t_1), \ldots q_m(t_m)$ by $E\left\{g\left[q_1, q_2 \ldots q_m\right]\right\}$

Then $$E\left\{g\left[q_1(t_1) \ldots q_m(t_m)\right]\right\} = \int_{-\infty}^{\infty} \ldots \int_{-\infty}^{\infty} g(x_1, x_2 \ldots x_m)\, f_m(x_1 \ldots x_m; t_1 \ldots t_m)\, dx_1 \ldots dx_m \qquad 2.2.3$$

For example the mean of $$q_i(t_k) = E\left\{q_i(t_k)\right\} = \int_{-\infty}^{\infty} x_i\, f_1(x_i, t_k)\, dx_i \qquad 2.2.4$$

It will be assumed, unless otherwise stated that processes have zero mean.

The variance of $q_i(t_k)$ can be obtained:

$$\text{var}\{q_i(t_k)\} = \sigma_i^2(t_k) = E\{q_i^2(t_k)\} \qquad \text{in the zero mean case.} \qquad 2.2.5$$

Further, define the autocorrelation function of the ith process:

$$R_{ii}(t_1, t_2) = E\{q_i(t_1).q_i(t_2)\} \qquad 2.2.6$$

For fixed t_1, t_2, this is essentially the covariance of the (zero mean) random variables $q_i(t_1)$ and $q_i(t_2)$, but for any t_1, t_2, this becomes a function defined on the t_1, t_2 plane. An extension of 2.2.6 leads to the cross-correlation function for a distinct pair of component processes:

$$R_{ij}(t_1, t_2) = E\{q_i(t_1).q_j(t_2)\} \qquad 2.2.7$$

An important class of process is the Gaussian or Normal case. If the random variables $q_1(t_1) \ldots q_m(t_m)$ are jointly normal, then f_m can be expressed in the following form:

$$f_m(x_1, x_2, \ldots x_m; t_1, t_2 \ldots t_m) = (2\pi)^{-\frac{m}{2}} |\Lambda|^{-\frac{1}{2}} \exp\left[-\frac{1}{2|\Lambda|}\sum_{ij}^{m} \Lambda_{ij}\, x_i\, x_j\right] \qquad 2.2.8$$

$[\Lambda]$ is the m square covariance matrix of the m random variables :

$$[\Lambda] = [R_{ij}(t_i, t_j)] = [E\{q_i(t_i).q_j(t_j)\}] \qquad 2.2.9$$

and Λ_{ij} are the cofactors of $[\Lambda]$.

An important property of the gaussian case is observed from 2.2.8. Complete specification of f_m is obtained if the covariance matrix of the set is specified. Consequently, complete probabilistic description of the n dimensional process is obtained in the gaussian case if the autocorrelation function for each member process and the cross-correlation function for each pair of member processes are specified for all points (t_1, t_2). The n square matrix $[R_{ij}(t_1, t_2)]$,

$$[R(t_1, t_2)] = \begin{bmatrix} R_{11}(t_1, t_2) & R_{12}(t_1, t_2) & \ldots & R_{1n}(t_1, t_2) \\ R_{21}(t_1, t_2) & R_{22}(t_1, t_2) & & \\ \ldots\ldots & & & \\ R_{n1}(t_1, t_2) & & & R_{nn}(t_1, t_2) \end{bmatrix} \qquad 2.2.10$$

defined for all pairs of time instants (t_1, t_2) implies a complete probabilistic description of the n dimensional process. It is clear that any covariance matrix $[\Lambda]$ of any order m, for an m dimensional random vector, obtained by sampling one or more member processes of the n dimensional set can be derived from 2.2.10.

Many random processes of practical interest can be assumed to be gaussian. The justification derives from the Central Limit Theorem (Papoulis 1965) and further, from the result that linear transformations of a gaussian process are also gaussian.

The following properties of the element functions of 2.2.10 may be readily derived:

$$R_{ij}(t_1,t_2) = R_{ji}(t_2,t_1) \qquad 2.2.11$$

$$R_{ii}(t_1,t_1) = \sigma_i^2(t_1) \qquad 2.2.12$$

$$0 \leqslant R_{ij}^2(t_1,t_2) \leqslant R_{ii}(t_1,t_1) \cdot R_{jj}(t_2,t_2) \qquad 2.2.13$$

If $R_{ij}(t_1,t_2)$ is identically zero for all t_1, t_2, the processes $q_i(t)$ and $q_j(t)$ are uncorrelated, or orthogonal in the zero mean case, while for gaussian processes, this implies statistical independence. The upper limit in 2.2.13:

$$R_{ij}^2(t_1,t_2) = \sigma_i^2(t_1) \cdot \sigma_j^2(t_2) \qquad 2.2.14$$

holds if and only if the random variables $q_i(t_1)$ and $q_j(t_2)$ are linearly dependent.

2.3 Stationary Random Processes

A further simplification of the description occurs if the processes are stationary. By definition a process is strictly stationary if

its finite dimensional distributions or density functions are invariant under a translation in time. A process is stationary in wide sense if its correlation functions are invariant with respect to a translation in time. Strict stationarity implies wide sense stationarity but the converse is not generally true. In the gaussian case the converse holds. In practice stationarity can only be inferred over some time interval T if the overall conditions under which the process is generated remain steady over this time. For a wide sense stationary process, it follows from 2.2.5 that the variances:

$$\sigma_i^2(t_k) = \sigma_i^2 \qquad 2.3.1$$

and from 2.2.6 with $t_2 = t_1 + \tau$:

$$R_{ii}(t_1, t_1+\tau) = R_{ii}(\tau) \qquad 2.3.2$$

Similarly from 2.2.7:

$$R_{ij}(t_1, t_1+\tau) = R_{ij}(\tau) \qquad 2.3.3$$

All correlation functions are functions of a single parameter τ, being the time interval between the pair of samples in 2.2.6 and 2.2.7.

In the stationary case, 2.2.11 implies that autocorrelation functions are even:

$$R_{ii}(\tau) = R_{ii}(-\tau) \qquad 2.3.4$$

and:

$$R_{ii}(0) = \sigma_i^2 \qquad 2.3.5$$

Also, the cross-correlation functions satisfy:

$$R_{ij}(\tau) = R_{ji}(-\tau) \qquad 2.3.6$$

The relation 2.2.13 becomes:

$$0 \leqslant R_{ij}^2(\tau) \leqslant R_{ii}(0).R_{jj}(0) \qquad 2.3.7$$

2.4 Ergodic Processes

Parameters of stationary random processes, such as auto and cross-correlation functions are in principle obtained from sampling the ensemble. This is not usually practicable since only a few sample records of finite length will be available in general. It is desirable that estimates of these parameters may be obtained from corresponding time averages, measured on a single sample function. Let $q_i(t,k)$ be a finite length of the kth sample function of the ith process, $t \in [0,T]$.

Then for example, the sample autocorrelation function is given by:

$$R_{ii}^{T}(\tau,k) = \frac{1}{T-\tau}\int_{0}^{T-\tau} q_i(t,k)\,q_i(t+\tau,k)\,dt \qquad 2.4.1$$

Clearly $R_{ii}^{T}(\tau)$ is itself a random variable and if this is to furnish a good estimate of $R_{ii}(\tau)$ for the process, then it is required that:

$$E\{R_{ii}^{T}(\tau)\} = R_{ii}(\tau) \qquad 2.4.2$$

and that:

$$\mathrm{var}\{R_{ii}^{T}(\tau)\} \to 0 \quad \text{as} \quad T \to \infty \qquad 2.4.3$$

Under these conditions, the time average autocorrelation function converges in mean square to the ensemble average. Processes for which time averages on a sample function converge in some sense to the corresponding ensemble functions are generally termed ergodic processes. Ergodicity of a stationary process implies in general that the fluctuations of any sample function are typical of the whole ensemble. Strictly, each average must be investigated to prove its ergodicity (Papoulis 1965, Section 9.8; Cramér and Leadbetter 1967, Section 7.10) but this requires knowledge of the finite dimensional distributions. A simple condition for ergodicity of the class of gaussian processes, having continuous autocorrelation functions is (Davenport and Root, 1958):

$$\int_{-\infty}^{\infty} |R(\tau)|\,d\tau < \infty \qquad 2.4.4$$

2.5 Description in Terms of Spectral Densities

For a stationary process $q_i(t)$, the spectral density may be defined as the fourier transform of the autocorrelation function:

$$S_{ii}(\omega) = \frac{1}{2\pi}\int_{-\infty}^{\infty} R_{ii}(\tau)\, exp(-i\omega\tau)\, d\tau \qquad 2.5.1$$

By the properties of fourier transforms, $S_{ii}(\omega)$ is a real, even function of circular frequency ω. It is also non-negative. The inverse relation may be written:

$$R_{ii}(\tau) = \int_{-\infty}^{\infty} S_{ii}(\omega)\, exp(i\omega\tau)\, d\omega \qquad 2.5.2$$

Hence for $\tau = 0$:

$$R_{ii}(0) \equiv E\left\{q_i^2(t)\right\} = \int_{-\infty}^{\infty} S_{ii}(\omega)\, d\omega \qquad 2.5.3$$

The mean square of the process is represented by the area under the spectral density curve.

An alternative definition is often given of the spectral density in terms of the sample functions of the process:

Let $q_k(t)$, $t \in [0,T]$, be the kth sample function of the process $q(t)$. Assume that $q_k(t)$ is zero outside the interval $[0,T]$. Then $q_k(t)$ has a fourier transform:

$$X_T^k(\omega) = \int_0^T q_k(t)\, exp(-i\omega t)\, dt$$

Let: $$S_T^k(\omega) = \frac{1}{2\pi T}\left|X_T^k(\omega)\right|^2 \qquad 2.5.4$$

Then: $$S^k(\omega) = \lim_{T\to\infty} S_T^k(\omega) \qquad 2.5.5$$

2.5.5. is the definition of spectral density of an arbitrary function from the theory of generalized harmonic analysis. Clearly $S_T^k(\omega)$ is a random variable, and the relationship of 2.5.5 to the spectral density of the process 2.5.1 is a delicate one. One may show (Lin 1967) that $\lim_{T\to\infty} E\left\{S_T^k(\omega)\right\}$ is equal to $S(\omega)$; but it is not true in general, not even for gaussian processes that $\lim_{T\to\infty} var\left\{S_T^k(\omega)\right\}$

tends to zero. So, $S_T^k(\omega)$ does not converge in mean square to the spectral density of the process, and hence would not give reliable estimates of $S(\omega)$. Estimates of the spectral density can be obtained from a single sample function in the form of a weighted average over an arbitrarily small frequency interval. Such an average may be shown to converge in mean square sense to the corresponding ensemble average for an ergodic process. (Crandall 1963, Chapter 2).

For an n dimensional process, the cross spectral densities may be defined as the fourier transforms of the cross-correlation functions:

$$S_{ij}(\omega) = \frac{1}{2\pi}\int_{-\infty}^{\infty} R_{ij}(\tau)\exp(-i\omega\tau)\,d\tau \qquad 2.5.6$$

$S_{ij}(\omega)$ is in general complex. From the properties of fourier transforms one may derive the Hermitian property of cross spectral densities:

$$S_{ij}(\omega) = S_{ji}^*(\omega) \qquad 2.5.7$$

and further:

$$S_{ij}(-\omega) = S_{ij}^*(\omega) \qquad 2.5.8$$

In the stationary case, one may take the fourier transform of the correlation function matrix 2.2.10 to obtain the n square spectral density matrix:

$$[S_{ij}(\omega)] \equiv \begin{bmatrix} S_{11}(\omega) & S_{12}(\omega) & \cdots & S_{1n}(\omega) \\ S_{21}(\omega) & S_{22}(\omega) & & \\ \cdots & & & \\ S_{n1}(\omega) & & \cdots & S_{nn}(\omega) \end{bmatrix} \qquad 2.5.9$$

Consequently, in the stationary and gaussian case, specification of the n square spectral density matrix at all frequencies ω implies a complete probabilistic description of the n dimensional process.

By 2.5.7 $[S(\omega)]$ is an Hermitian matrix at any frequency. A further property of $[S(\omega)]$ is that of non-negative definiteness. Indeed for any pair of component processes, $q_i(t)$, $q_j(t)$, the coherence relations hold at any frequency:

$$0 \leqslant |S_{ij}(\omega)|^2 \leqslant S_{ii}(\omega) . S_{jj}(\omega) \qquad 2.5.10$$

and the non-negative definiteness of 2.5.9 follows. The property 2.5.10 seems to have been reported first by Cramér (1940), and may be considered as a form of the Cauchy - Schwarz inequality on the space of complex valued, zero-mean random variables, having inner product defined as:

$$(\xi, \eta) \equiv E\{\xi \eta^*\} \qquad 2.5.11$$

where ξ, η are elements of the space.

(ξ, η) satisfies the Cauchy - Schwarz inequality:

$$0 \leqslant |(\xi, \eta)| \leqslant (\xi, \xi)^{\frac{1}{2}} . (\eta, \eta)^{\frac{1}{2}} \qquad 2.5.12$$

Now, let $$X_T(\omega, k) = \int_0^T q_i(t, k) \exp(-i\omega t)\, dt$$

and $$Y_T(\omega, k) = \int_0^T q_j(t, k) \exp(-i\omega t)\, dt \qquad 2.5.13$$

X_T and Y_T are the fourier transforms of the kth sample functions of the ith and jth processes and are complex random variables.

One has, by 2.5.5:

$$S_{ii}(\omega) = \lim_{T \to \infty} \frac{E\{|X_T(\omega, k)|^2\}}{2\pi T} \text{ , with a similar expression for } S_{jj} .$$

Further, $S_{ij}(\omega)$ may be expressed in the following form:

$$S_{ij}(\omega) = \lim_{T \to \infty} \frac{E\{X_T . Y_T^*\}}{2\pi T} \qquad 2.5.14$$

Using 2.5.12, one may write:

$$0 \leqslant |E\{X_T . Y_T^*\}|^2 \leqslant E\{|X_T|^2\} . E\{|Y_T|^2\}$$

Divide through by $(2\pi T)^2$:

$$0 \leqslant \left| \frac{E\{X_T \cdot Y_T^*\}}{2\pi T} \right|^2 \leqslant \frac{E\{|X_T|^2\}}{2\pi T} \cdot \frac{E\{|Y_T|^2\}}{2\pi T}$$

Now let $T \to \infty$ and 2.5.10 follows.

2.6 Response of a General Elastic Structure to Excitation Forces

Consider a continuous elastic structure S, excited by time dependent forces on its boundary C (Figure 2.6.1)

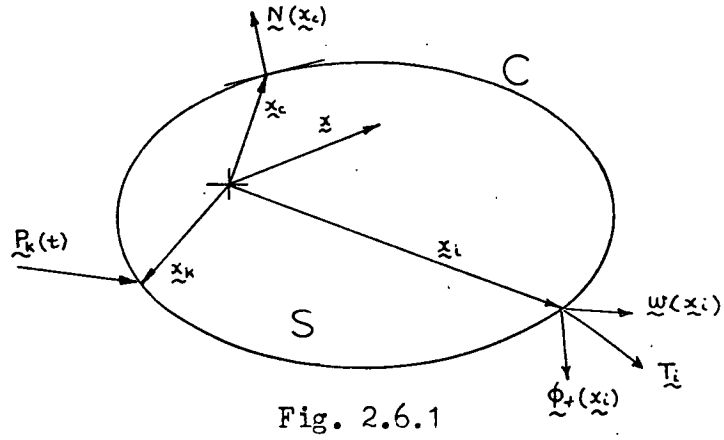

Fig. 2.6.1

General Elastic Structure.

For such a structure, the normal mode shapes of free undamped vibration $\underset{\sim}{\phi}_r(\underset{\sim}{x})$ constitute a complete orthogonal set. The response $\underset{\sim}{w}$ at any point in S with position vector $\underset{\sim}{X}$ can be written in terms of the normal co-ordinates ξ_r , $r = 1, 2, 3, \ldots \infty$.

$$\underset{\sim}{w}(\underset{\sim}{x}, t) = \sum_r \underset{\sim}{\phi}_r(\underset{\sim}{x})\, \xi_r(t) \qquad 2.6.1$$

The scalar response recorded by a transducer, having its sensitive axis aligned in the direction of the unit vector $\underset{\sim}{T}_i$ at position $\underset{\sim}{x}_i$ is $w_i(t)$ where:

$$w_i(t) = \underset{\sim}{w}(\underset{\sim}{x}_i, t) \cdot \underset{\sim}{T}_i \qquad 2.6.2$$

$$= \sum_r \underset{\sim}{\phi}_r(\underset{\sim}{x}_i) \cdot \underset{\sim}{T}_i \; \xi_r(t)$$

or

$$w_i(t) = \sum_r \phi_{ri}\, \xi_r(t) \qquad 2.6.3$$

Where ϕ_{ri} is the projection of the rth mode shape on the transducer axis at $\underset{\sim}{x}_i$.

It is important to note that an expression similar to 2.6.3 may be obtained for any response quantity of interest such as velocity, acceleration, stress or strain components in a prescribed direction at the point. For example the velocity response at $\underset{\sim}{x}_i$ in direction $\underset{\sim}{T}_i$ can be obtained from 2.6.3 by differentiation:

$$\dot{w}_i = \sum_r \phi_{ri} \dot{\xi}_r \qquad 2.6.4$$

while responses such as stress or strain may be obtained in terms of the derivatives of $\underset{\sim}{\phi}_r$ at $\underset{\sim}{x}_i$. This type of response may be written in the general form:

$$q_i(t) = \sum_r C_{ri} . \xi_r(t) \qquad 2.6.5$$

C_{ri} is the influence coefficient relating the amplitude of some response at $\underset{\sim}{x}_i$ for a unit displacement of the rth normal mode.

For the idealized, conservative structure, the equations of motion may be obtained in terms of the normal co-ordinates by well known techniques:

$$\ddot{\xi}_r + \omega_r^2 \xi_r = \frac{Z_r}{M_r} \quad ; r = 1,2,\cdots \infty \qquad 2.6.6$$

where ω_r is the rth natural frequency and M_r is the generalized mass of the rth mode.

$$M_r = \int_s m(\underset{\sim}{x}_c)\ \underset{\sim}{\phi}_r(\underset{\sim}{x}_c) \cdot \underset{\sim}{\phi}_r(\underset{\sim}{x}_c)\, ds \qquad 2.6.7$$

$Z_r(t)$ is the generalized force in the rth mode, and may be derived from considerations of work done in virtual displacements.

For a force $\underset{\sim}{P}$ at a discrete point $\underset{\sim}{x}_c$, consider the work done in a set of virtual displacements of the normal co-ordinates.

$$\sum_r Z_r \delta\xi_r = \underset{\sim}{P} \cdot \delta\underset{\sim}{w}(\underset{\sim}{x}_c) = \underset{\sim}{P} \cdot \sum_r \underset{\sim}{\phi}_r(\underset{\sim}{x}_c)\delta\xi_r \qquad 2.6.8$$

Since the normal co-ordinates are independent, the $\delta\xi_r$ are arbitrary.

Hence : $$Z_r = \underset{\sim}{P} \cdot \underset{\sim}{\phi}_r(\underset{\sim}{x}_c) \qquad 2.6.9$$

For a force fixed in direction, $\underset{\sim}{P}_K = P_K \underset{\sim}{F}_K$, where $\underset{\sim}{F}_K$ is a unit vector at $\underset{\sim}{x}_c$.

Hence : $$Z_r = P_K \phi_{rK} \text{ , where } \quad \phi_{rK} = \underset{\sim}{\phi}_r(\underset{\sim}{x}_c) \cdot \underset{\sim}{F}_K \text{ .} \qquad 2.6.10$$

Consider now a distributed normal pressure $p(\underset{\sim}{x}_c, t)$. Let $\underset{\sim}{N}(x_c)$ be the unit outward normal to the surface at $\underset{\sim}{x}_c$. Then the normal force on an element of area dA at $\underset{\sim}{x}_c$ is $p\, dA\, \underset{\sim}{N}$ and the generalized force for the rth mode follows from 2.6.9:

$$Z_r(t) = \int_c p(\underset{\sim}{x}_c, t)\, \underset{\sim}{N}(\underset{\sim}{x}_c) \cdot \underset{\sim}{\phi}_r(\underset{\sim}{x}_c)\, dA \qquad 2.6.11$$

or $$Z_r(t) = \int_c p(x_c, t)\, \phi_{rN}(\underset{\sim}{x}_c)\, dA$$

where $\phi_{rN}(\underset{\sim}{x}_c)$ is the component of the rth mode shape normal to the surface at $\underset{\sim}{x}_c$.

The equations of motion 2.6.6 do not allow for energy dissipation which is always present in real structures.. This may be allowed for in the mathematical model by (a) introducing a complex stiffness to allow for hysteresis or (b) introducing a representative coefficient of viscous damping in each mode. In practice a distributed damping force in the structure will lead to damping coupling terms in the equations 2.6.6. However experimental evidence on aircraft and similar structures suggests that the expedient of neglecting damping coupling between the modes gives a satisfactory representation of vibrations in these structures. (Pendered 1965). The question of damping coupling will be re-examined in a subsequent section. Strictly, the approach (a) is limited to steady-state harmonic excitation. Following (b), assume some representative coefficient of damping in each mode:

$$\ddot{\xi}_r + 2\delta_r \omega_r \dot{\xi}_r + \omega_r^2 \xi_r = \frac{Z_r}{M_r} \text{ ; } r = 1, 2, \ldots \infty \qquad 2.6.12$$

It is useful to refer to particular cases of 2.6.12. Let $Z_r(t)$ be a unit impulse applied at $t = 0$. Then the response $h_r(t)$ is termed the modal impulse response. Secondly let $Z_r(t)$ be a harmonic force with frequency ω .

$$Z_r(t) = Z_r e^{i\omega t}$$

Then the steady state response may be found from 2.6.12 in the form:

$$q_r(t) = \alpha_r(\omega) Z_r e^{i\omega t}$$

where

$$\alpha_r(\omega) = \frac{1}{M_r\left[\omega_r^2 - \omega^2 + i\,2\delta_r\omega_r\omega\right]} \qquad 2.6.13$$

$\alpha_r(\omega)$ is the modal receptance of the rth mode. It may be shown that α_r and h_r are fourier transform pairs.

The structure may also be characterized by its set of impulse responses. $h_{ik}(t) \equiv h_{ik}(\underset{\sim}{x}_i, \underset{\sim}{T}_i ; \underset{\sim}{x}_k, \underset{\sim}{T}_k ; t)$ is the response in a prescribed direction $\underset{\sim}{T}_i$ at position $\underset{\sim}{x}_i$ for a unit impulse applied at $\underset{\sim}{x}_k$ in direction $\underset{\sim}{T}_k$. Only stable structures will be considered, in the sense that any $h_{ik}(t)$ is absolutely integrable:

$$\int_{-\infty}^{\infty} |h_{ik}(t)|\,dt < \infty \qquad 2.6.14$$

2.6.14 is a sufficient condition for the existence of the fourier transform of h_{ik}. Let $\alpha_{ik}(\omega) \equiv \alpha_{ik}(\underset{\sim}{x}_i, \underset{\sim}{T}_i ; \underset{\sim}{x}_k, \underset{\sim}{T}_k ; \omega)$ be the fourier transform of h_{ik}. α_{ik} will in general be complex. It may be shown that $\alpha_{ik}(\omega)$ represents the steady state response at $\underset{\sim}{x}_i$ in direction $\underset{\sim}{T}_i$ for a unit harmonic force $e^{i\omega t}$ applied at $\underset{\sim}{x}_k$ in direction $\underset{\sim}{T}_k$ i.e. $\alpha_{ik}(\omega)$ are the complex receptances of the structure. (Bishop and Johnson 1960).

2.7 Response of a General Elastic Structure to Random Excitation

Consider an excitation which can be satisfactorily modelled as a stationary, gaussian random process. Such a process is described by its correlation functions or its spectral densities. The response of the structure, after the initial transient has diedout, will be stationary, and may be described by its correlation functions or spectral densitites.

Consider excitation by a set of discrete random forces $P_k(t)$, $k = 1, 2, \ldots N$.

Then, by 2.6.10, the generalized force in the rth mode at time t can be written:

$$Z_r(t) = \sum_{K}^{N} P_K(t)\ \phi_{rK} \qquad 2.7.1$$

Similarly, the generalized force in the sth mode at time $t + \tau$ can be written:

$$Z_s(t+\tau) = \sum_{L}^{N} P_L(t+\tau)\ \phi_{sL} \qquad 2.7.2$$

Multiplying and taking the ensemble average of both sides:

$$R^{Z}_{rs}(\tau) = E\Big\{ \sum_{K,L}^{N} \phi_{rK}.\phi_{sL}\ P_K(t).P_L(t+\tau) \Big\} \qquad 2.7.3$$

$$= \sum_{K,L}^{N} \phi_{rK}\,\phi_{sL}\ R^{P}_{KL}(\tau) \qquad 2.7.4$$

2.7.4 follows because the operation $E\{\ \}$ is linear.

Taking fourier transforms of both sides:

$$S^{Z}_{rs}(\omega) = \sum_{KL}^{N} \phi_{rK}\,\phi_{sL}\ S^{P}_{KL}(\omega) \qquad 2.7.5$$

2.7.5. expresses the cross spectral density of the generalised forces in the rth and sth modes in terms of the excitation force spectral densities at any frequency.

For a random pressure field using 2.6.12 the cross correlation of

the generalized forces in the rth and sth modes may be obtained:

$$R^{Z}_{rs}(\tau) = E\left\{ \int_C \int_C \phi_{rN}(\underset{\sim}{x}_1) \cdot \phi_{sN}(\underset{\sim}{x}_2)\, p(\underset{\sim}{x}_1, t) \cdot p(\underset{\sim}{x}_2, t+\tau)\, dA_1\, dA_2 \right\} \qquad 2.7.6$$

The order of integration and ensemble averaging in 2.7.6 may be interchanged:

$$R^{Z}_{rs}(\tau) = \int_C \int_C \phi_{rN}(\underset{\sim}{x}_1) \cdot \phi_{sN}(\underset{\sim}{x}_2)\, R^{p}(\underset{\sim}{x}_1, \underset{\sim}{x}_2, \tau)\, dA_1\, dA_2 \qquad 2.7.7$$

Taking fourier transforms of both sides:

$$S^{Z}_{rs}(\omega) = \int_C \int_C \phi_{rN}(\underset{\sim}{x}_1) \cdot \phi_{sN}(\underset{\sim}{x}_2)\, S^{p}(\underset{\sim}{x}_1, \underset{\sim}{x}_2, \omega)\, dA_1\, dA_2 \qquad 2.7.8$$

This expresses the cross spectral density of generalized force of the rth and sth modes in terms of the cross spectral density of the pressure field over the whole surface of the structure.

Now consider the response in terms of the generalized co-ordinates ξ_r, to a set of arbitrary random generalized forces. The equations of motion are given in 2.6.12. For the rth mode, the response to an arbitrary generalized force $Z_r(t)$ can be written as a convolution with $h_r(t)$:

$$\xi_r(t) = \int_{-\infty}^{\infty} h_r(u)\, Z_r(t-u)\, du \qquad 2.7.9$$

Similarly, the response of the sth generalized co-ordinate at time $t + \tau$ may be written:

$$\xi_s(t+\tau) = \int_{-\infty}^{\infty} h_s(v)\, Z_s(t+\tau-v)\, dv \qquad 2.7.10$$

Taking an ensemble average of the product of 2.7.9 and 2.7.10 leads to:

$$R^{\xi}_{rs}(\tau) = E\left\{ \int \int h_r(u) \cdot h_s(v)\, Z_r(t-u)\, Z_s(t+\tau-v)\, du\, dv \right\} \qquad 2.7.11$$

$$= \int_{-\infty}^{\infty} \int_{-\infty}^{\infty} h_r(u)\, h_s(v)\, R^{Z}_{rs}(\tau + u - v)\, du\, dv$$

Finally taking fourier transforms of both sides leads to the cross spectral density of the response in terms of the cross spectral density

of the generalized forces and the modal receptances:

$$S^{f}_{rs}(\omega) = \alpha^{*}_{r}(\omega)\,\alpha_{s}(\omega)\,S^{z}_{rs}(\omega) \qquad 2.7.12$$

In particular, the direct spectral density of the rth generalized co-ordinate is:

$$S^{f}_{rr}(\omega) = |\alpha_{r}(\omega)|^{2}\,S^{z}_{rr} \qquad 2.7.13$$

Observe that the cross-spectral densities of the generalized co-ordinate velocities or accelerations may be obtained in a similar manner, using the appropriate modal receptances. Indeed:

$$S^{\dot{f}}_{rs} = \omega^{2}\,S^{f}_{rs} \quad \text{and} \quad S^{\ddot{f}}_{rs} = \omega^{4}\,S^{f}_{rs} \qquad 2.7.14$$

Finally, expression for the cross spectral density between any pair of responses at $\underset{\sim}{x}_i$ and $\underset{\sim}{x}_j$ in prescribed directions may be obtained from the generalized co-ordinate cross spectral densities using 2.6.3 or 2.6.5. For example:

$$S^{w}_{ij}(\omega) = \sum_{r,s} \phi_{ri}\,\phi_{sj}\,S^{f}_{rs}(\omega) \qquad 2.7.15$$

2.7.15 may be generalized in the following way for any pair of response quantities in prescribed directions. Let C_{ri} be the (complex) harmonic response of q_i for a unit harmonic response of the rth mode. Then $S^{q}_{ij}(\omega)$ may be written with appropriate response co-efficients:

$$S^{q}_{ij}(\omega) = \sum_{r,s} C^{*}_{ri}\,C_{sj}\,S^{f}_{rs} \qquad 2.7.16$$

2.7.16 is appropriate to velocity, acceleration, stress or strain responses. These relations constitute a formal solution to the response of a linear elastic structure to stationary random excitation. For discrete forces, an alternative expression of response in terms of receptances will be useful.

Consider a set of discrete forces $P_K(t)$; K = 1, 2, ... N. Then the response at $\underset{\sim}{x}_i$ in direction $\underset{\sim}{T}_i$ can be written:

$$q_i(t) = \sum_{K=1}^{N} \int_{-\infty}^{\infty} h_{iK}(u_K)\, P_K(t-u_K)\, du_K \qquad 2.7.17$$

Similarly, the response at $\underset{\sim}{x}_j$ in direction $\underset{\sim}{T}_j$ can be written:

$$q_j(t+\tau) = \sum_{L=1}^{N} \int_{-\infty}^{\infty} h_{jL}(u_L)\, P_L(t+\tau-u_L)\, du_L \qquad 2.7.18$$

Taking ensemble average of the product leads to:

$$R^q_{ij}(\tau) = \sum_{K,L}^{N} \int_{-\infty}^{\infty}\int_{-\infty}^{\infty} h_{iK}(u_K)\, h_{jL}(v_L)\, R^P_{KL}(\tau+u_K-v_L)\, du_K\, dv_L \qquad 2.7.19$$

Finally taking fourier transforms of both sides leads to the cross-spectral density of the responses:

$$S^q_{ij}(\omega) = \sum_{K,L=1}^{N} \alpha^*_{iK}\ \alpha_{jL}\ S^P_{KL}(\omega) \qquad 2.7.20$$

This may be written using matrices. Let $[S^P] \equiv [S^P_{KL}]$ be the N square matrix of the spectral densities of the applied forces. Let $\{\alpha_i\} \equiv \{\alpha_{i1}, \alpha_{i2} .. \alpha_{iN}\}$ and $\{\alpha_j\} \equiv \{\alpha_{j1}, \alpha_{j2} .. \alpha_{jN}\}$ be row matrices of complex receptances for the ith and jth locations. Then:

$$S^q_{ij} = \{\overline{\alpha_i}\}[S^P]\{\alpha_j\}' \qquad 2.7.21$$

The bar denotes the conjugate of the matrix. For a set of n responses, the n square spectral density matrix $[S^q] \equiv [S^q_{ij}]$ may be written:

$$[S^q] = [\overline{\alpha}][S^P][\alpha]' \qquad 2.7.22$$

where $[\alpha]$ is the $n \times N$ matrix whose rows are $\{\alpha_i\}$, $i = 1, 2, \ldots n$.

CHAPTER 3

THEORETICAL BASIS FOR SIMULATION

3.1 Introduction

In this chapter, the simulation of the random motions of a general elastic structure is considered, simulation being interpreted as the replacement of an arbitrary form of random excitation corresponding to the service environment, by another representing the laboratory test, controlled to produce a response which is equivalent in some sense. The service excitation is assumed to be well represented as stationary and gaussian. In particular, the replacement of such a service load by a set of force generators is considered.

The assumption of randomness of the excitation makes it necessary to base the equivalence of the two situations, service and simulation, on some probabilistic measure of the type discussed in chapter 2. It is considered that spectral densities represent the most useful measure of randomness from the practical point of view that control of a random vibration test is most easily effected by frequency selective filtering, which acts directly on the spectral densities.

3.2 Necessary Conditions for Simulation

The degree of equivalence of a simulated response must be based upon a comparison with the response of the structure in the service situation. The reproduction of the actual time history of any service response would be a valid simulation test, but in the first place this would lead to extreme practical difficulties, and in the second place, it is not necessary since in the context of the random

behaviour, such a time history cannot be regarded as the unique outcome of the service environment, but only as a typical sample record. Consequently there is no point in faithfully reproducing the detailed fluctuations of any one sample record.

The characterization of the responses as a set of random processes implies that equivalence can be reasonably based on probabilistic measures, and leads to the following conditions for simulation.

Let $q_i(t)$, $i = 1,2...m$ be any set of responses at defined locations within S. The responses need not be distinct. Consider the following event:

$$A \equiv \left\{ x_1 < q_1(t+\tau_1) \leq x_1+\delta x_1 \ \underline{\text{and}} \ x_2 < q_2(t+\tau_2) \leq x_2+\delta x_2 \ \underline{\text{and}} \ldots \right.$$
$$\left. \ldots \underline{\text{and}} \ x_m < q_m(t+\tau_m) \leq x_m + \delta x_m \right\} \qquad 3.2.1$$

Then a necessary condition for simulation is that the probability of this event be the same in the service and in the simulated motion for any set of time differences τ_1, τ_2 $\ldots \tau_m$ and for any interval of the m dimensional sample space.

$$\text{Prob } A_{(I)} = \text{Prob } A_{(II)} \qquad 3.2.2.$$

The subscripts I and II are used to represent the service and simulated cases.

The statement 3.2.2 implies that the finite dimensional density and distribution functions of the m dimensional process $\{q_1(t), q_2(t), \ldots q_m(t)\}$ must be reproduced. Let $F_m(x_1,x_2..x_m ; \tau_1,\tau_2..\tau_m)$ be the joint distribution function of the random variables $q_i(t+\tau_1)$, $\ldots q_m(t+\tau_m)$. Then the condition for simulation is:

$$F_{m(II)} = F_{m(I)} \qquad 3.2.3$$

for any m, τ_1 , τ_2 ... τ_m , and for all points (x_1, x_2... x_m)

This basis for simulation will be termed simulation in distribution. Stationarity has been assumed in 3.2.3. For a gaussian process it has been demonstrated in chapter 2 how the finite dimensional distributions may be derived wholly from the set of correlation functions. Let $q_i(t)$, $q_j(t)$ be a pair of responses within S. Then for a gaussian process, by 3.2.3, a necessary condition for simulation in distribution is that the cross-correlation function $R^q_{ij}(\tau)$ be the same in the simulated case for any q_i, q_j and for all τ.

$$R^q_{ij}(\tau)_{II} = R^q_{ij}(\tau)_I \qquad 3.2.4$$

Finally, taking fourier transforms of both sides leads to a statement of spectral density simulation.

$$S^q_{ij}(\omega)_{II} = S^q_{ij}(\omega)_I \qquad 3.2.5$$

A necessary condition for simulation in probability of all events of the type 3.2.1 is that the cross spectral density of the responses of any pair of co-ordinates in S be reproduced at all frequencies ω . While 3.2.5 represents a simplification of the statement of simulation in probability 3.2.1, it must apply to all pairs of responses in S, and in this form does not suggest a practical solution to the simulation problem. By considering the general response relations for the structure, outlined in chapter 2, further simplifications are possible.

The cross spectral density of the responses q_i and q_j may be written:

$$S^{q}_{ij} = \sum_{r,s=1}^{\infty} C^{*}_{ri}\, C_{sj}\, S^{f}_{rs} \qquad 3.2.6$$

$$= \sum_{r,s=1}^{\infty} C^{*}_{ri}\, C_{sj}\, \alpha^{*}_{r}\, \alpha_{s}\, S^{z}_{rs} \qquad 3.2.7$$

where C_{ri}, C_{sj} are the previously defined influence coefficients of the responses for unit harmonic response of the normal co-ordinates, and α_r, α_s are the modal receptances. It follows that spectral density simulation of the whole structure requires that the cross spectral density of any pair of normal co-ordinates is reproduced at any frequency ω :

$$S^{f}_{rs\,(II)} = S^{f}_{rs\,(I)} \qquad 3.2.8$$

or that the corresponding generalized force cross spectra are reproduced:

$$S^{z}_{rs\,(II)} = S^{z}_{rs\,(I)} \qquad 3.2.9$$

Strictly, conditions 3.2.8 and 3.2.9 must be satisfied at all frequencies for the infinite set of modes but this cannot lead to a practical basis for simulation.

3.3 Finite Degree of Freedom Approximation

It is possible to justify a finite series description of response of the form of 3.2.6 :

$$S^{q}_{ij} = \sum_{r,s=1}^{n} C^{*}_{ri}\, C_{sj}\, S^{f}_{rs} = \sum_{r,s=1}^{n} C^{*}_{ri}\, C_{sj}\, \alpha^{*}_{r}\alpha_{s}\, S^{z}_{rs} \qquad 3.3.1$$

or:

$$S^{q}_{ij} = \sum_{r=1}^{n} C^{*}_{ri}\, C_{rj}\, |\alpha_{r}|^{2} S^{z}_{rr} + \sum_{r\neq s}^{n} C^{*}_{ri}\, C_{sj}\, \alpha^{*}_{r}\alpha_{s}\, S^{z}_{rs} \qquad 3.3.2$$

Recall the form of the modal receptances:

$$\alpha_r(\omega) = \frac{1}{M_r[\omega_r^2 - \omega^2 + i2\delta_r\omega_r\omega]} \qquad 3.3.3$$

Hence:

$$(\alpha_r^* \alpha_s) = \frac{1}{M_r M_s[\omega_r^2 - \omega^2 - i2\delta_r\omega_r\omega][\omega_s^2 - \omega^2 + i2\delta_s\omega_s\omega]} \qquad 3.3.4$$

$$= |\alpha_r||\alpha_s| e^{i(\psi_s - \psi_r)} \quad \text{where} \quad \psi_r = \tan^{-1}\frac{2\delta_r\omega_r\omega}{[\omega_r^2 - \omega^2]} \qquad 3.3.5$$

and:

$$|\alpha_r|^2 = \frac{1}{M_r^2[(\omega_r^2 - \omega^2)^2 + 4\delta_r^2\omega_r^2\omega^2]} \qquad 3.3.6$$

For a typical structure the modal receptances are highly selective in frequency, exhibiting a peak at the corresponding natural frequency. Such characteristics are illustrated in Figure 3.3.1. It is also clear from Figure 3.3.1 that cross products of modal receptances of the type 3.3.4 will be small at any frequency unless the natural frequencies of the two modes are close enough such that the peaks of α_r and α_s overlap.

In the first place, a finite degree of freedom approximation (3.3.1) may be based on the fact that any physically realisable excitation has an upper frequency limit, but on this basis alone, n will be large in general. Further simplification can be made by considering the resonant motions of the structure.

In the general case, the forms of the response spectral densities are determined by the shapes of the excitation spectra and by the receptances. If the excitation spectra, represented by the $S_{rs}^{xx}(\omega)$ terms in 3.3.2 are slowly varying functions of frequency compared with the fluctuations of the $\alpha(\omega)$ terms, then any response spectral density will parallel the form of the receptances and will exhibit a series of

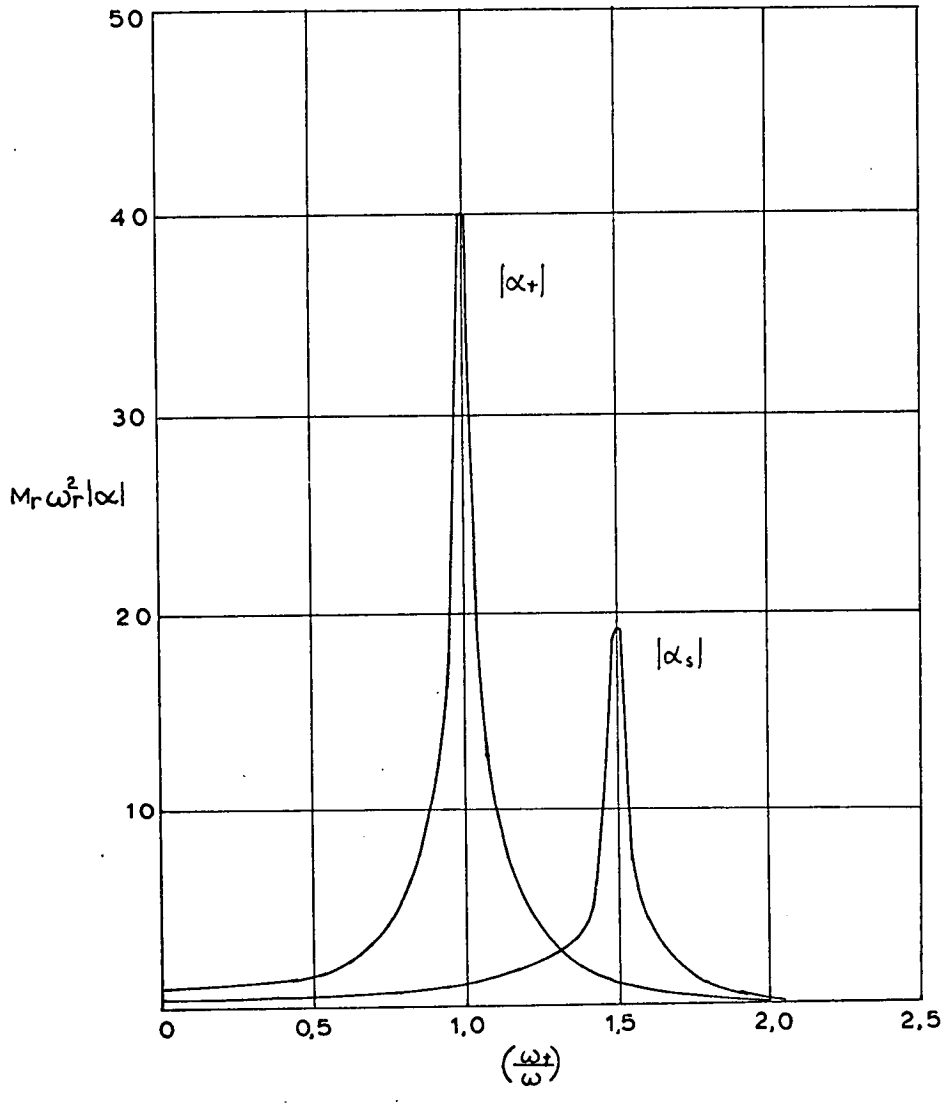

Fig. 3.3.1

Modal Receptance Characteristics.

$Q_r = Q_s = 40$; $\omega_s/\omega_r = 1.5$

peaks at the natural frequencies. This is the common experience with practically important excitations and structures. Significant levels of response spectral density occur in the neighbourhood of the structure natural frequencies and represent the resonant motions of the structure. Under these circumstances, at a frequency ω near, say, the rth resonant frequency, the leading term in the first series of 3.3.2 will be the rth term because of the weight of the rth modal receptance. Significant contributions might also come from the adjacent terms. The second series of 3.3.2 represents the contributions arising from correlations between the generalized forces in the different modes, weighted by receptance cross products, and the magnitudes of these contributions depend on the closeness of the natural frequencies. These considerations suggest that at frequencies near a resonant frequency, the representation of the response by the motions in only a few modes would be satisfactory, so that n might be reasonably low. Indeed for structures possessing low damping, n might be taken to be one over frequency intervals where the natural frequencies were widely spaced.

3.4 Theoretical Basis for the Simulation of Resonant Motion

Consider spectral density simulation of the structure S over an interval of frequency. Suppose that the response over this frequency interval may be represented by the motions of n modes. The following statements may be made.

Necessary and sufficient conditions for the simulation in spectral density of the motions of the whole structure over this frequency interval are that (a) the n square spectral density matrix of a set of

n reference responses be reproduced and (b) the n square matrix of the modal influence coefficients of the reference co-ordinates be non-singular.

In addition, the motions may be simulated by a set of n force generators, subject to the condition that the n square matrix of the projections of the n mode shapes on the lines of action of the forces be non-singular.

Proof of these statements follows:

Let q_i, q_j be a pair of response co-ordinates within S. Then by 3.3.1 their cross spectral density may be expressed as:

$$S^q_{ij}(\omega) = \sum_{r,s=1}^{n} C^*_{ri}\, C_{sj}\, S^f_{rs} \qquad 3.4.1$$

or in matrix form:

$$S^q_{ij} = [c_i]^\dagger [S^f] [c_j] \qquad 3.4.2$$

It follows that for simulation of all such responses in S, it is required that the n square spectral density matrix of the normal co-ordinates be reproduced over the frequency interval:

$$[S^f]_{II} = [S^f]_{I} \qquad 3.4.3$$

Now, let q_a, a = 1,2,...n be a set of reference response co-ordinates of S. The n square spectral density matrix of these co-ordinates may be expressed as:

$$[S^q] = [C^a]^\dagger [S^f] [C^a] \qquad 3.4.4$$

where $[C^a]$ is the n square matrix of modal influence coefficients for the n modes at the reference co-ordinates.

It follows from 3.2.5 that a necessary condition for simulation is :

$$[S^a]_{II} = [S^a]_I \qquad 3.4.5$$

Condition 3.2.5 is also sufficient provided that $\det [C^a] \neq 0$. Then $[C^a]^{-1}$ exists and is unique. 3.4.4 may be written:

$$[S^q] = [C^{a-1}]^T [S^a] [C^{a-1}] \qquad 3.4.6$$

In 3.4.6 $[S^q]$ is unique so that condition 3.4.5 implies :

$$[S^q]_{II} = [S^q]_I$$

and it follows from 3.4.2 that:

$$S^q_{ij\,(II)} = S^q_{ij\,(I)}$$

for any q_i, q_j in S.

Simulation in spectral density of all responses of S over the frequency interval follows if the spectral densities of the n reference co-ordinates are reproduced. The reference transducers must be placed so that $\det [C^a] \neq 0$. This means that no rows or columns of $[C^a]$ may be zero, and that all rows or columns must be linearly independent. The condition would not be satisfied if a transducer had its sensitive axis orthogonal to the vectors of the deformation in each of the n modes at the transducer location.

Now consider excitation by a set of n force generators P_k, $k = 1,2,\ldots n$ with controllable spectral densities. Let $[S^P] \equiv [S^P_{k\ell}]$ $k,\ell = 1,\ldots n$ be the spectral density matrix of the forces.

The responses of the structure at the n reference points may be expressed in terms of the receptances between the excitation locations and the reference locations:

$$[S^a] = \overline{[A]}[S^p][A]' \qquad 3.4.7$$

where $[A] = [\alpha_{ak}]$ is the matrix of complex receptances (2.7.22). Suppose $\det[A] \neq 0$, then $[A]^{-1}$ exists and is unique.

also:

$$\overline{[A]}^{-1} \equiv \overline{[A^{-1}]} \qquad 3.4.8$$

Hence 3.4.7 may be written:

$$[S^p] = \overline{[B]}[S^a][B]' \text{ where } [B] = [A]^{-1} \qquad 3.4.9$$

Provided $\det[A] \neq 0$, there exists a unique spectral density matrix of the n forces which will reproduce a given set of response spectra of n reference points, and which will therefore achieve spectral density simulation of the whole structure over the prescribed frequency interval. The required spectral density matrix $[S^p]$ may be determined from measured receptances of the structure, or it may be possible to adjust the levels by feedback from the responses.

The condition of non-singularity of the receptance matrix is a restriction on the siteing of the force generators, similar to the condition imposed on the reference transducers. In practice, non-singularity may be checked from the measured receptances. On the basis of the n degree of freedom approximation with no damping coupling, the receptance matrix $[A]$ may be expressed as:

$$[A] = [C^a]'[\alpha][f] \qquad 3.4.10$$

where $[\alpha] = \text{diag}[\alpha_1, \alpha_2 \ldots \alpha_n]$ is the matrix of the n modal receptances, $[C^a]$ is the matrix of modal influence coefficients and $[f] = [\phi_{rk}]$ is the n square matrix of the projections of the n mode shapes $r = 1,2,\ldots n$ on the lines of action of the forces at the locations $k = 1,2,\ldots n$.

Hence $\det [A] = \det [C^a] . \det [\alpha] . \det [f]$ 3.4.11

and non-singularity of $[A]$ requires that $[C^a]$ and $[f]$ be non-singular.

It is suggested that the relevant value of n at any frequency ω is the number of modes having resonant frequency 'near' ω. This presupposes that significant levels of response spectra are always a consequence of resonant motion. The question of a quantitative measure of 'nearness' will be discussed presently. It is clear that the complexity of the simulation experiment increases with n, and that only at low orders of n does the procedure become a practical possibility.

3.5 Single Vibrator Simulation

If, over some range of frequency a structure has widely spaced natural frequencies and low damping, then at frequencies in the neighbourhood of a resonant frequency, significant response of any co-ordinate will be associated with a large contribution from the term in expression 3.3.2 which relates to the corresponding mode. A one degree of freedom approximation of the response would be valid, and the general theory with n = 1 states that simulation in spectral density of the whole structure would be obtained by reproducing the direct spectral density at a single point using a single vibrator. The siteing conditions for the force and transducer locations are simply that $\phi_{+k} \neq 0$ and $C_{+a} \neq 0$.

From 3.4.1 the response cross spectral density of any pair of co-ordinates of the structure can be written:

$$S^q_{ij} = C^*_{+i} C_{+j} S^f_{++} = C^*_{+i} C_{+j} |\alpha_+|^2 S^E_{++} \qquad 3.5.1$$

Let q_a be the reference transducer. Then in the service case:

$$S^{q}_{aa(I)} = |C_{+a}|^2 S^{f}_{++(I)} \qquad 3.5.2$$

If, in the simulation test, a force P_k is adjusted so that $S^{q}_{aa(II)} = S^{q}_{aa(I)}$

i.e. $$S^{p}_{kk} = \frac{S^{q}_{aa(I)}}{|\alpha_{ak}|^2} \qquad 3.5.3$$

This will be possible provided $\phi_{+k} \neq 0$. Then from 3.5.2, if $C_{+a} \neq 0$:

$$S^{f}_{++(II)} = S^{f}_{++(I)} \qquad 3.5.4$$

By 3.5.1 this implies $S^{q}_{ij(II)} = S^{q}_{ij(I)}$ for any q_i, q_j in S. 3.5.5.

It would seem however that the assumptions would only be valid for certain types of service excitations. It is clear that for $\omega \doteqdot \omega_+$, the mode adjacent to ω_+ might well contribute significantly at ω by virtue of its generalized force spectral density being sufficiently large to overcome the attenuation of the response by its modal receptance. Consequently the one degree of freedom assumption need not be valid in the neighbourhood of each resonance if the service excitation caused a wide range of values of generalized force spectra. Observe however, that if $S^{z}_{++1} >> S^{z}_{+}$ so that the one degree of freedom model is not valid near ω_+, then at frequencies near ω_{++1} the accuracy of the one degree of freedom assumption is improved by the fact that $S^{z}_{++1} >> S^{z}_{+}$ and further, the peak at ω_{++1} is the more severe. Consequently, for the case of widely spaced natural frequencies the use of one vibrator simulation might lead to errors due to non-uniformity of the service generalized force spectra but the accuracy of the simulation would increase with the severity of the resonance.

At frequencies between the resonant frequencies, the one dimensional model would not be valid, since several terms of 3.3.1 would be required

to represent the motion. It may be reasonably assumed that such off-resonant contributions would be small however so that the possibility of simulation errors at these frequencies need not detract seriously from the validity of the method, and must be viewed in the light of the ability of the method to reproduce the severe resonant response of the whole structure on such a simple basis.

3.6 Two Vibrator Simulation

It is expected that the single vibrator simulation would be relevant to many practical structures at low frequencies. If two modes have close natural frequencies, however, the expression for the response spectra 3.3.1 would require n = 2 over the frequency interval containing the natural frequencies. From the general case of simulation with n significant modes, it is inferred that spectral density simulation of the whole structure over the resonant frequency interval can be achieved if the direct and cross spectral densities between two reference responses are reproduced, and this can be obtained by adjusting the direct and cross spectral densities of two suitably located vibrators.

It is of interest to note that reproduction of only the direct spectral densities of the reference responses does not guarantee simulation of the whole structure. Suppose q_a, q_b are the reference responses. Then for a general service excitation, the direct spectral densities may be written:

$$\left.\begin{aligned} S^{q}_{aa} &= |C_{ra}|^2 S^{f}_{rr} + |C_{sa}|^2 S^{f}_{ss} + 2\,\mathrm{Re}\{C^{*}_{ra}\, C_{sa}\, S^{f}_{rs}\} \\ S^{q}_{bb} &= |C_{rb}|^2 S^{f}_{rr} + |C_{sb}|^2 S^{f}_{ss} + 2\,\mathrm{Re}\{C^{*}_{rb}\, C_{sb}\, S^{f}_{rs}\} \end{aligned}\right\} \qquad 3.6.1$$

This relation does not have a unique inverse, so the conditions:

$$S^{q}_{aa\,(II)} = S^{q}_{aa\,(I)} \qquad \text{and} \qquad S^{q}_{bb\,(II)} = S^{q}_{bb\,(I)} \qquad 3.6.2$$

do not guarantee the condition for simulation :

$$\begin{bmatrix} S^{f}_{++} & S^{f}_{+s} \\ S^{f}_{s+} & S^{f}_{ss} \end{bmatrix}_{II} = \begin{bmatrix} S^{f}_{++} & S^{f}_{+s} \\ S^{f}_{s+} & S^{f}_{ss} \end{bmatrix}_{I} \qquad 3.6.3$$

3.7 Errors in One Vibrator Simulation

Arguments for the justification of one or two vibrator simulation have been based upon the closeness or otherwise of the natural frequencies of the normal modes and upon corresponding assumptions of a one or two mode representation of the structure. Such assumptions are approximate because strictly, every modal receptance exists at all frequencies. In view of the useful simplicity of the single vibrator case, it is of some interest to obtain some quantitative measure of how close two natural frequencies must be before the one dimensional representation becomes inadequate. This is obtained in the present section.

Consider a pair of modes, denoted the rth and sth, having natural frequencies ω_+ and ω_s . Let q_i be an arbitrary response co-ordinate and let q_a be a reference co-ordinate for one vibrator simulation. For simplicity these will be taken to be displacements. It is assumed that at frequencies near ω_+ and ω_s, a two mode representation of the structure response is adequate. Any service excitation may be represented by the generalized force spectral density matrix:

$$[S^{F}] \equiv \begin{bmatrix} S^{F}_{rr} & S^{F}_{rs} \\ S^{F}_{sr} & S^{F}_{ss} \end{bmatrix}$$

Using 3.3.1 , the direct spectral densities of the responses q_i and q_a may be written:

$$S^{q}_{ii(I)} = \phi^{2}_{ri} |\alpha_r|^2 S^{F}_{rr} + \phi^{2}_{si} |\alpha_s|^2 S^{F}_{ss} + 2\phi_{ri}\phi_{si} \mathrm{Re}\{\alpha^{*}_{r}\alpha_s S^{F}_{rs}\} \qquad 3.7.1$$

$$S^{q}_{aa(I)} = \phi^{2}_{ra} |\alpha_r|^2 S^{F}_{rr} + \phi^{2}_{sa} |\alpha_s|^2 S^{F}_{ss} + 2\phi_{ra}\phi_{sa} \mathrm{Re}\{\alpha^{*}_{r}\alpha_s S^{F}_{rs}\} \qquad 3.7.2$$

Now suppose a single vibrator is used to reproduce $S^{q}_{aa(I)}$. Let P_K be the force and ϕ_{rK}, ϕ_{sK} be the projections of the rth and sth modes on its line of action.

Then the required spectral density is:

$$S^{P}_{KK} = \frac{S^{q}_{aa(I)}}{|\alpha_{aK}|^2} \qquad 3.7.3$$

So that the simulated response at q_i is given by:

$$S^{q}_{ii(II)} = \frac{|\alpha_{iK}|^2}{|\alpha_{aK}|^2} S^{q}_{aa(I)} \qquad 3.7.4$$

The ratio $S^{q}_{ii(II)} / S^{q}_{ii(I)}$ gives a measure of the accuracy of the simulation at any frequency where:

$$\frac{S^{q}_{ii(II)}}{S^{q}_{ii(I)}} = \frac{|\alpha_{iK}|^2}{|\alpha_{aK}|^2} \frac{S^{q}_{aa(I)}}{S^{q}_{ii(I)}} \qquad 3.7.5$$

In 3.7.5, the receptances may be expressed in terms of the two contributing modes :

$$\alpha_{iK} = \phi_{ri}\phi_{rK}\alpha_r + \phi_{si}\phi_{sK}\alpha_s \qquad 3.7.6.$$

Whence : $$|\alpha_{iK}|^2 = \phi^{2}_{ri}\phi^{2}_{rK}|\alpha_r|^2 + \phi^{2}_{si}\phi^{2}_{sK}|\alpha_s|^2 + 2\phi_{ri}\phi_{rK}\phi_{si}\phi_{sK}\mathrm{Re}\{\alpha^{*}_{r}\alpha_s\} \qquad 3.7.7$$

with a similar expansion for $|\alpha_{aK}|^2$.

For accurate simulation, the ratio 3.7.5 must be close to unity, and by 3.7.1, 3.7.2, 3.7.7 this ratio depends on the service excitation properties, the force, reference and test locations and the natural frequencies and damping factors of the two modes. By making reasonable assumptions about the force, reference and test locations it is possible to obtain bounds for the ratio 3.7.5 which demonstrate how the simulation error depends on the closeness of the natural frequencies.

In 3.7.1 and 3.7.2, S^{z}_{+s} may be written using the coherence relations (2.5.10) as:

$$S^{z}_{+s} = \nu \left[S^{z}_{++} . S^{z}_{ss} \right]^{\frac{1}{2}} e^{i\theta_{+s}} \qquad 3.7.8$$

where $\nu = \frac{|S^{z}_{+s}|}{[S^{z}_{++} . S^{z}_{ss}]^{\frac{1}{2}}}$ is the coherence ratio. ; $0 \leqslant \nu \leqslant 1$. 3.7.9

Now θ_{+s} may be such that $\{\alpha^{*}_{+} \alpha_{s} e^{i\theta_{+s}}\}$ is a real number, positive or negative, so that the third term in 3.7.2 must lie within the limits:

$$\pm \; 2 \phi_{+a} \phi_{sa} \nu \left[S^{z}_{++} . S^{z}_{ss} \right]^{\frac{1}{2}} |\alpha_{+}||\alpha_{s}| \qquad 3.7.10$$

which take on the greatest magnitude in the fully coherent case, $\nu = 1$. This defines limits for $S^{q}_{aa(I)}$ for arbitrary S^{z}_{+s} :

S^{q}_{aa} in range $\left[\phi^{2}_{+a}|\alpha_{+}|^{2} S^{z}_{++} + \phi^{2}_{sa}|\alpha_{s}|^{2} S^{z}_{ss} \pm 2\phi_{+a}\phi_{sa}|\alpha_{+}||\alpha_{s}| \{S^{z}_{++} . S^{z}_{ss}\}^{\frac{1}{2}}\right]$ 3.7.11

or S^{q}_{aa} in range $\left[\, \phi_{+a}|\alpha_{+}| \pm \gamma^{\frac{1}{2}} \phi_{sa} |\alpha_{s}| \,\right]^{2} S^{z}_{++}$ 3.7.12

where $\gamma = \frac{S^{z}_{ss}}{S^{z}_{++}}$.

Similarly from 3.7.1, S^{q}_{ii} lies in the range:

$$\left[\phi_{+i} |\alpha_{+}| \pm \gamma^{\frac{1}{2}} \phi_{si} |\alpha_{s}|\right]^{2} S^{z}_{++} \qquad 3.7.13$$

and the limiting values in 3.7.12 and 3.7.13 are obtained at the same value of θ_{+s} . Also, for close natural frequencies the phase difference

between the modal receptances will be less than $\pi/2$ so that $\mathrm{Re}\{\alpha_r^* \alpha_s\} > 0$. Using the limiting values of $S^q_{aa\,(I)}$ and $S^q_{ii\,(I)}$ in 3.7.5 it is possible to determine the limits for the ratio $S^q_{ii\,(II)}/S^q_{ii\,(I)}$ in terms of the single parameter of the service excitation γ. By considering the most unfavourable phasing of all the mode shape components (it is convenient to regard the mode shape components at the reference location, ϕ_{ra}, ϕ_{sa} as positive) so that the numerator in 3.7.5 has maximum value while the denominator has minimum value, the upper limit for the ratio 3.7.5 may be expressed in terms of γ, the absolute values of the modal components and the modal receptances:

$$\frac{S^q_{ii\,(II)}}{S^q_{ii\,(I)}} \leqslant \frac{[\phi_{ri}^2\phi_{rk}^2|\alpha_r|^2 + \phi_{si}^2\phi_{sk}^2|\alpha_s|^2 + 2|\phi_{ri}\phi_{rk}\phi_{si}\phi_{sk}|\mathrm{Re}\{\alpha_r^*\alpha_s\}][|\phi_{ra}||\alpha_r| + \gamma^{\frac{1}{2}}|\phi_{sa}||\alpha_s|]^2}{[\phi_{ra}^2\phi_{rk}^2|\alpha_r| + \phi_{sa}^2\phi_{sk}^2|\alpha_s| - 2|\phi_{ra}\phi_{rk}\phi_{sa}\phi_{sk}|\mathrm{Re}\{\alpha_r^*\alpha_s\}][|\phi_{ri}||\alpha_r| - \gamma^{\frac{1}{2}}|\phi_{si}||\alpha_s|]^2} \qquad 3.7.14$$

Similarly, a lower limit exists for this ratio when the numerator of 3.7.5 has least value and the denominator has greatest value. This is found from 3.7.14 by changing the signs of all the cross product terms.

$$\frac{S^q_{ii\,(II)}}{S^q_{ii\,(I)}} \geqslant \frac{[\phi_{ri}^2\phi_{rk}^2|\alpha_r|^2 + \phi_{si}^2\phi_{sk}^2|\alpha_s|^2 - 2|\phi_{ri}\phi_{rk}\phi_{si}\phi_{sk}|\mathrm{Re}\{\alpha_r^*\alpha_s\}][|\phi_{ra}||\alpha_r| - \gamma^{\frac{1}{2}}|\phi_{sa}||\alpha_s|]^2}{[\phi_{ra}^2\phi_{rk}^2|\alpha_r|^2 + \phi_{sa}^2\phi_{sk}^2|\alpha_s|^2 + 2|\phi_{ra}\phi_{sa}\phi_{rk}\phi_{sk}|\mathrm{Re}\{\alpha_r^*\alpha_s\}][|\phi_{ri}||\alpha_r| + \gamma^{\frac{1}{2}}|\phi_{si}||\alpha_s|]^2} \qquad 3.7.15$$

It is apparent from 3.7.14 and 3.7.15 that serious departures from unity of the response ratio 3.7.5 can occur in particular cases. The lower limit 3.7.15 may be zero for a non trivial service excitation if $|\phi_{ra}||\alpha_r| / |\phi_{sa}||\alpha_s| = \gamma^{\frac{1}{2}}$ and the $z_r(t)$ and $z_s(t)$ processes are fully coherent and critically phased. This means that the response spectral density at the reference location is zero and the simulation gives a solution $S^p_{kk} = 0$. A corresponding result leads to the ratio 3.7.5. having infinite value if the service response in the test position $S^q_{ii\,(I)}$ is zero, and the simulated response $S^q_{ii\,(II)}$ is finite. These results demonstrate the severe effects on the single vibrator approach of overlapping of the modal responses. For the purposes of studying

the onset of small departures from unity of the ratio 3.7.5 it may be reasonably assumed that all mode shape components are of a similar order in absolute value, so that they may be cancelled out of 3.7.14 and 3.7.15. The lower limit 3.7.15 then becomes the reciprocal of the upper limit which is given by:

$$\frac{S^{q}_{ii(II)}}{S^{q}_{ii(I)}} \leqslant \frac{\left[|\alpha_r|^2 + |\alpha_s|^2 + 2\,Re\{\alpha_r^* \alpha_s\}\right]\left[|\alpha_r| + \gamma^{\frac{1}{2}}|\alpha_s|\right]^2}{\left[|\alpha_r|^2 + |\alpha_s|^2 - 2\,Re\{\alpha_r^* \alpha_s\}\right]\left[|\alpha_r| - \gamma^{\frac{1}{2}}|\alpha_s|\right]^2} \qquad 3.7.16$$

Computed curves for the limits of the ratio $S^{q}_{ii(II)}/S^{q}_{ii(I)}$ are plotted in Figure 3.7.1 against the natural frequency ratio of the two modes for four values of the service generalized force spectral density ratio γ for the same value of damping (assumed equal in both modes). The limits are evaluated at the natural frequency of the rth mode, and the generalized masses of the two modes are assumed equal. In Figure 3.7.2 the limits are shown for four different values of damping for a value of γ of one. The curves show that the range of possible simulation errors increases as R approaches one, and that for fixed R, the range of possible errors increases with γ and with the amount of damping.

A difficulty in using such curves to determine the limits of accurate one vibrator simulation is that the parameter γ depends on the service excitation and will not in general be known. It may be inferred that the case $\gamma = 1$ represents the most useful assumption. For $\gamma < 1$ the errors will be smaller while $\gamma > 1$ implies that the adjacent mode is the more significant of the two, and that this latter mode has the ratio S^{z}_{rr}/S^{z}_{ss} as the parameter of its error limits where $S^{z}_{rr}/S^{z}_{ss} = 1/\gamma < 1$.

Taking $\gamma = 1$, it is useful to represent the separation of the resonant frequencies of the two modes in terms of the sharpness of the

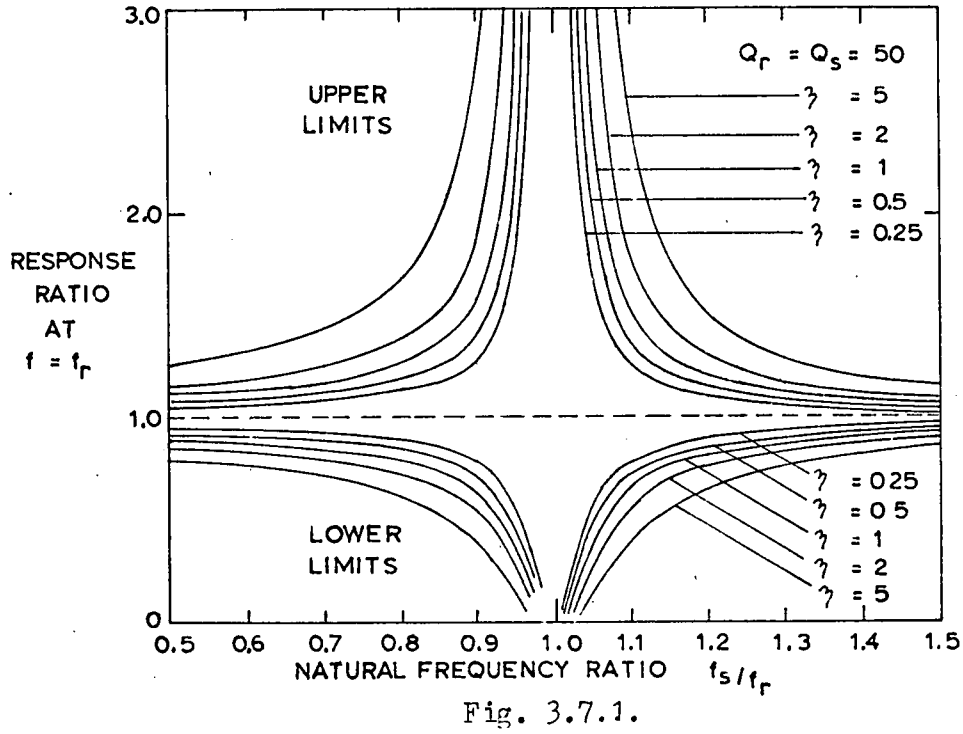

Fig. 3.7.1.

Theoretical Limits for Ratio of Service Response to Simulated Response for Single Vibrator Simulation.

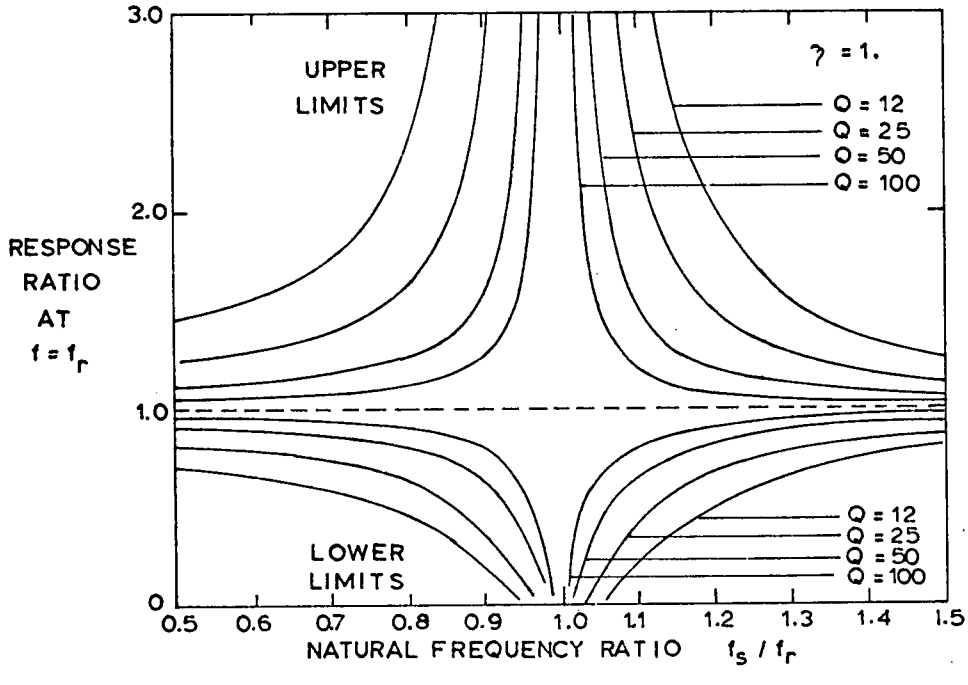

Fig. 3.7.2

Theoretical Limits for Ratio of Service Response to Simulated Response for Single Vibrator Simulation. (Damping Assumed Equal in r^{th} and s^{th} Modes.)

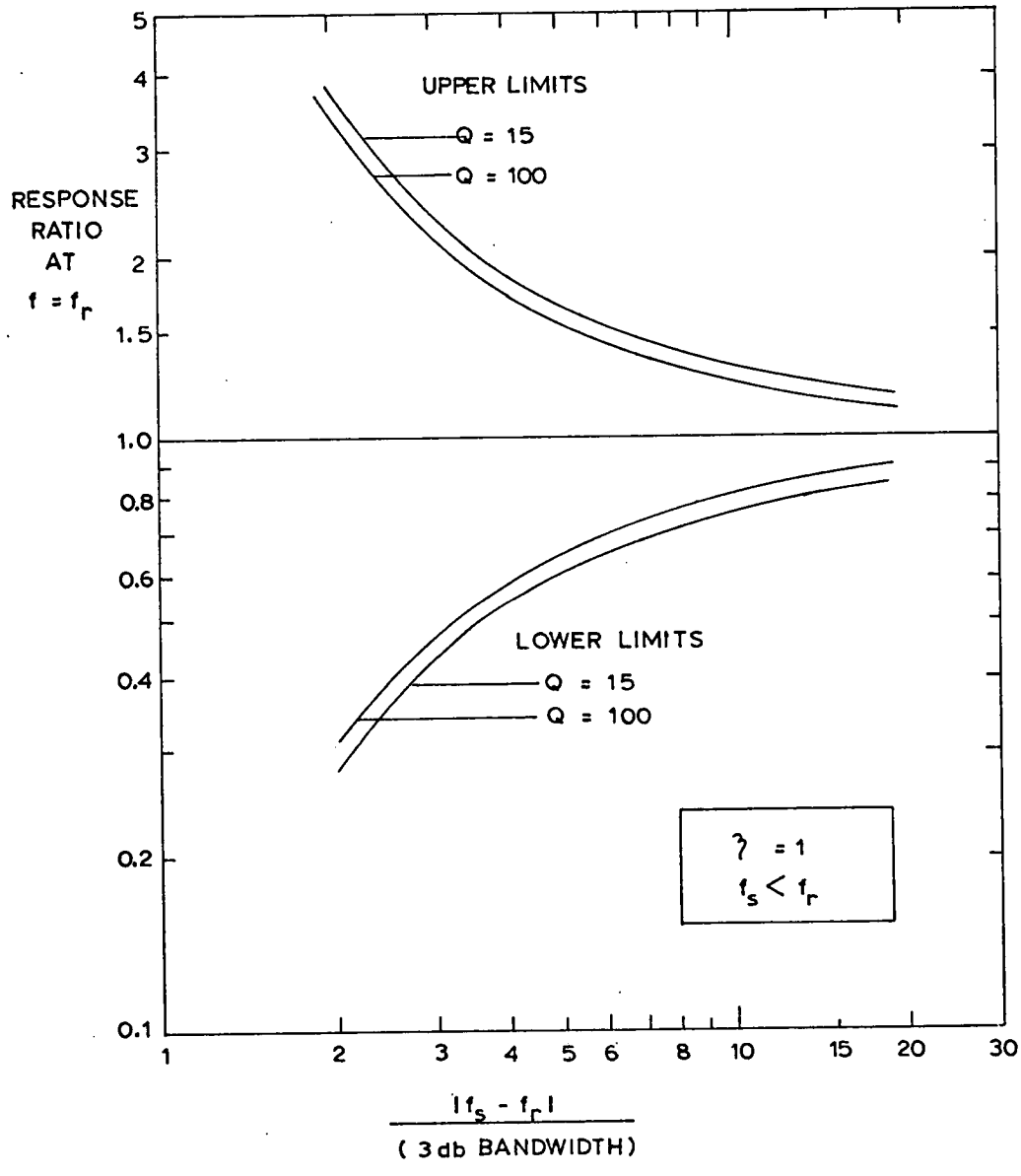

Fig. 3.7.3

Theoretical Limits for Ratio of Service Response to Simulated Response for Single Vibrator, Single Reference Simulation.
(Damping Assumed Equal in r^{th} and s^{th} Modes.)

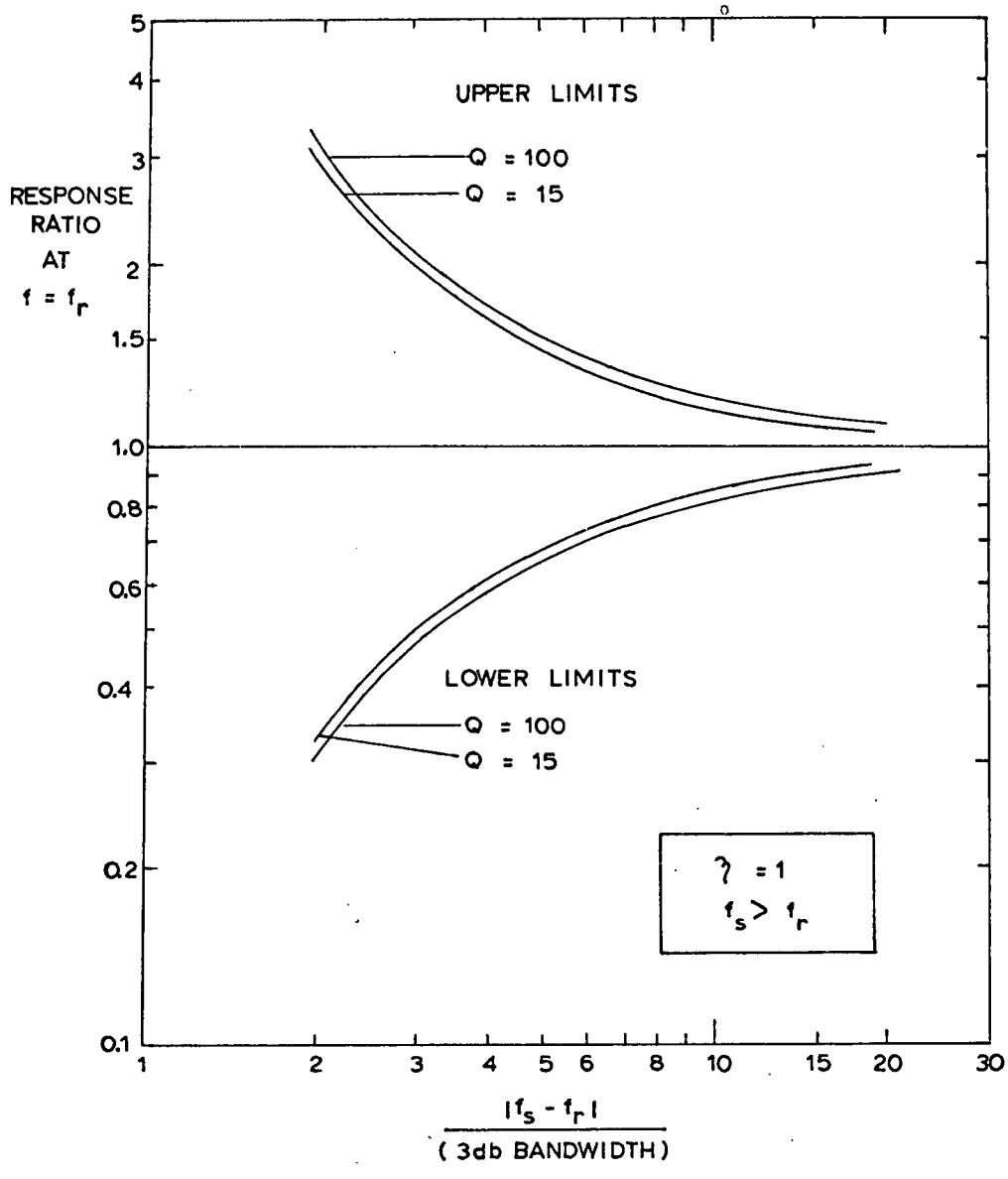

Fig. 3.7.4

Theoretical Limits for Ratio of Service Response to Simulated Response for Single Vibrator, Single Reference Simulation.
(Damping Assumed Equal in r^{th} and s^{th} Modes.)

resonance peaks. The ratio of the frequency difference to the three decibel band width of the modal receptance:- $(\omega_s - \omega_r)/2\delta\omega_r$, is a convenient measure of this. Figures 3.7.3 and 3.7.4 show the error limits for a range of Q factors of 15 to 100 plotted against the number of bandwidths of separation of the resonant frequencies. It is seen that on this basis the curves pratically coincide and that errors of 20% are possible at separations of less that ten times the three decibel bandwidth. This figure may be taken as an approximate but useful guide to the application of single vibrator simulation.

3.8 Effects of Damping Coupling

It is of interest to discuss the case where damping coupling exists between the modes. Using the mode shapes of free undamped vibration to define a set of generalized co-ordinates as before:

$$\underset{\sim}{w}(\underset{\sim}{x},t) = \sum_{r=1}^{\infty} \underset{\sim}{\phi}_r(\underset{\sim}{x})\, \xi_r(t) \qquad 3.8.1$$

The equations of motion now have the general form:

$$M_r \ddot{\xi}_r + \sum_{s=1}^{\infty} \delta_{rs} \dot{\xi}_s + K_r \xi_r = Z_r(t)\,; \quad r = 1,2 \ldots \infty. \qquad 3.8.2$$

An n degree of freedom approximation may be justified over a limited frequency range as before. It follows from 3.8.1 that simulation of the n square spectral density matrix of the generalized co-ordinates leads to spectral density simulation of the whole structure over this frequency range, and this is achieved if the responses of a suitable set of n reference co-ordinates are simulated, as in section 3.4. The possibility of simulating the responses of the n reference co-ordinates by a set of n random forces $P_k(t)$, k = 1, 2 ... n, is now considered.

As in section 3.4. the responses of the reference co-ordinates may be expressed in terms of the spectral density matrix of the forces and the receptances between the respective force and response locations:

$$[S^a] = [\overline{A}][S^p][A]' \qquad 3.8.3$$

The existence of $[A]$ is still guaranteed by the stability assumption. As in section 3.4, a solution to the simulation is assured if $[A]$ is non-singular. Let $[C]$ be the matrix of modal influence coefficients at the n reference locations. Then for harmonic response in the n modes:

$$[q_a] = [C]'[\xi] \qquad 3.8.4$$

Also let $[f]$ be the matrix of the projections of the n mode shapes on the lines of action of the forces. Then for harmonic forces:

$$[Z] = [f][P] \qquad 3.8.5$$

By definition:

$$[q_a] = [A][P]$$

Provided $[C]$ and $[f]$ are non-singular, then:

$$[\xi] = [C^{-1}]'[q_a] = [C^{-1}]'[A][f^{-1}][Z] \qquad 3.8.6$$

or:

$$[\xi] = [\alpha][Z] \qquad 3.8.7$$

where $[\alpha]$ is the modal receptance matrix and by 3.8.6 exists at all ω. $[\alpha]$ will not be diagonal if damping coupling exists between the modes. It remains to show that $[\alpha]$ is non-singular.

From 3.8.2 with a harmonic set of generalized forces:

$$[V][\xi] = [Z] \qquad 3.8.8$$

where:

$$[V] = [K] - \omega^2[M] + i\omega[\delta_{rs}] \qquad 3.8.9$$

$[K]$ and $[M]$ are diagonal matrices, while $[\delta_{rs}]$ is symmetric, positive definite. By 3.8.8, $[V]$ is the inverse of $[\alpha]$ and by inspection of 3.8.9 it is seen that $[V]$ exists at all frequencies. Hence $[\alpha]$ is non-singular and by 3.8.6 $[A]$ is non-singular, so that the presence of damping coupling between the modes does not invalidate the theoretical basis of simulation.

3.9 Conclusions

A theoretical basis for simulation has been presented which shows that spectral density simulation implies simulation in distribution, and that simulation of resonant motion of the whole of certain structures may be reasonably achieved using simple facilities. In particular if the natural frequencies are widely separated and the damping is small, a single vibrator may be used to achieve simulation of the service environment. In general the minimum number of vibrators required corresponds to the number of modes n which may contribute to the motion at any frequency, and these vibrators must be controlled to reproduce the service magnitudes of direct spectral density and cross spectral density at a set of n suitable reference co-ordinates. This result is valid even if there is appreciable damping coupling between the modes. It has been demonstrated that significant errors in the simulation using a single vibrator are probable if the natural frequencies of a pair of adjacent modes are closer than ten times the three decibel bandwidth of the modes.

On a practical level, the results for single vibrator simulation should not be taken to mean that the whole simulation test can be carried out using a single vibrator, but only that over any frequency sub-interval a single vibrator will be adequate.

The possibility of the same vibrator being adequate over the whole frequency range of the service response depends entirely upon the set of relevant structure mode shapes, and whether these allow all the modes to be excited from a single position. This possibility must be considered to be remote since the modes involved will generally consist of both the overall modes of the structure and of localized modes of loosely coupled distinct structure parts and sub-systems. It is impossible to generalize about this but a multiplicity of vibrators and of reference response spectral densities may be required to cover the whole of the relevant frequency range over all of the structure and its sub-systems, although in the context of single vibrator simulation these may be operated independently over different frequency intervals.

CHAPTER 4

EXPERIMENTAL INVESTIGATION OF ONE AND TWO VIBRATOR SIMULATION

4.1 Introduction

At the time when experimental verification of the theory of simulation was considered, several difficulties were encountered. In the first place, the desired degree of resolution of spectral density measurements could not be obtained using the available instruments and facilities for the measurement of cross spectral density were not available. A high degree of accuracy in the spectral density estimates was also required and it was felt that this could not be easily obtained. These considerations led to the development of a discrete frequency analogue of the response relations of the structure in terms of spectral density. The theoretical basis of this is presented in section 4.4 and its usefulness derives from the fact that random forces with prescribed spectral densities may be represented by harmonic forces and that the corresponding response spectral densities may be inferred from measurements, made quickly and accurately, of harmonic responses. In the second place, the range of possible simulation experiments was restricted by available facilities. The easiest method of exciting a model structure was by using electrodynamic vibrators attached at discrete points to the structure. It was considered that a valid demonstration of one and two vibrator simulation would be to excite some response of the structure using say n vibrators, record the motions of some sample points and then to attempt to reproduce these motions using one or two vibrators. This course was adopted.

4.2 The Experimental Model

The experimental model was required to have the following facilities: (a) frequency intervals of approximately unimodal response; (b) frequency intervals of approximately bi-modal response; (c) means of adjustment of the frequency ratio of a pair of adjacent modes; (d) ease of determination of the natural frequencies and mode shapes; (e) ease of interchangeability of the excitation and (f) adjustment of damping.

The experimental model is shown in Figure 4.2.1 and consisted of a horizontal brass cantilever 20 inches long and having a circular cross section of 0.875 inches diameter. The cantilever was clamped in a lathe chuck and carried at its free end a horizontal steel cross bar. The cross bar was screwed and jockey weights could be locked at any position on its length. The purpose of the cross bar was to provide a different rotatory inertia at the tip for motions in the horizontal and vertical planes. In the case of a plain round cantilever bar, the flexural modes occur in pairs, having very close natural frequencies which are separated only by the effects of imperfections in the symmetry of the clamping and by imperfections in the mass distribution. Further the modes are fixed in preferred planes in the model, but these are not predictable. By introducing the horizontal cross bar at the free end, mass is added at the tip which causes a drop in frequency of each mode, but in addition rotatory inertia is added which is much larger for rotations about a vertical axis at the tip than for rotations about a horizontal axis. This gross imperfection tends to make the mode pairs align themselves to the horizontal and vertical planes and reduces the frequencies of the horizontal modes relative to the vertical modes. The effect could be varied by altering the positions of jockey weights on the cross bar.

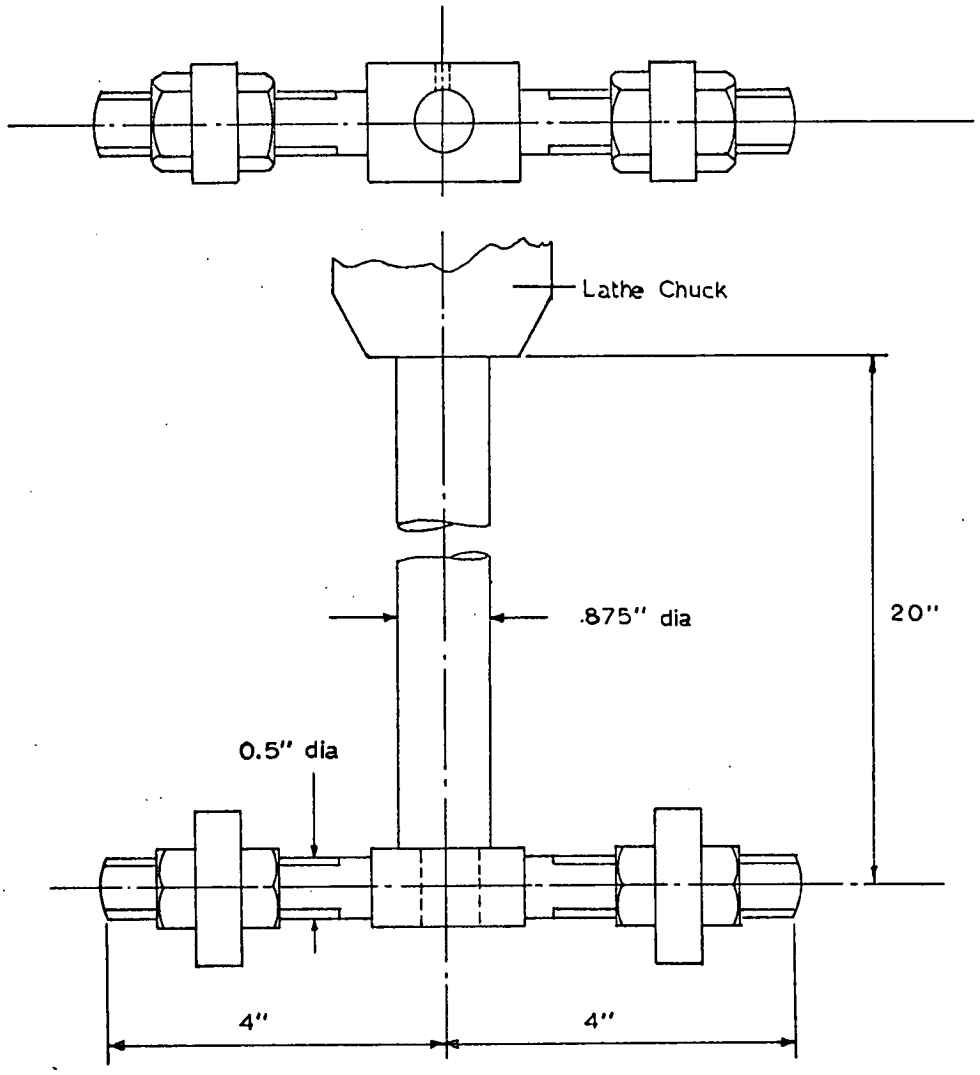

Fig. 4.2.1

Plan and Elevation of Experimental Model.

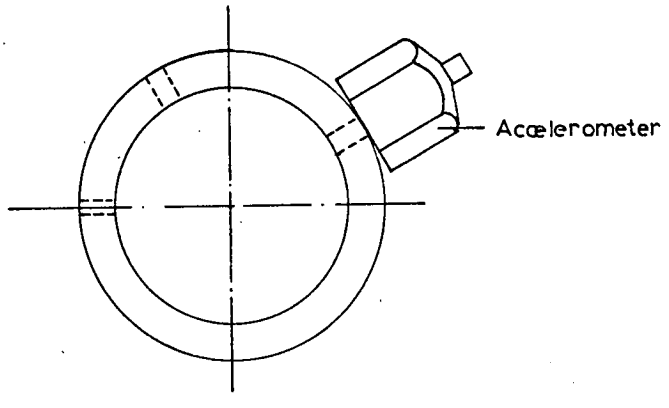

Fig. 4.2.2

Accelerometer Mounting Ring.

A suitable size of tip inertia was found by trial and error. A useful range of natural frequency ratios was easily obtained for the mode pair corresponding to the second flexural mode. Using the tip inertia shown in Figure 4.2.1 the mode shapes were found to be within a few degrees of the horizontal and vertical planes and for a constant natural frequency of the vertical mode f_v of 164.4 Hz frequency ratios, f_v/f_H, in the range 1.05 to 1.23 were obtainable.

The mode pair corresponding to the fundamental flexural frequency occurred at about 38 Hz and only a relative separation of 0.5 Hz could be produced by adding the cross bar. The observed frequencies corresponding to the third flexural mode were at 656 Hz and 492 Hz for the vertical and horizontal modes respectively in the case of the plain cross bar. It was felt that the frequency range in the neighbourhood of the second pair of natural frequencies provided a useful area for simulation tests.

Bruel and Kjaer accelerometers were used to detect the motions, and these were mounted on aluminium rings which could be slid along the bar and locked by means of grub screws at any angle. Figure 4.2.2 shows the arrangement. Small Pye-Ling vibrators, type V47, were used to excite the model and these were coupled through 4BA screwed brass rod to aluminium rings similar to the transducer rings, which could be locked at any angle at any axial plane. To support the vibrators, an aluminium bracket was clamped on the lathe bed at right angles to the model axis. The model passed through a clearance hole in the bracket, while a concentric slot in the bracket enabled vibrators mounted in individual brackets to be supported at various angles. Vibrators could be mounted on both sides of this bracket so that the points of attachment to the model were dispersed along its axis and up to four vibrators could be

used simultaneously. The arrangement is shown in Figure 4.2.3. A fifth vibrator was mounted on the lathe tool post to provide an additional horizontal excitation.

A Hewlett-Packard Oscillator type 203A was obtained to excite the model. This was an extremely useful oscillator, having a reference output section with sine and square waves available simultaneously, and a similar output section driven from the reference section through a continuously adjustable phase shift. Two vibrators could be driven simultaneously via power amplifiers, having any prescribed phase shift. Alternatively, when using a single vibrator to make receptance measurements, the variable phase section could be used to obtain the phase lag of the response. This was achieved by feeding the transducer signal to the Y amplifier of an oscilloscope, feeding the variable phase output to the X amplifier and adjusting the phase lag control to obtain a straight line with positive slope. The phase lag could be read off the calibrated dial to 2^{o} accuracy. The method proved more versatile than a commercial phasemeter in its ability to handle a wide range of signal levels and to deal with distorted signals at low levels. An alternative method was used for phase measurements when both sine channels of the oscillator were being used to drive vibrators. This is described later. The square wave output was used to drive a digital counter for period measurement. The outputs of the 5VA power amplifiers were connected to the five vibrators through a switch system, and the vibrator currents were monitored on avometers.

The accelerometer outputs were connected through a five way switch to the Bruel and Kjaer preamplifier type 1606, and then to the Bruel and Kjaer frequency analyser type 2107. This was used essentially as a valve voltmeter but its frequency selective section could be switched

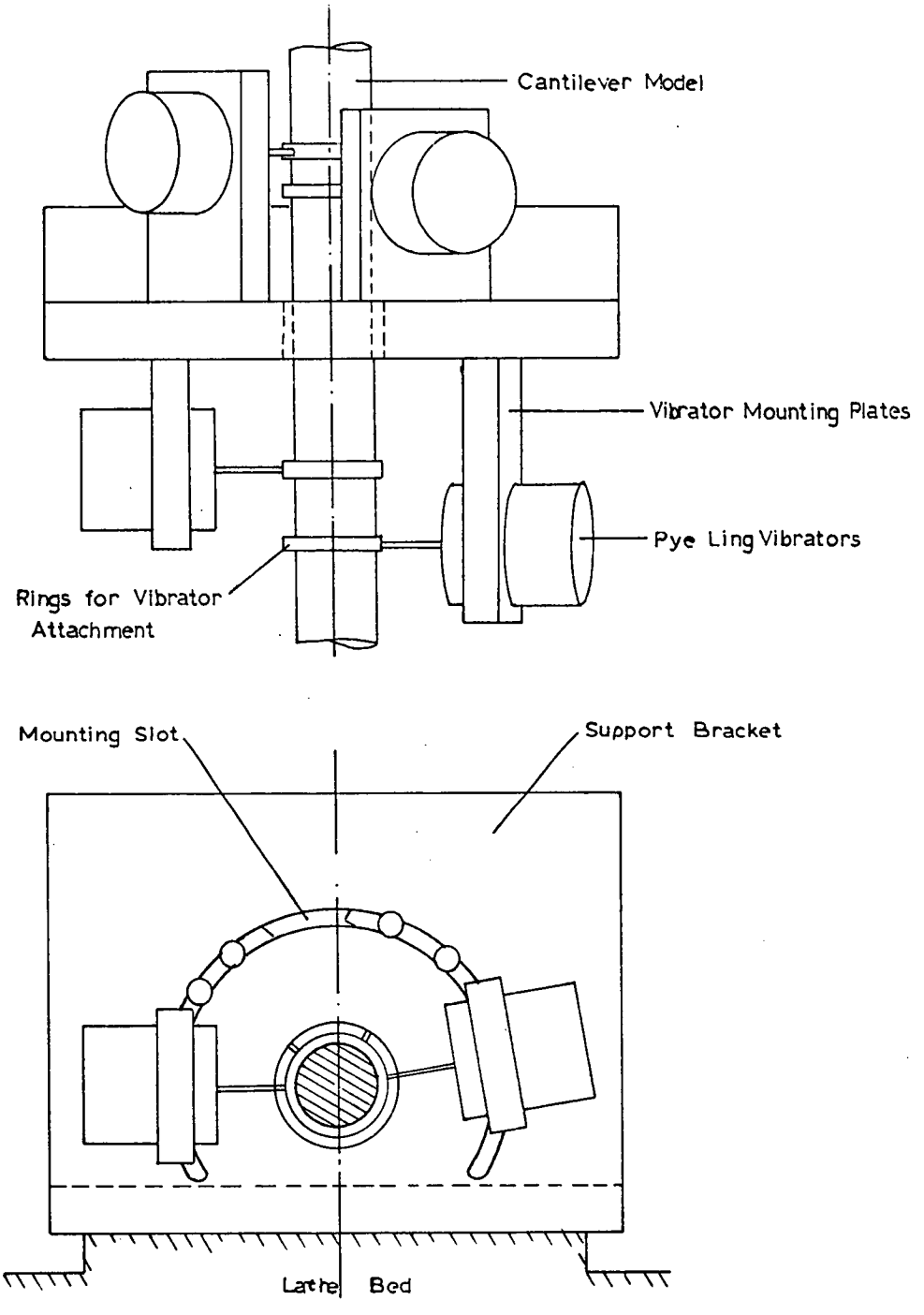

Fig. 4.2.3

Vibrator Mounting Arrangement.

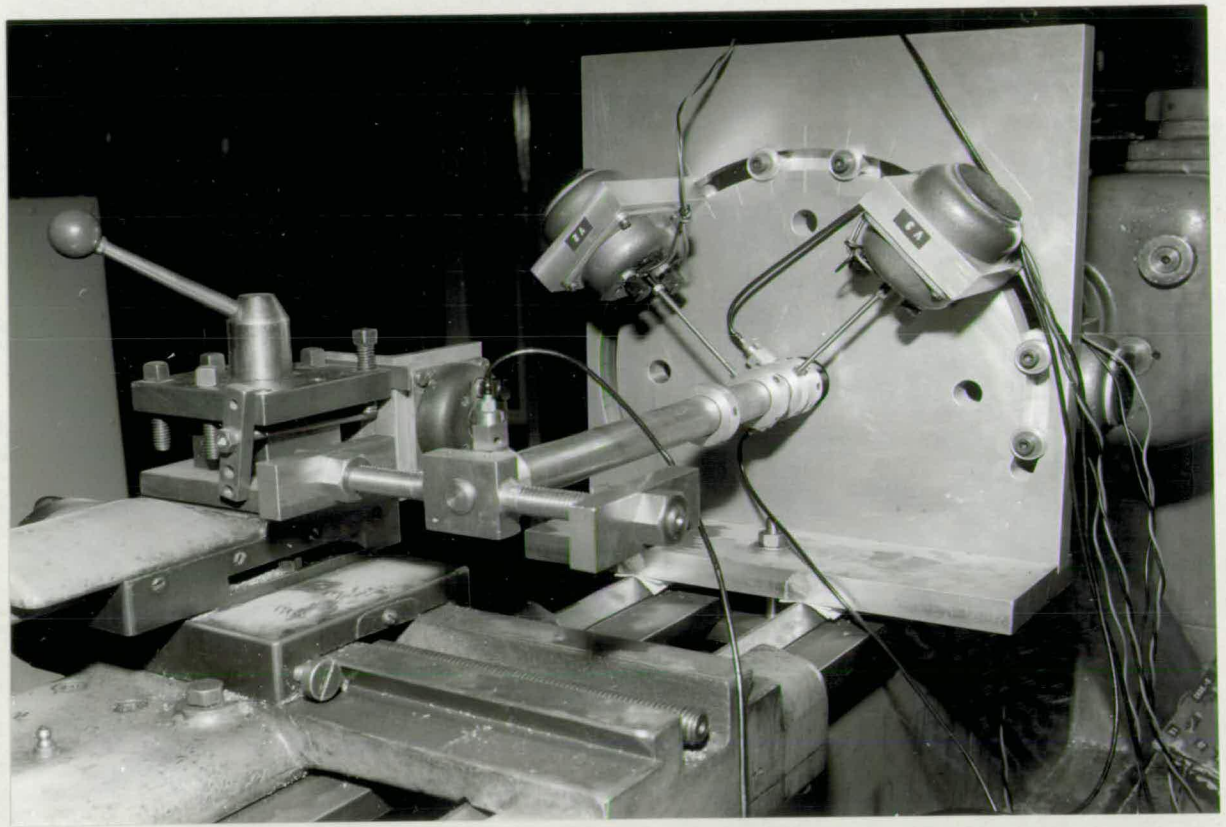

Fig. 4.2.4

Photograph of Experimental Model.

in to deal with distorted signals if necessary. The output from the 2107 was displayed on an oscilloscope for phase measurement purposes. Figure 4.2.4 shows a photograph of the experimental model.

4.3 Preliminary Measurements

Tests to determine the dynamical characteristics were carried out. Four accelerometers were mounted on the model. The natural frequencies of the modes were found by observing the frequencies at which peak responses were obtained using horizontal and vertical vibrators. At such peaks all accelerometers were examined to check that in-phase response was taking place. Figure 4.3.1 shows the natural frequencies of the second flexural mode in the horizontal and vertical directions as a function of the spacing of the jockey weights on the cross bar. Towards the innermost limit of the weights it was found that the H and V modes were not quite in the horizontal and vertical planes, but up to 5° out of plane. It became necessary to change the angles of the vibrators to obtain unimodal responses. This was probably due to lack of symmetry in the cantilever clamp stiffness. Linearity of response was investigated at several frequencies for a range of vibrator current. It was found that large departures from linearity took place at currents in excess of 0.250 amps, at frequencies near resonance and that the non linear behaviour was accompanied by changes in phase lag of the order of 30° with increasing vibrator current. A limit of 0.200 amps was imposed to ensure approximately linear behaviour for future tests.

Receptance plots relating accelerometer response to vibrator current are shown in Figure 4.3.2. These demonstrate unimodal response

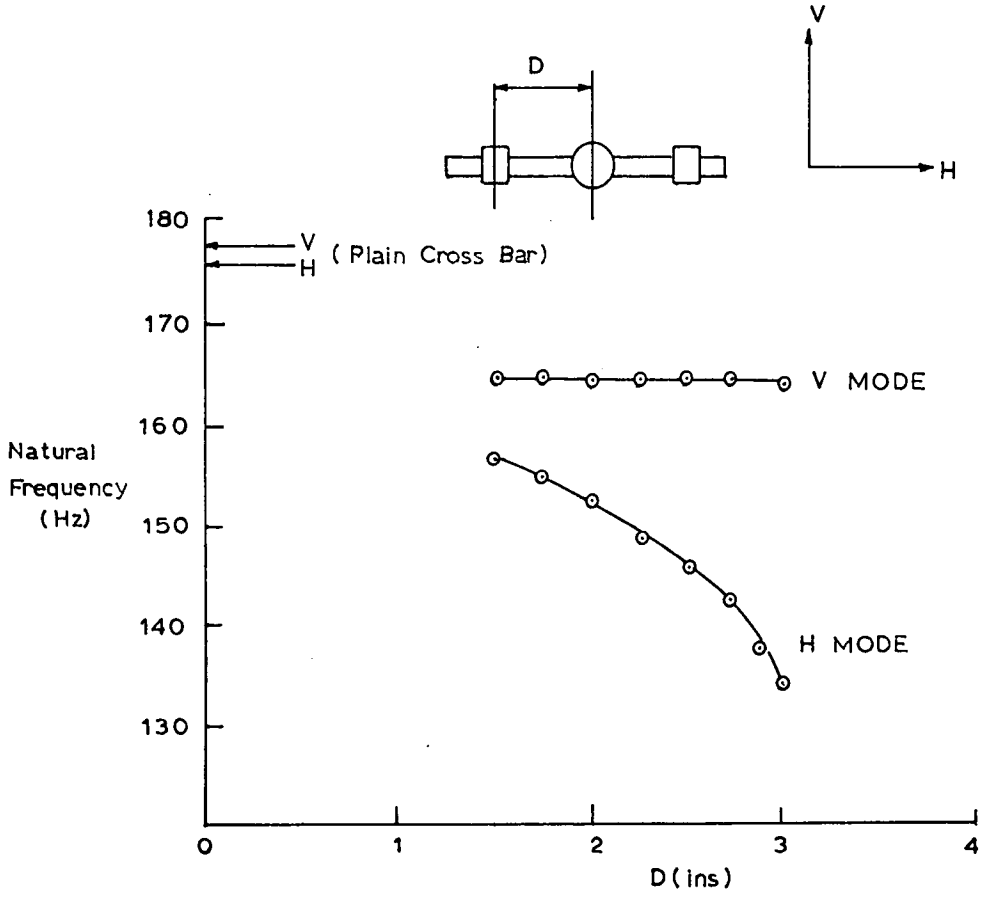

Fig. 4.3.1

Effect of Tip Weight Spacing on
Natural Frequencies of 2nd. Flexural Mode.

Weight of Cross Bar = 0.571bs.
Jockey Weights (each) = 0.491bs.
(Including Lock Nuts)

(a) Uni-modal Response

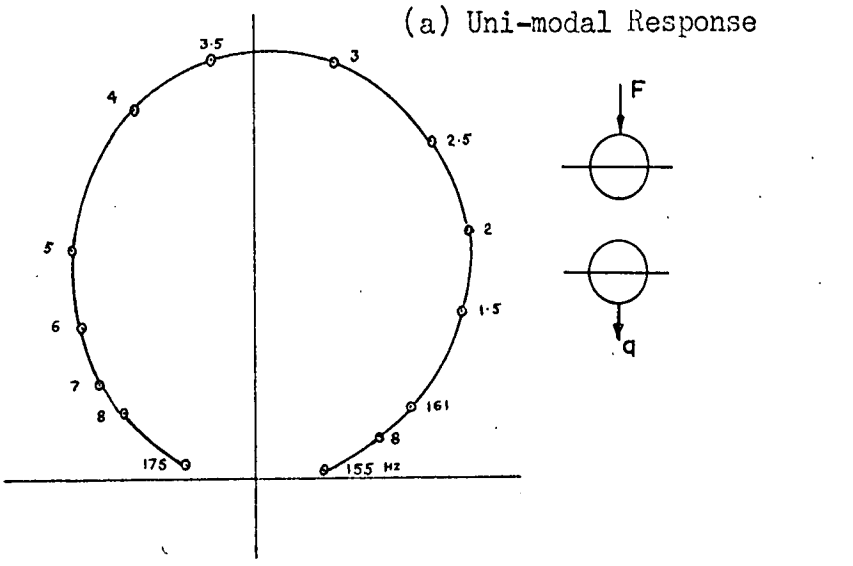

(b) Bi-modal Response

R = 1.24

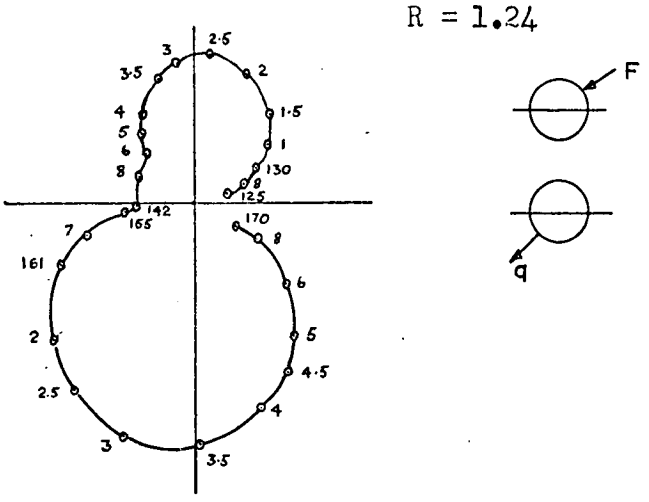

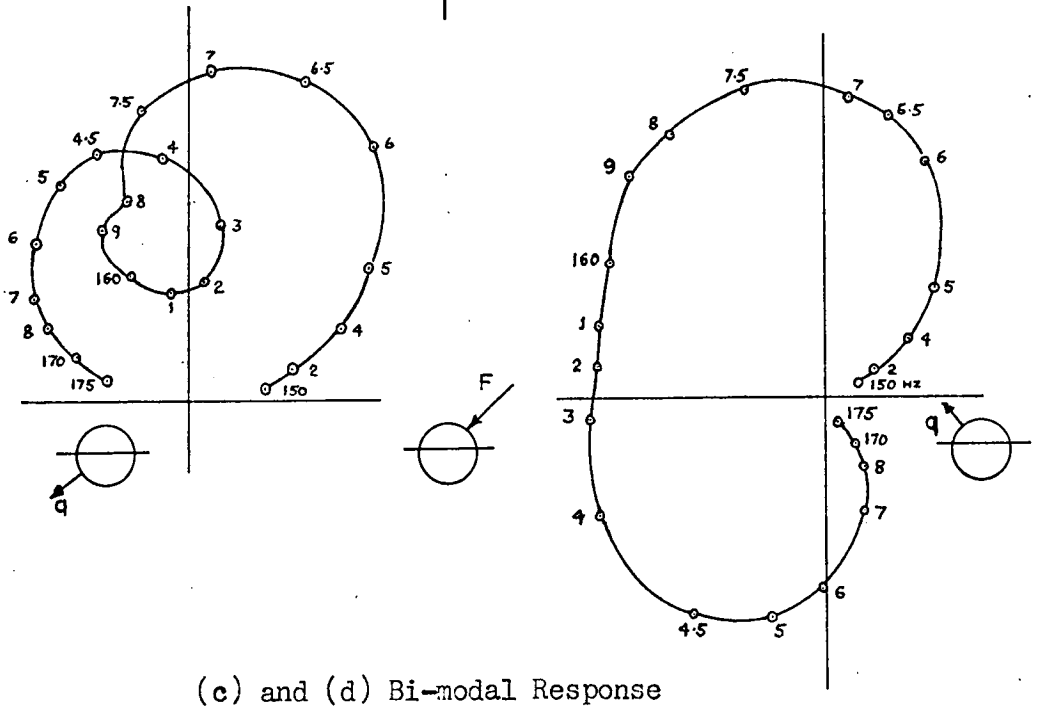

(c) and (d) Bi-modal Response

R= 1.04

Fig. 4.3.2

Receptance Plots of Model Response.

(100mA Vibrator Current.)

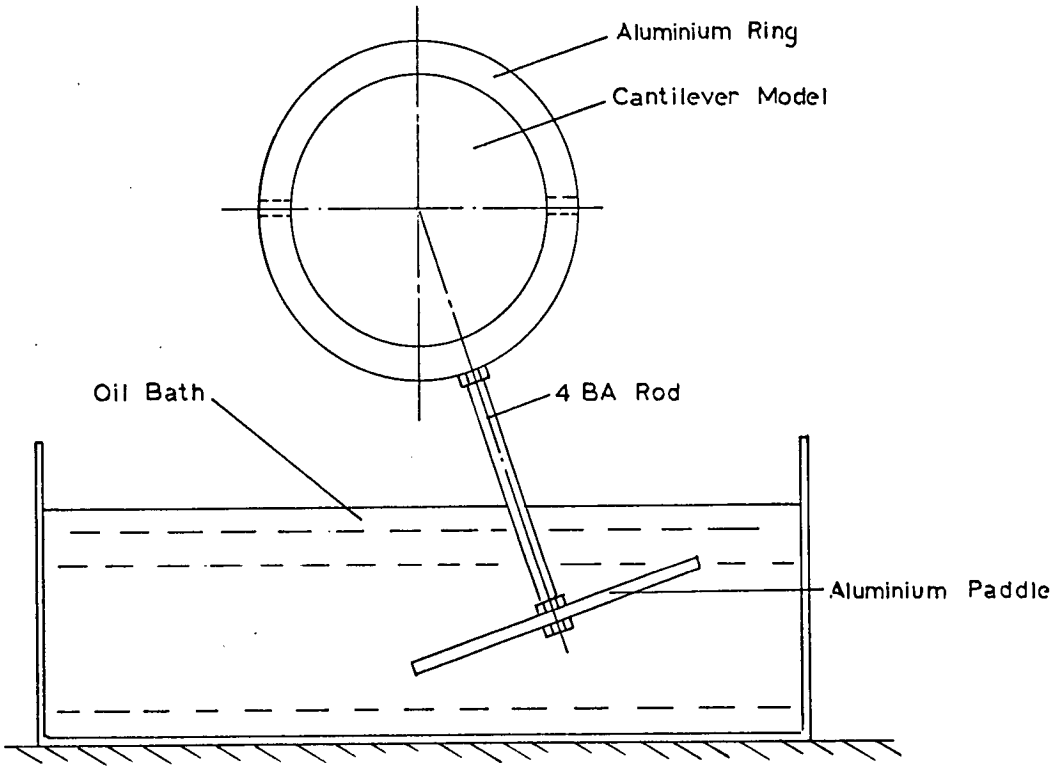

Fig. 4.3.3

Oil Bath Damper.

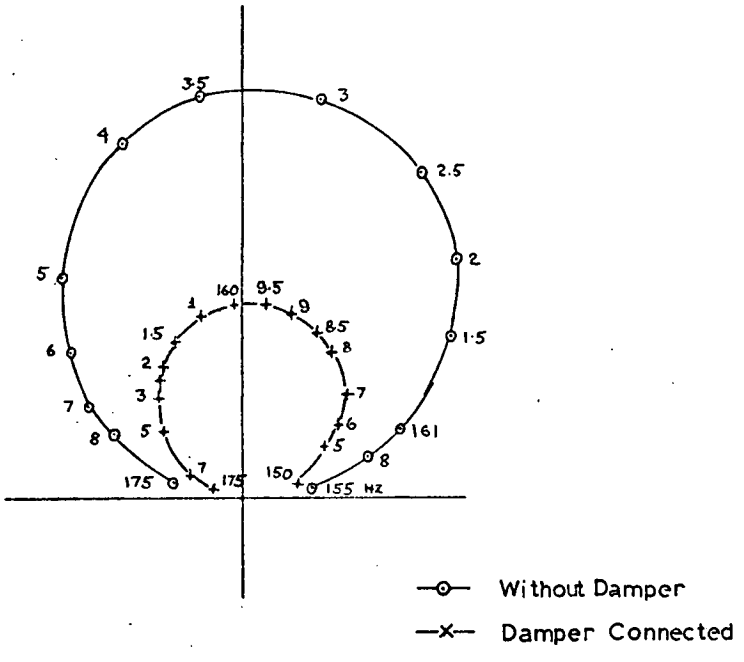

Fig. 4.3.4

Effect of the Damper on The Response of the second V Mode.
(Damper Vertical.)

when the exciter is aligned in the horizontal or vertical plane, and bi-modal response when the exciter is able to excite both modes and the transducer is sensitive to motions in both modes.

The damping factors of the modes were measured using the three decibel bandwidth method, taking care to ensure that in-phase motion of the whole structure was obtained over the band. Values of magnification factor Q of 40 to 45 were obtained. Additional damping was introduced if desired by attaching a rectangular paddle to the end of a piece of 4BA screwed rod. The rod was screwed into a transducer ring and the paddle was immersed in an oil bath. The arrangement is shown in Figure 4.3.3.

Figure 4.3.4 shows the effect of connecting the damper at mid-span on the response of the second flexural vertical mode. There is a small reduction in resonant frequency and the Q factor of the mode was reduced from 42 to 20. The damper could be inclined up to 45° to introduce damping coupling between the modes.

4.4 Harmonic Analogue of the Response of a Structure to Random Forces.

The problems of measuring spectral densities are well known. Such measurements take the form of estimates in the statistical sense and accuracy can only be gauged in terms of a variance or standard error of the estimate. When dealing with vibrations, narrow bandwidths are necessary to resolve accurately the variations in spectral density with frequency, and extremely long records are required to ensure confidence of the estimates. It was envisaged that many such measurements

would be required to demonstrate simulation, so an alternative method was adopted.

For the case of a linear elastic structure excited by N random forces it is shown (a) that a set of N harmonic forces can represent the excitation spectral densities at any frequency and that the response spectral densities at that frequency may be inferred from measurements of the harmonic response, provided that the N random forces are fully coherent at that frequency.

Further, (b) any general N dimensional spectral density matrix may be expressed as a sum of spectral density matrices representing fully coherent processes, so that the harmonic representation may be extended to the general case by superposition.

Recall the expression for the cross spectral density between a pair of co-ordinates q_i and q_j in terms of receptances for a set of random forces $P_L(t)$, $L = 1,2,\ldots N$.

$$S^q_{ij} = \overline{[\alpha_i]}\,[S^P]\,[\alpha_j]' \qquad 4.4.1$$

where $[\alpha_i]$ is the row matrix $[\alpha_{i1}, \alpha_{i2} \ldots \alpha_{iN}]$ of complex receptances and $[S^P] \equiv [S^P_{LM}]$ is the N square spectral density matrix of the forces.

Now let $P_L(t)$, $L = 1,2,\ldots N$ be a set of harmonic forces:

$$P_L(t) = \hat{P}_L \cos(\omega t - \phi_L) \qquad 4.4.2$$

$$= \mathrm{Re}\left\{ \hat{P}_L\, e^{i\omega t}\, e^{-i\phi_L} \right\}$$

or: $P_L(t) = \mathrm{Re}\left\{P_L e^{i\omega t}\right\}$ 4.4.3

with complex amplitude $P_L \equiv \hat{P}_L e^{-i\phi_L}$

Now define the quantity $H^P_{LM} \equiv \hat{P}_L \hat{P}_M \left[\cos(\phi_L - \phi_M) + i \sin(\phi_L - \phi_M)\right]$ 4.4.4

H^P_{LM} may be expressed in terms of the complex representation of the harmonic forces:

$$\begin{aligned} H^P_{LM} &= \mathrm{Re}\left[\hat{P}_L \hat{P}_M e^{i(\phi_L - \phi_M)}\right] + i\, \mathrm{Im}\left[\hat{P}_L \hat{P}_M e^{i(\phi_L - \phi_M)}\right] \\ &= \hat{P}_L \hat{P}_M e^{i(\phi_L - \phi_M)} \\ &= \hat{P}_L e^{i\phi_L} \cdot e^{i\omega t} \cdot \hat{P}_M e^{-i\phi_M} e^{-i\omega t} \\ &= P_L^* P_M \end{aligned} \qquad 4.4.5$$

It follows that the N square matrix $[H^P] \equiv [H^P_{LM}]$ is given by:

$$[H^P] = [P_L^* P_M] \qquad 4.4.6$$

or

$$[H^P] = \overline{[P]}\,[P]' \qquad 4.4.7$$

where $[P]$ is the column matrix of force complex amplitudes.
By inspection of 4.4.5 it follows that $[H^P]$ is Hermitian. Further it is seen from 4.4.6 that $[H^P]$ is positive semi-definite of rank 1, since every minor of $[H^P]$ of order 2 is zero and the diagonal elements are non-negative.

Now let $q_i(t)$, $q_j(t)$ be the responses of any pair of co-ordinates of the system.

Write:
$$q_i(t) = \hat{q}_i \cos(\omega t - \psi_i) \qquad 4.4.8$$

$$= \mathrm{Re}\left\{\hat{q}_i e^{i(\omega t - \psi_i)}\right\}$$

$$= \mathrm{Re}\left\{q_i e^{i\omega t}\right\} \quad \text{with} \quad q_i \equiv \hat{q}_i e^{-i\psi_i}. \qquad 4.4.9$$

Similarly:
$$q_j(t) = \mathrm{Re}\left\{q_j e^{i\omega t}\right\} \quad \text{with} \quad q_j \equiv \hat{q}_j e^{-i\psi_j}. \qquad 4.4.10$$

Now the quantity H^q_{ij} can be defined as :

$$H^q_{ij} \equiv \hat{q}_i \hat{q}_j \cos(\psi_i - \psi_j) + i\, \hat{q}_i \hat{q}_j \sin(\psi_i - \psi_j) \qquad 4.4.11$$

$$= \hat{q}_i \hat{q}_j\, e^{i(\psi_i - \psi_j)}$$

$$= q_i^* q_j \qquad 4.4.12$$

(Note that $H^q_{ii} = \hat{q}_i \hat{q}_i = \hat{q}_i^2$.)

By definition of complex receptance:

$$q_i = \sum_{K=1}^{N} \alpha_{iK} P_K = [\alpha_i][P] \qquad 4.4.13$$

$$q_j = [\alpha_j][P] = [P]'[\alpha_j]' \qquad 4.4.14$$

Hence : $H^q_{ij} = [\overline{\alpha_i}]\,[\overline{P}][P]'[\alpha_j]'$

or: $$H^q_{ij} = [\overline{\alpha_i}][H^P][\alpha_j]' \qquad 4.4.15$$

Comparison of 4.4.1 and 4.4.15 shows that the transformation of $[H^P]$ into H^q_{ij} is identical to the transformation of $[S^P]$ into S^q_{ij} . It follows that if a set of phased harmonic forces can be arranged such that $[H^P]$ as defined in 4.4.4 takes on the same set of values as $[S^P]$ then the cross spectral density of the response S^q_{ij} may be inferred from H^q_{ij} which is derived as in 4.4.11 from measured responses to the harmonic force system. Since $[H^P]$ is of rank one, the harmonic representation is restricted so far to spectral density matrices of rank one. It remains to show for part (a) that any spectral density matrix of rank one can be represented by the form 4.4.6.

Let $[S^P]$ be an arbitrary spectral density matrix of rank $r \leqslant N$.

Then since $[S^P]$ is positive semi-definite Hermitian, it is conjunctive to the canonical matrix: $\begin{bmatrix} I_r & 0 \\ 0 & 0 \end{bmatrix}$; where $[I_r]$ is the identity matrix of order r. 4.4.16

That is, there exists a non-singular matrix $[Q]$ with complex elements such that:

$$[S^p] = \overline{[Q]} \begin{bmatrix} I_r & 0 \\ 0 & 0 \end{bmatrix} [Q]' \qquad 4.4.17$$

Indeed $[S^p]$ is conjunctive to any positive semi-definite Hermitian matrix of order N and rank r, which in turn is conjunctive to 4.4.16. In particular, a non-singular matrix $[T]$ exists with complex elements such that: $[S^p] = \overline{[T]}$ Diag $[g_{11}\ g_{22}..g_{rr},0,0,..0][T]'$ 4.4.18

where g_{11} .. g_{rr} are arbitrary positive elements.

4.4.18 implies that any N dimensional random process having arbitrary correlation between its component processes may be considered to be derived from a set of r statistically independent random processes where r is the rank of the spectral density matrix, by linear filtering. Further, the generating set of independent processes is not unique.

Now let the columns of $[T]$ be: $[T_1]$, $[T_2]$, .. $[T_N]$. Then:

$$[S^p] = [\bar{T}_1\ \bar{T}_2..\bar{T}_N]\ \text{diag}[g_{11}..g_{rr},0\ 0] \begin{bmatrix} T_1' \\ T_2' \\ \vdots \\ T_N' \end{bmatrix} \qquad 4.4.19$$

or:
$$[S^p] = \sum_{k=1}^{r} g_{kk} \overline{[T_k]} [T_k]' \qquad 4.4.20$$

In the case where r = 1 , $[S^p]$ can be expressed as:

$$[S^p] = g_{11} \overline{[T_1]} [T_1]' = \overline{[P_1]} [P_1]' \text{ , say.} \qquad 4.4.21$$

It follows from 4.4.7 and 4.4.21 that in this case a harmonic representation of $[S^p]$ can always be derived. Note that in 4.4.21, $[P_i]$ is determined up to an arbitrary phase angle.

In the general case, $r \leqslant N$, the expansion 4.4.20 shows that $[S^p]$ may be written as a sum of N square matrices and further, each matrix in the sum is of rank 1.

$$[S^p] = \sum_{K=1}^{r} g_{KK}[T_K][T_K]' = \sum_{K=1}^{r} [S_K^p] \quad \text{say,} \qquad 4.4.22$$

where each $[S_K^p]$ is of rank 1.

Introducing this expansion into 4.4.1:

$$S_{ij}^q = [\overline{\alpha_i}][\sum_K^r [S_K^p]][\alpha_j]' = \sum_K^r [\overline{\alpha_i}][S_K^p][\alpha_j]' = \sum_K^r S_{ij(K)}^q \quad \text{say, where } S_{ij(K)}^q = [\overline{\alpha_i}][S_K^p][\alpha_j]' \qquad 4.4.23$$

Relations 4.4.22 and 4.4.23 indicate how the harmonic analogue may be extended to the general case of the spectral density matrix having rank $r \leqslant N$. Each of the component matrices $[S_K^p]$ of the expansion 4.4.22, being of rank one has a harmonic representation $[H_K^p] \equiv [\overline{P_K}][P_K]'$. If each corresponding harmonic force set $[P_K]$ is applied to the structure, the amplitudes and phases of a pair of responses may be used to construct a harmonic representation of a cross spectral density component.

e.g. $q_i = [\alpha_i][P_K]$; $q_j = [\alpha_j][P_K]$.

$$H_{ij(K)}^q = q_i^* q_j = [\overline{\alpha_i}][\overline{P_K}][P_K]'[\alpha_j]' = [\overline{\alpha_i}][H_K^p][\alpha_j]'$$

By applying each force set $[P_k]$ in turn, K = 1,2,...r, and adding the complex harmonic representations $H^q_{ij(k)}$ according to 4.4.23, a final harmonic representation of any response spectral density or cross spectral density may be obtained. The expansion 4.4.22 is not unique and consequently there is a whole set of equivalent harmonic representations of a given spectral density matrix. This concludes the proof of statement (b). In the case of a direct spectral density, the harmonic representation of the kth component response $H^q_{ii(k)}$ is obtained from $(q^*_i\, q_i)_{(k)} \equiv |q_i|^2_{(k)} \equiv \hat{q}^2_{i(k)}$. Consequently the final representation of the response spectral density is a sum of squares of harmonic amplitudes.

In the case of a general 2 x 2 spectral density matrix it is easily seen that many expansions of the type 4.4.22 can be found by inspection.

Given: $$[S^p] \equiv \begin{bmatrix} S^p_{11} & S^p_{12} \\ S^p_{21} & S^p_{22} \end{bmatrix}$$

Write: $$\begin{bmatrix} S^p_{11} & S^p_{12} \\ S^p_{21} & S^p_{22} \end{bmatrix} \equiv \begin{bmatrix} a_{11} & a_{12} \\ a_{21} & a_{22} \end{bmatrix} + \begin{bmatrix} b_{11} & b_{12} \\ b_{21} & b_{22} \end{bmatrix}$$

Now the expansion must satisfy:

$$\left.\begin{aligned} a_{11} + b_{11} = S^p_{11} \;;\quad & Re\{a_{12}\} + Re\{b_{12}\} = Re\{S^p_{12}\} \\ a_{22} + b_{22} = S^p_{22} \;;\quad & Im\{a_{12}\} + Im\{b_{12}\} = Im\{S^p_{12}\} \end{aligned}\right\} \quad 4.4.24$$

and the component matrices must have rank 1:

$$\left.\begin{aligned} |a_{12}|^2 = a_{11}\, a_{22} \quad ;\quad |b_{12}|^2 = b_{11}\, b_{22} \end{aligned}\right\}$$

Eight real numbers must be chosen to satisfy six equations, so the expansion is not unique. For example let $b_{12} = 0$. Then either b_{11}

or b_{22} is zero. Taking the former, the expansion is obtained:

$$[S^p] = \begin{bmatrix} S^p_{11} & S^p_{12} \\ S^p_{21} & S^{p\prime}_{22} \end{bmatrix} + \begin{bmatrix} 0 & 0 \\ 0 & S^{p\prime\prime}_{22} \end{bmatrix} \qquad 4.4.25$$

$S^{p\prime}_{22}$ is chosen so that $S^p_{11} S^{p\prime}_{22} = |S^p_{12}|^2$ and $S^{p\prime\prime}_{22} = S^p_{22} - S^{p\prime}_{22}$.

To apply the harmonic analogue, complex vectors $[P_1]$ and $[P_2]$ are derived such that:

$$[\overline{P_1}][P_1]' \equiv \begin{bmatrix} b^*_{11} \\ b^*_{21} \end{bmatrix} [b_{11}\ b_{21}] = \begin{bmatrix} S^p_{11} & S^p_{12} \\ S^p_{21} & S^{p\prime}_{22} \end{bmatrix}$$

and :

$$[\overline{P_2}][P_2]' \equiv \begin{bmatrix} b^*_{12} \\ b^*_{22} \end{bmatrix} [b_{12}\ b_{22}] = \begin{bmatrix} 0 & 0 \\ 0 & S^{p\prime\prime}_{22} \end{bmatrix} \qquad 4.4.26$$

Since $[P_1]$ and $[P_2]$ are determined up to an arbitrary phase angle, it is convenient to set p_{11} and p_{22} real initially. The values of the elements follow easily from 4.4.26, and these represent the amplitudes of harmonic forces which may be applied in sequence to the structure.

For orders of $[S^p]$ greater that 2 x 2, an expansion of the form 4.4.22 may be found from the eigenvalues and eigenvectors of $[S^p]$:

If $[S^p]$ is of rank $r \leqslant N$ then it has r positive eigenvalues $\lambda_1 \cdots \lambda_r$ and (N - r) zero eigenvalues. A result in the theory of matrices is that $[S^p]$ is unitarily similar to a diagonal matrix :

$$[S^p] = [U]\, \mathrm{diag}[\lambda_1, \lambda_2 \cdots \lambda_N][U]^{-1} \qquad 4.4.27$$

where $[U]$ is a unitary matrix; $[U]^{-1} = [U]^{\dagger}$; whose columns $[U_1] \cdots [U_N]$ are the eigenvectors of $[S^p]$, normalized to have unit length. 4.4.27 is a special case of the conjunctive transformation 4.4.13, in that

the columns of $[U]$ are prescribed to be mutually orthogonal.

Hence:

$$[S^p] = \sum_{k=1}^{r} \lambda_k [U_k] \overline{[U_k]}' = \sum_{k=1}^{r} [S_k^p] \qquad 4.4.28$$

In this case, the expansion 4.4.28 is unique.

Although originally devised as a means of demonstrating simulation of spectral densities, it is considered that the harmonic analogue has application in many experimental aspects of random vibrations. For example the responses of a complex structure to discrete random forces with prescribed spectral densities may be evaluated accurately by experiments based on the analogue, and the method is easily extended to the case of prescribed random support motions of equipment.

4.5 Application of the Harmonic Analogue to Simulation Experiments

It has been stated in the introduction that the most feasible method of testing the validity of the simulation theory was to attempt to replace one set of point forces by another set, using small vibrators. It may be argued that this restricted form of experiment would constitute a valid test of the possibility of simulating more general environments because in chapter 2 it has been shown that any general environment, consisting of distributed or discrete forces with spatial and temporal correlations, generates a set of generalized force spectral densities from which the response of the structure follows. Simulation is therefore concerned with reproducing these generalized force terms without reference to their origin. On this basis, the laboratory tests are essentially equivalent to the more general types of excitation in that

the vibrators are capable of producing a range of generalized force spectral densities in a highly convenient manner.

The harmonic analogue representation of the random forces and responses was used in conjunction with the Hewlett-Packard Two-Phase Oscillator. The two output sections of the oscillator could be used to drive two vibrators simultaneously with a prescribed phase lag between their currents. In this way and by superposition, random forces with a wide range of correlation could be represented. The method required that phase angles of the harmonic response be measured, and since both sections of the oscillator were being used to excite the structure, an alternative method was used. The square wave output of the oscillator was used to drive a Servomex function generator Type LF141 in synchronism and the variable phase output of this instrument was used in conjunction with an oscilloscope display to determine phase angles in the manner described in section 4.2 The arrangement of the instrumentation is shown diagrammatically in Figure 4.5.1. During the tests all vibrators were coupled to the model so that the dynamical characteristics would not be changed. It was felt that vibrator current was a convenient and sufficient guide to the excitation, and that force transducers were not necessary. Consequently receptance measurements were based on force units of 0.100 amps of vibrator current.

Tests were carried out to demonstrate (a) single vibrator simulation (b) two vibrator simulation and (c) the growth of errors in single vibrator simulation, and these are now described.

In the case of single vibrator simulation, the procedure was as follows. Having set up the model to have the required dynamic characteristics, an arrangement of vibrators was chosen to represent the

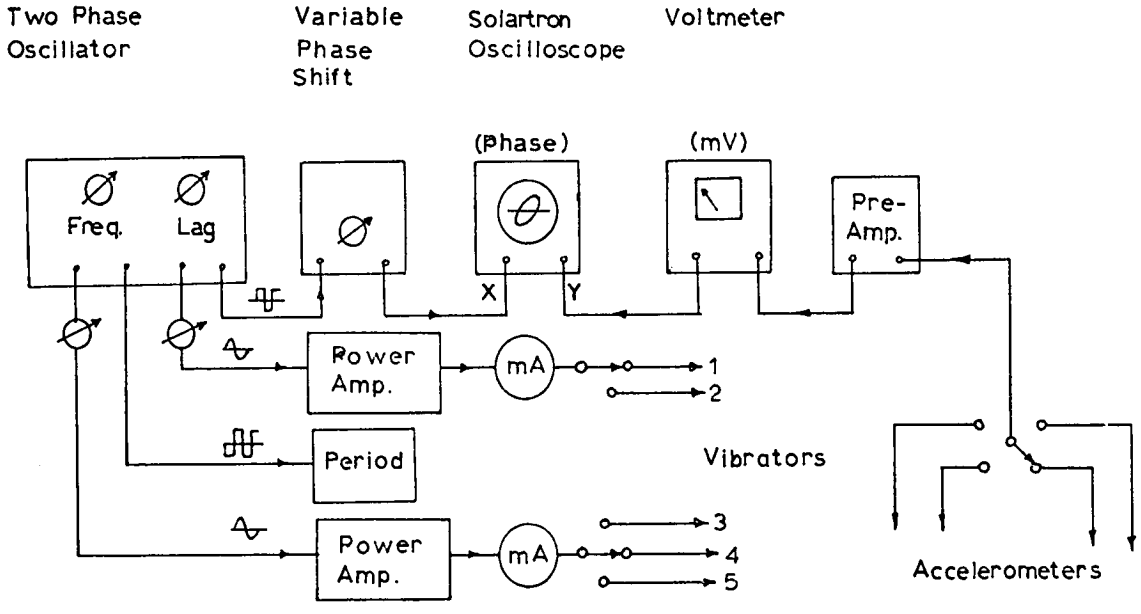

<u>Data Tape</u>

(1) Harmonic amplitudes and phases of 4 accelerometers.
(2) Amplitudes and phase lags of receptances between simulating forces and reference accelerometers.(for 100mA vibrator current)

<u>K.D.F.9 Computer Program.</u>

(1) Compute the equivalent 4×4 spectral density matrix from harmonic responses using 4.4.11.
(2) Compute the complex elements of the receptance matrix.
(3) Invert the receptance matrix.
(4) Compute the required simulating force spectral density matrix from 3.4.9 .
(5) Resolve the force spectral density matrix into the equivalent set of harmonic forces using 4.4.25 and 4.4.26.

<u>Output</u>

(1) Equivalent response spectral densities.
(2) Simulating force spectral densities.
(3) Equivalent harmonic force system. (Vibrator currents and phase lags.)

Fig. 4.5.1

Apparatus and Data Processing Scheme

for Simulation Tests.

the service environment. At least three were used. These were energised in pairs with arbitrary phase angles to represent a fairly general load. For each pair, amplitude and phase data was obtained from four accelerometers. The tests were repeated at a number of frequency points around the resonant frequency intervals. It was convenient to keep the same force amplitudes and phases over the frequency interval.

Simulation of the environment was attempted at each frequency point by choosing a reference accelerometer and energising a further vibrator to reproduce the reference response spectral density. In the context of the harmonic representation, this meant that the mean square of the reference harmonic response was set to be equal to the sum of the mean squares of reference responses to each of the set of harmonic forces representing the service environment. Having done this, the amplitudes and phases of other accelerometers were recorded. The calculations involved in reducing the amplitude and phase data of the accelerometers to the equivalent spectral densities and cross spectral densities were somewhat tedious and an Atlas Autocode program was written to do this. Finally, the accuracy of the simulation was gauged from a comparison of the two sets of spectral densities.

The procedure in the case of two vibrator simulation was to represent the service loading by a system of vibrators as above, but in this case a pair of reference accelerometers were used and two further vibrators were used to simulate the motion. It was necessary to obtain first of all the 2 x 2 spectral density matrix of the required vibrator currents. In general, this matrix would be non-singular. There was no hope of obtaining simulation by a trial and error adjustment of currents and phase because a superposition of two harmonic force sets would be required (see 4.4.25). It was necessary to calculate the

required force spectral density matrix using relation 3.4.9 together with measured receptances between the simulating forces and the reference transducers and then resolve the resulting matrix into a pair of harmonic force sets according to 4.4.26. This was a tedious calculation and in the end was computerized. The final method adopted was to make the service measurements at all frequency points; prepare a data tape from the accelerometer amplitudes and phases and measured receptances, compute (a) the equivalent spectral densities; (b) the spectral density matrix of required simulating forces and (c) the resolution of this matrix into its harmonic force representation. Finally the computed force system was applied to the model and a further data tape prepared from the measured responses to compute the equivalent spectral densities for the simulated case.

4.6 Results of Simulation Tests

The results of five tests are presented to demonstrate one and two vibrator simulation. Details of the locations of the vibrators and accelerometers for these tests are recorded in Appendix I.

Test A

In this test, single vibrator simulation of a system having an isolated resonant peak was investigated. By confining the service and simulating vibrators to the horizontal plane, only motion of the H mode was produced. The transducers were not confined to the horizontal plane. The results are given in Fig. 4.6.1. The encircled points represent the service reponse while the crosses represent the simulated response. S44 (Fig. 4.6.1(d)) is the reference response.

The other responses show excellent agreement between service and simulated responses with the exception of S33, (c), which shows a small error. This is due to the relative largeness of the non-resonant response at the tip of the cantilever. In (e) and (f) C14 and C23 are the real parts of the cross spectral densities, and show good agreement. The imaginary parts are not shown, being virtually zero throughout.

Test B

In this test single vibrator simulation of a system having a pair of reasonably well separated resonant frequencies was investigated. The system was set up with a tip inertia to produce a frequency ratio f_V/f_H of 1.23. The service forces were not confined to any plane. The accelerometers were positioned so that (1) and (2) had large responses in both modes but with phase differences. (3) and (4) were positioned so as to be nearly unimodal. The simulating force was positioned to produce good response in both modes and accelerometer (1) was used as reference. The results are shown in Fig. 4.6.2. The reference response spectral density S11 clearly shows the two peaks. It is clear from the other responses that fairly accurate simulation is obtained in the neighbourhood of the resonant peaks. Although the imaginary part of the cross spectral density, Q12, (e), shows some disparity, it is drawn to a large scale compared with C12. The outstanding feature is the large discrepancy which appears at frequencies between the resonant frequencies. S22, (b), shows the effect as an additional peak in the spectral density at 148 Hz and there is evidence of similar distortions in all the other responses. This is due to an anti-resonance effect in the receptance between the simulating vibrator and the reference transducer. This is shown in the plot of Fig. 4.6.3 in which the receptance reaches a minimum at about 148 Hz. The receptance between the simulating vibrator and accelerometer (2) is also drawn and shows

no such strong anti-resonance. At 148 Hz this receptance is almost seven times the value of the reference receptance so that for excitation by the single random force, the response spectral density S22 will be 49 times S11. It is clear therefore why the peak arises. This is an interesting result. It had previously been assumed that large errors might occur at frequencies away from resonant frequencies because of the breakingdown of the uni-modal assumption, but it was assumed that the absolute values of spectral density produced would still be insignificiant compared with values in the resonant frequency region. The experiment shows that such errors can cause serious distortions of spectral densities. The effect can be minimised by judicious choice of reference response. For example if accelerometer (2) had been used as reference, the simulated response of S11 would have been 49 times less than the simulated response S22, and this would have represented an acceptable error in S11. The anti-resonant effect was noticeable during the test, because the vibrator current required to maintain a fairly low response at accelerometer (1) increased substantially in the frequency interval around 148 Hz.

Test C

In test C, single vibrator simulation was attempted on a model having close natural frequencies, with a frequency ratio f_V/f_H of 1.05. This was obtained by clamping the jockey weights at the innermost position on the cross bar. The service loading was identical to that for test B and accelerometer (1) was used as reference. The results are shown in Figure 4.6.4. All the responses show large errors between service and simulated values, particularly at frequencies between the resonant frequencies. Single vibrator simulation is clearly not accurate for such a system.

Test D

In test D the system and service loading were identical to that of test C, but in this case two additional vibrators were used to simulate the motions of two reference accelerometers. The simulating vibrators were inclined at 45° to the horizontal plane and on opposite sides of the model, so that each vibrator could excite responses in both H and V modes. The reference accelerometers were similarly positioned, being sensitive to both modes, but with phase differences. In the context of the simulation theory, the relevant modal influence coefficient matrices were far from singular. The other two accelerometers were mounted at different axial planes in the horizontal and vertical directions respectively. The required currents and phase angles for the simulating vibrators were obtained from the computer program and since this involved a time delay, a minor difficulty was found in reproducing the reference responses because of small changes in the receptances of the structure. It was found that receptances measured on two successive days did not correspond exactly so that when computed solutions were applied to the model, the reference spectral densities were not exactly reproduced. The errors involved were fairly small. The results of the test are shown in Figure 4.6.5 and show very good agreement between service and simulated cases for all direct and cross responses.

Test E

In this test one and two vibrator simulation was attempted on a model having very close natural frequencies with damping coupling between the modes. The cantilever was used with a plain cross bar to obtain a frequency ratio of 1.005. After checking the natural frequencies and mode shape components at the accelerometers, the dashpot was attached at an angle of 45° to the vertical to obtain damping coupling. The simulating vibrators were again inclined at 45° to the horizontal on

either side of the model. Only one was used to try single vibrator simulation. The two reference accelerometers were in the same positions as for test D. The results are shown in Figure 4.6.6. Circles indicate the service response points, crosses indicate the two vibrator simulation response and squares indicate the single vibrator response using accelerometer (1) as reference. It is seen that the single vibrator approach produces gross errors in the responses, while the two vibrator approach reproduces all the responses extremely well. Small errors are a consequence of the fluctuations in the measured receptances mentioned above.

These tests are representative of the tests carried out on the model and it is considered that they verify the theory of simulation. Further tests were carried out at particular frequencies to verify the effects of having poorly conditioned reference locations in two vibrator simulation. This is achieved by having the reference accelerometers almost parallel and at close axial positions on the model. The effect was that the solutions for the simulating vibrator currents obtained from the computer were too large to be applied and the situation was made worse by adjusting the simulating force positions to be almost parallel.

Finally a range of tests were carried out to determine experimentally the effects of different correlations between generalized forces in the service loads on the errors produced by single vibrator simulation. Using the theory of section 3.7 it was possible to make theoretical predictions of the limits of the ratio $S^q_{ii(x)}/ S^q_{ii(r)}$ for the whole range of possible correlations between the generalized forces in the service case. These predictions were for a particular

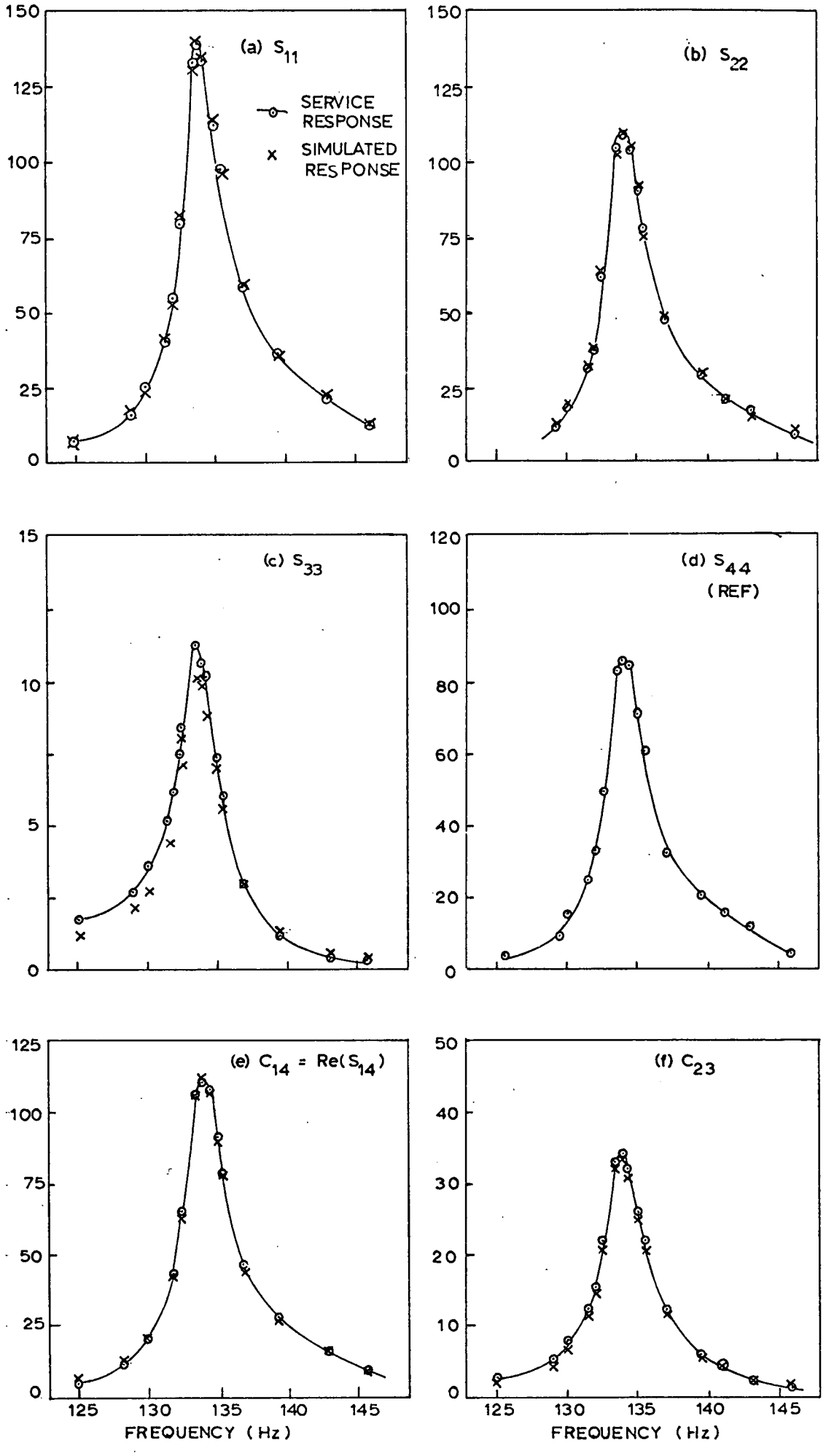

Fig. 4.6.1

Test A: Single Vibrator Simulation

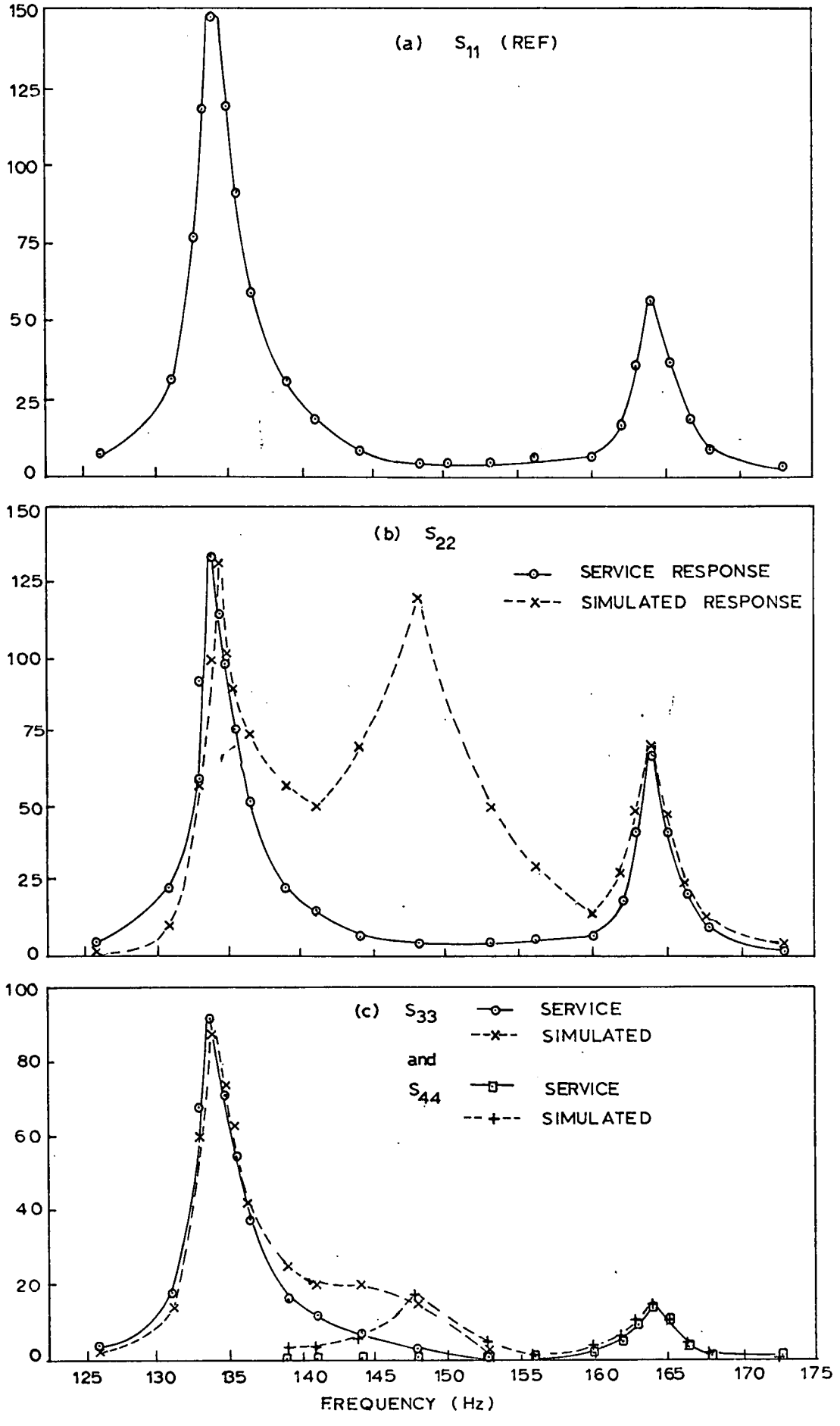

Fig. 4.6.2

Test B: Single Vibrator Simulation

Frequency Ratio of Adjacent Modes = 1.23

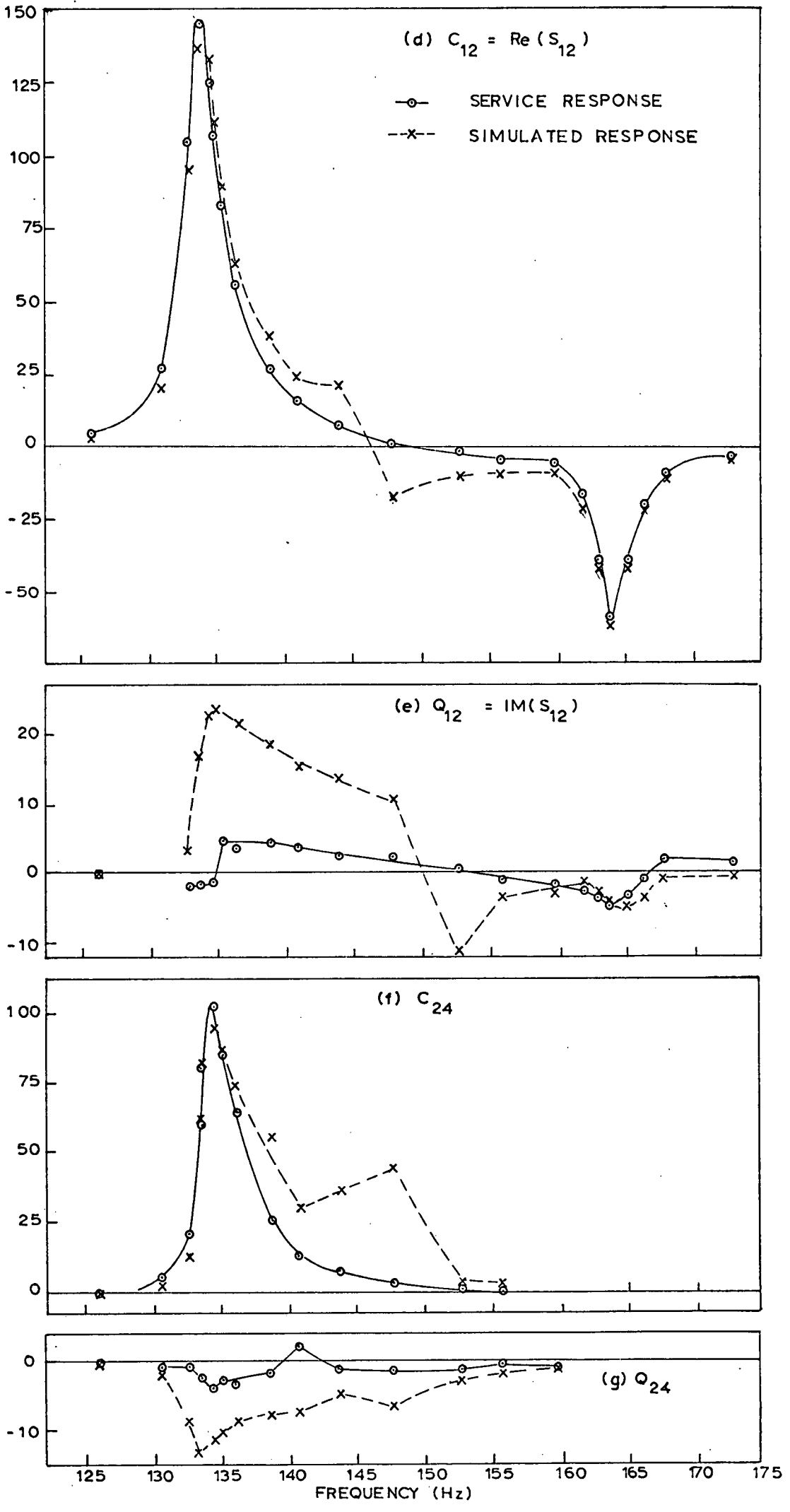

Fig. 4.6.2 (Continued)

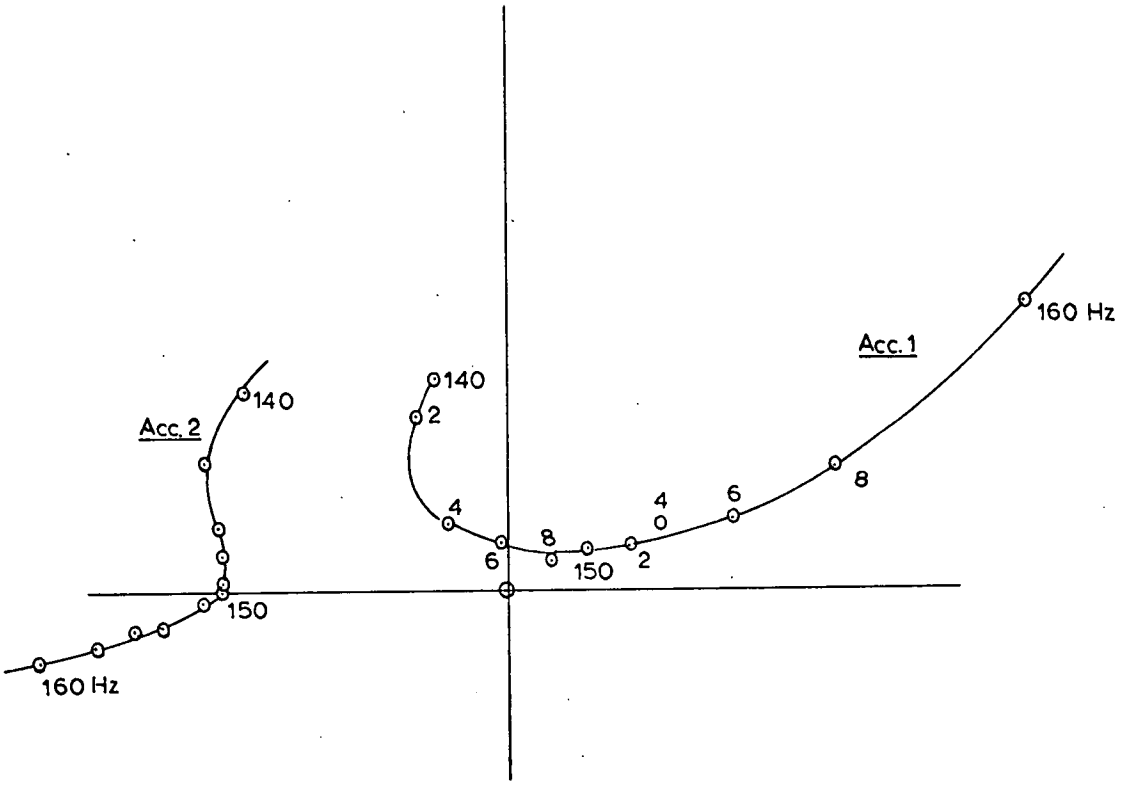

Fig. 4.6.3

Test B: Receptance Plots between Accelerometers (1) and (2) and the Simulating Force, showing Anti-resonance Effect at 148Hz.

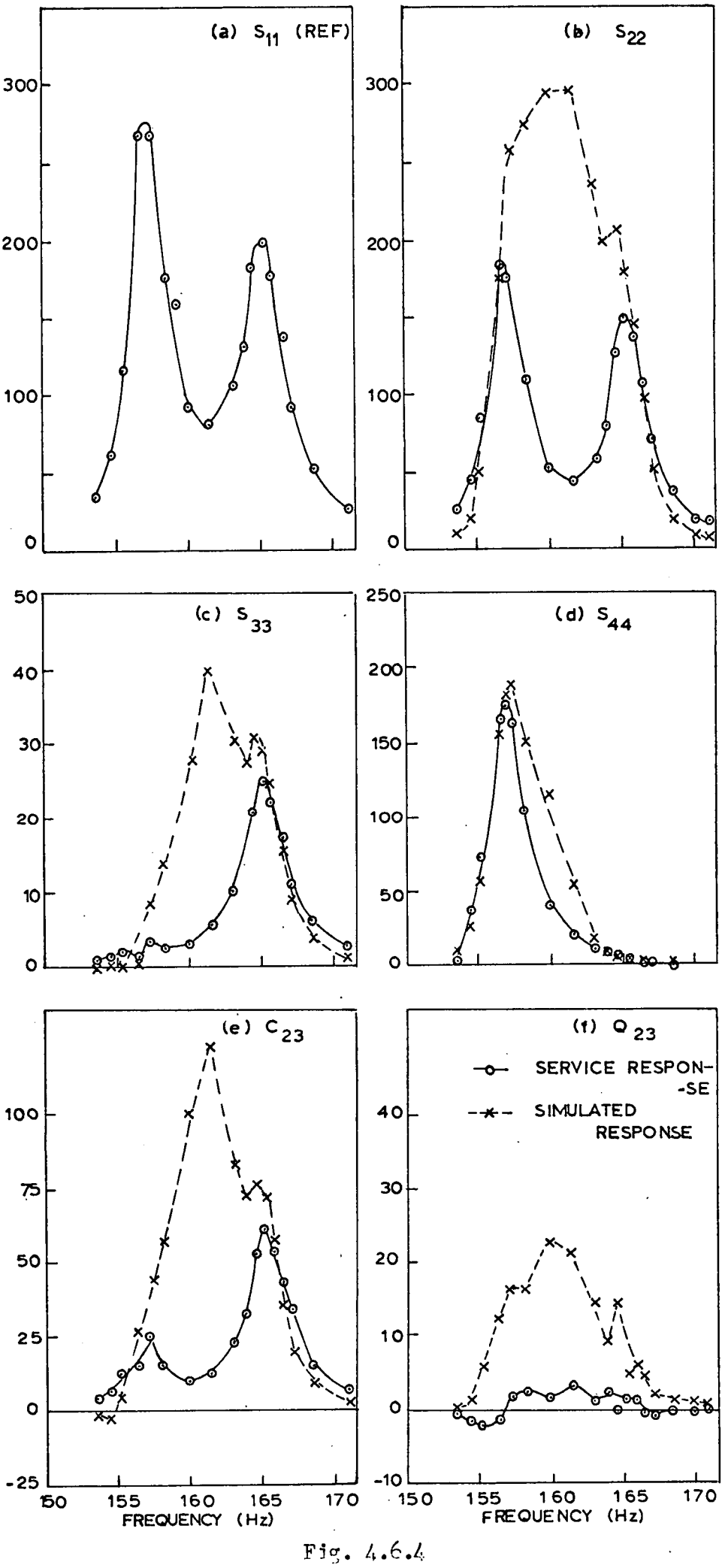

Fig. 4.6.4

Test C; Single Vibrator Simulation.
Frequency Ratio of Adjacent Modes = 1.05

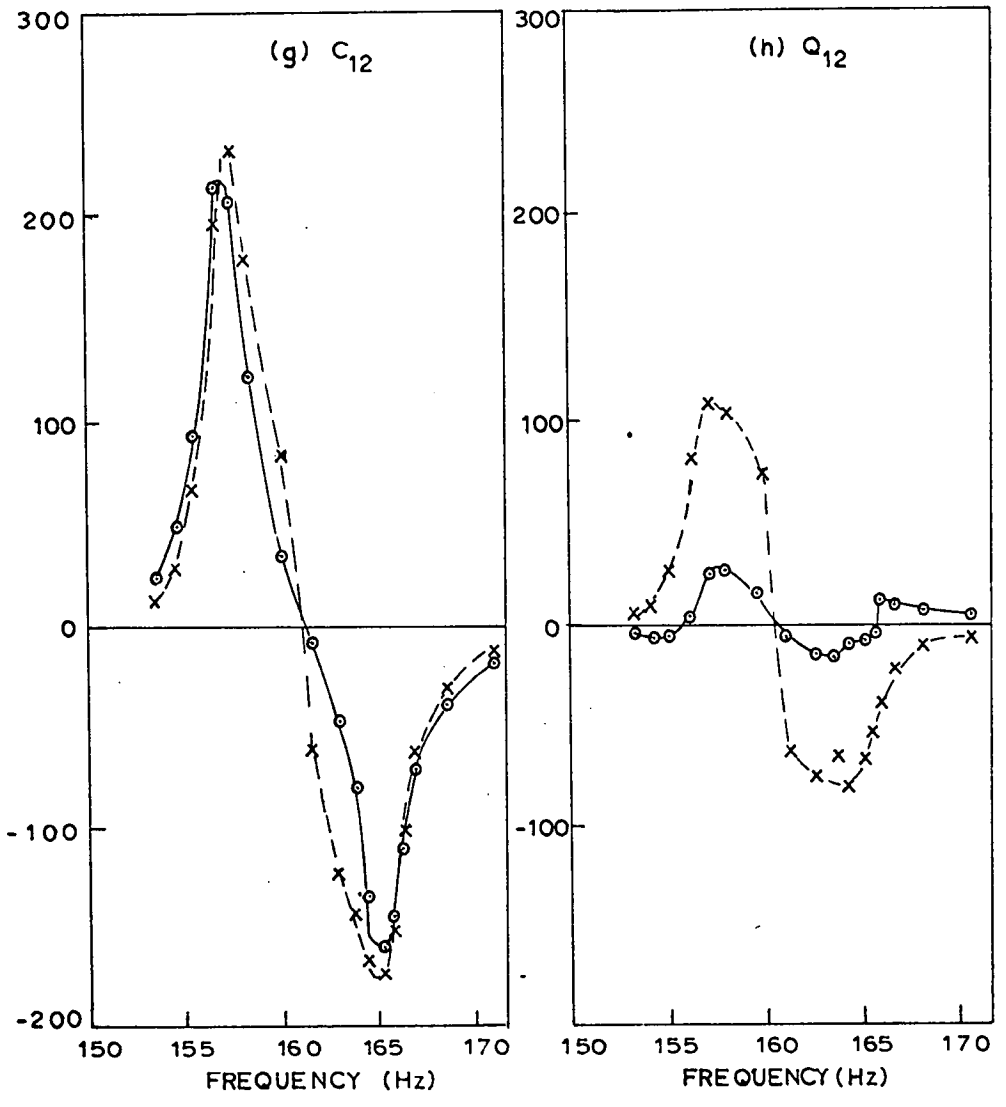

Fig. 4.6.4 (Continued)

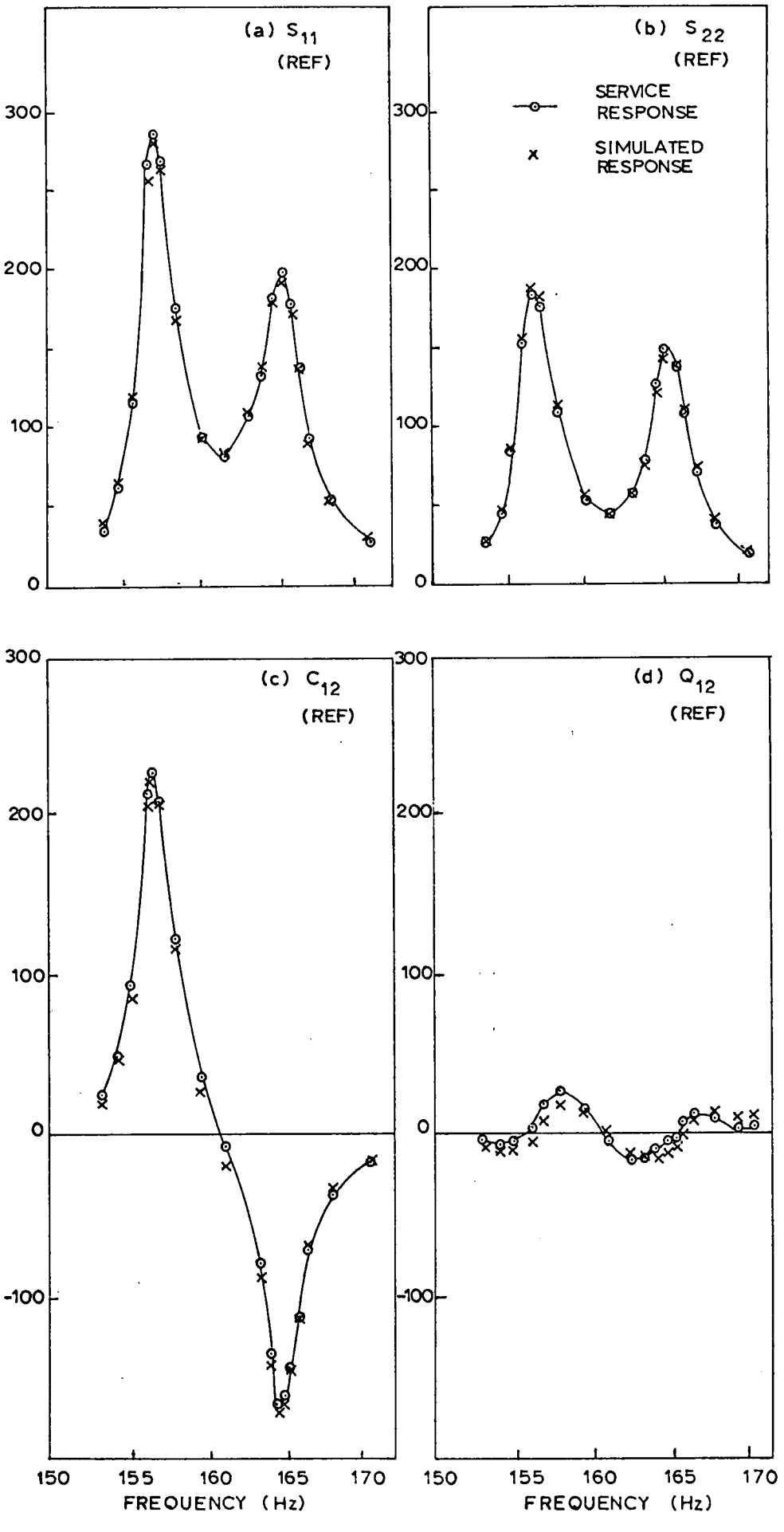

Fig. 4.6.5

Test D: Two Vibrator Simulation

Frequency Ratio of Adjacent Modes = 1.05

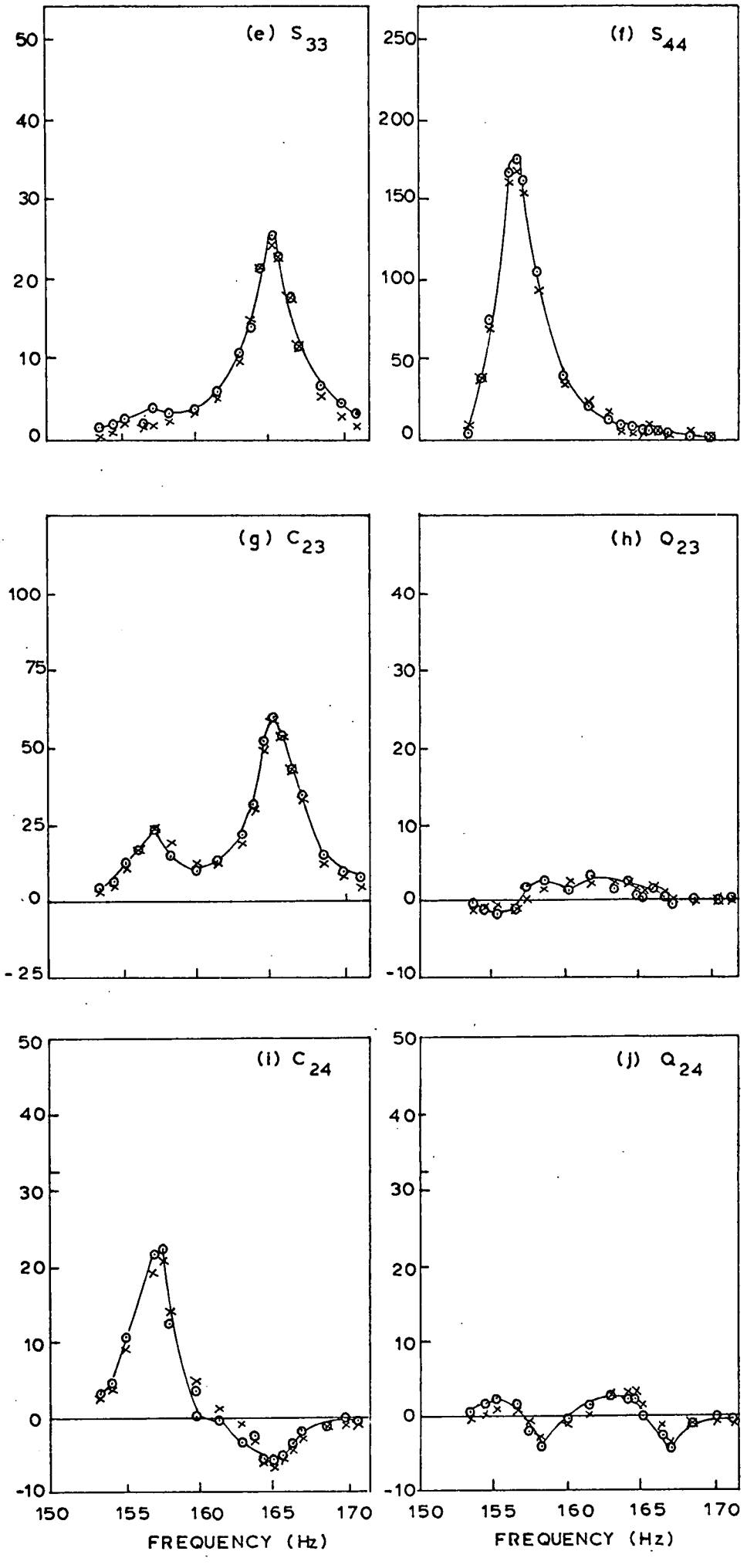

Fig. 4.6.5 (Continued)

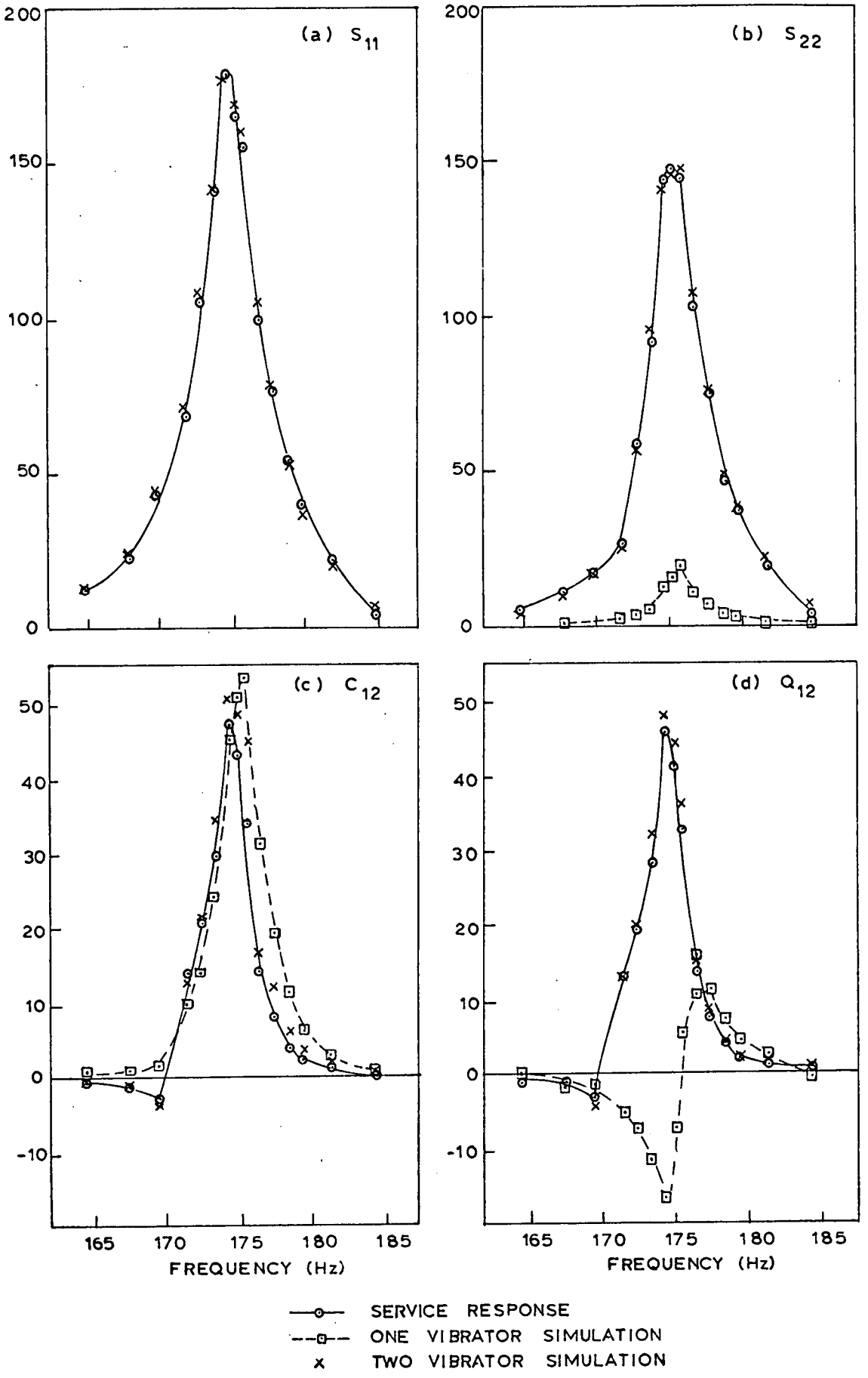

Fig. 4.6.6

Test E: One and Two Vibrator Simulation.
Frequency Ratio of Adjacent Modes = 1.005.

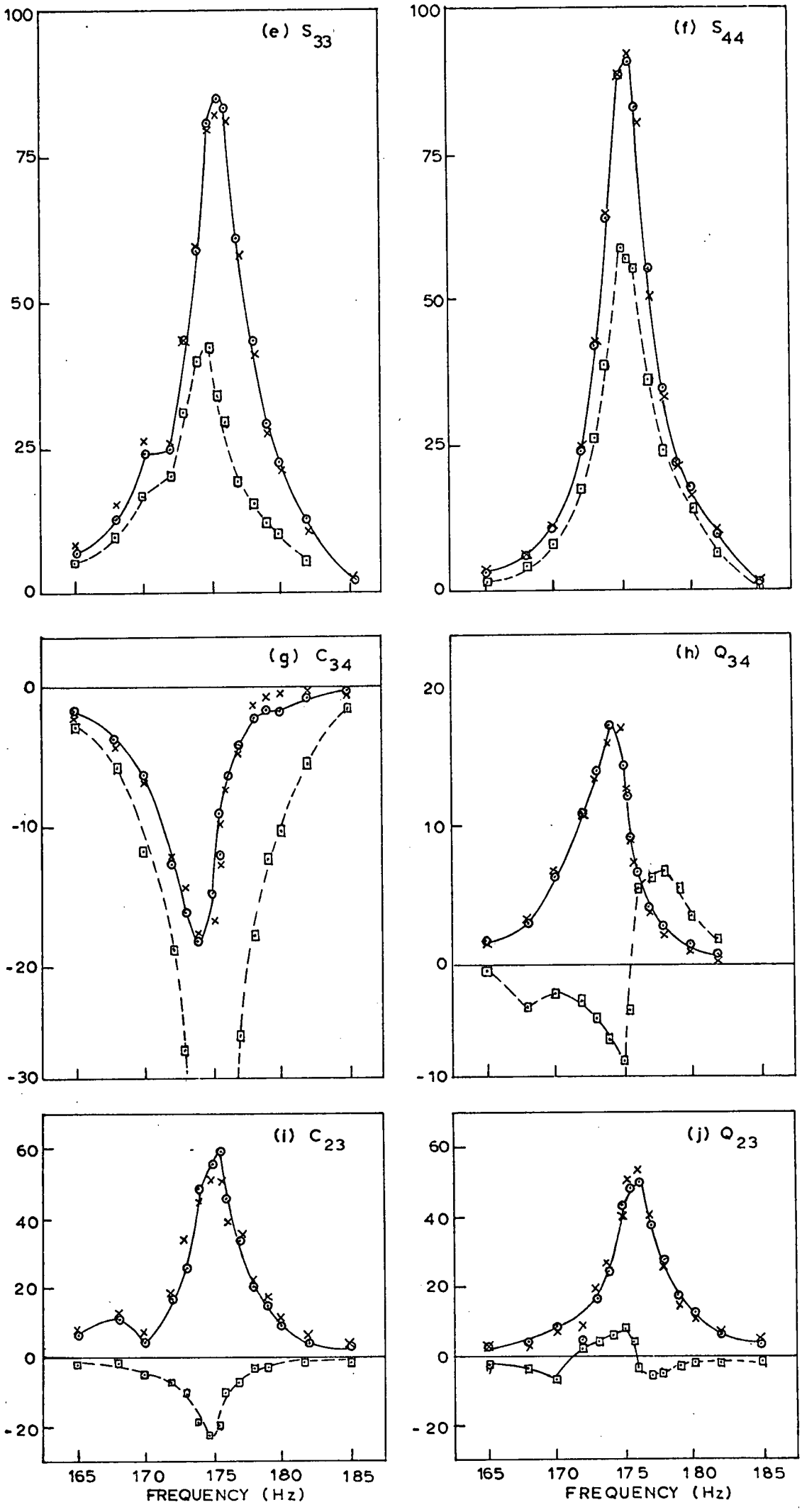

Fig. 4.6.6 (Continued)

ratio of generalized force spectral densities in the service case, denoted $\gamma = S^{z}_{ss}/S^{z}_{rr}$ and for specific locations of the simulating force, reference transducer and sample response. The theoretical limits were obtained for different values of the resonant frequency ratio R, and were evaluated at the single frequency ω_r, for ω_s above and below ω_r. The ratio of the generalized masses of the two modes was required for accurate prediction of these limits. This was obtained experimentally by the method of displaced frequencies. A small amount of mass (plasticine) was added to the model at the reference section, (12 inches from the clamp) where the mode shapes of the H and V modes were considered to have unit radial amplitude. The change in natural frequency or period caused by this was obtained accurately for each mode and the ratio of generalized masses found from the measurements. Let ω_r, ω_s be the unperturbed natural frequencies.

Then $\omega_r^2 = \frac{K_r}{M_r}$; with K_r and M_r generalized stiffness and mass. For a small change in generalized mass δM_r :

$$\delta\omega_r = \frac{-\omega_r \delta M_r}{2 M_r}$$

Since δM_r is caused by the addition of a small mass m at x_m

$$\delta M_r = \phi_r^2(x_m).\, m = m .$$

Taking the ratio of changes in the rth and sth frequencies:

$$\frac{M_s}{M_r} = \frac{\omega_s \delta\omega_r}{\omega_r \delta\omega_s} \qquad 4.6.1$$

It was found that changing the position of the jockey weights on the cross bar altered the generalized mass ratio appreciably and this is shown in Fig. 4.6.7.

The theoretical limits for the ratio $S^{q}_{ii(x)}/ S^{q}_{ii(x)}$ are shown in Fig. 4.6.8. The curves are drawn for the case where all mode shape components at the various locations have the same amplitude and

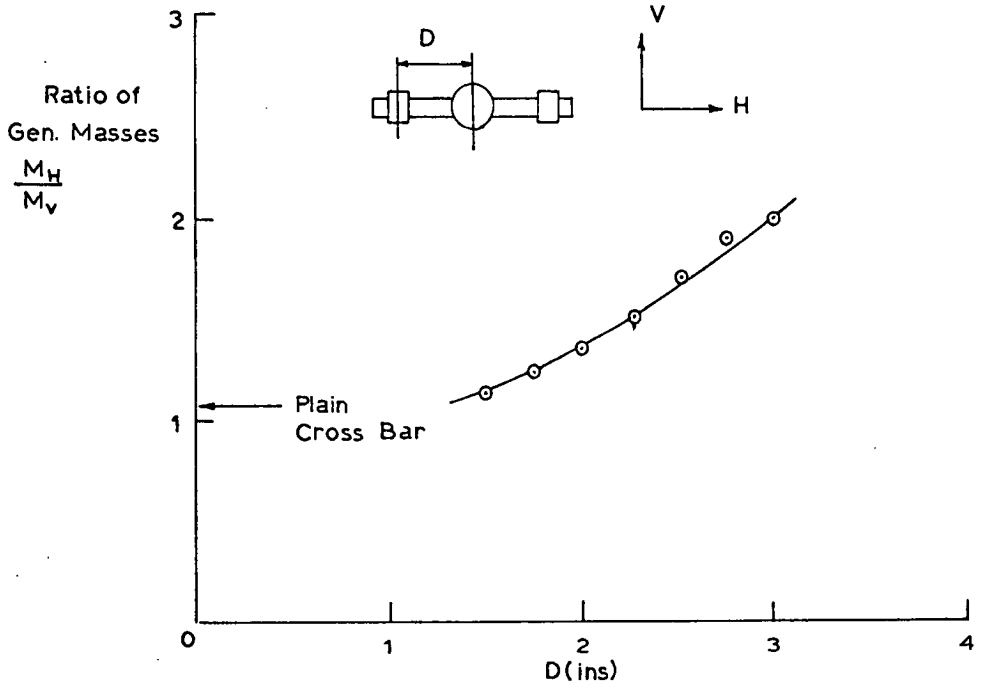

Fig, 4.6.7

Measured Ratio of Generalized Masses
of Second Flexural Modes.

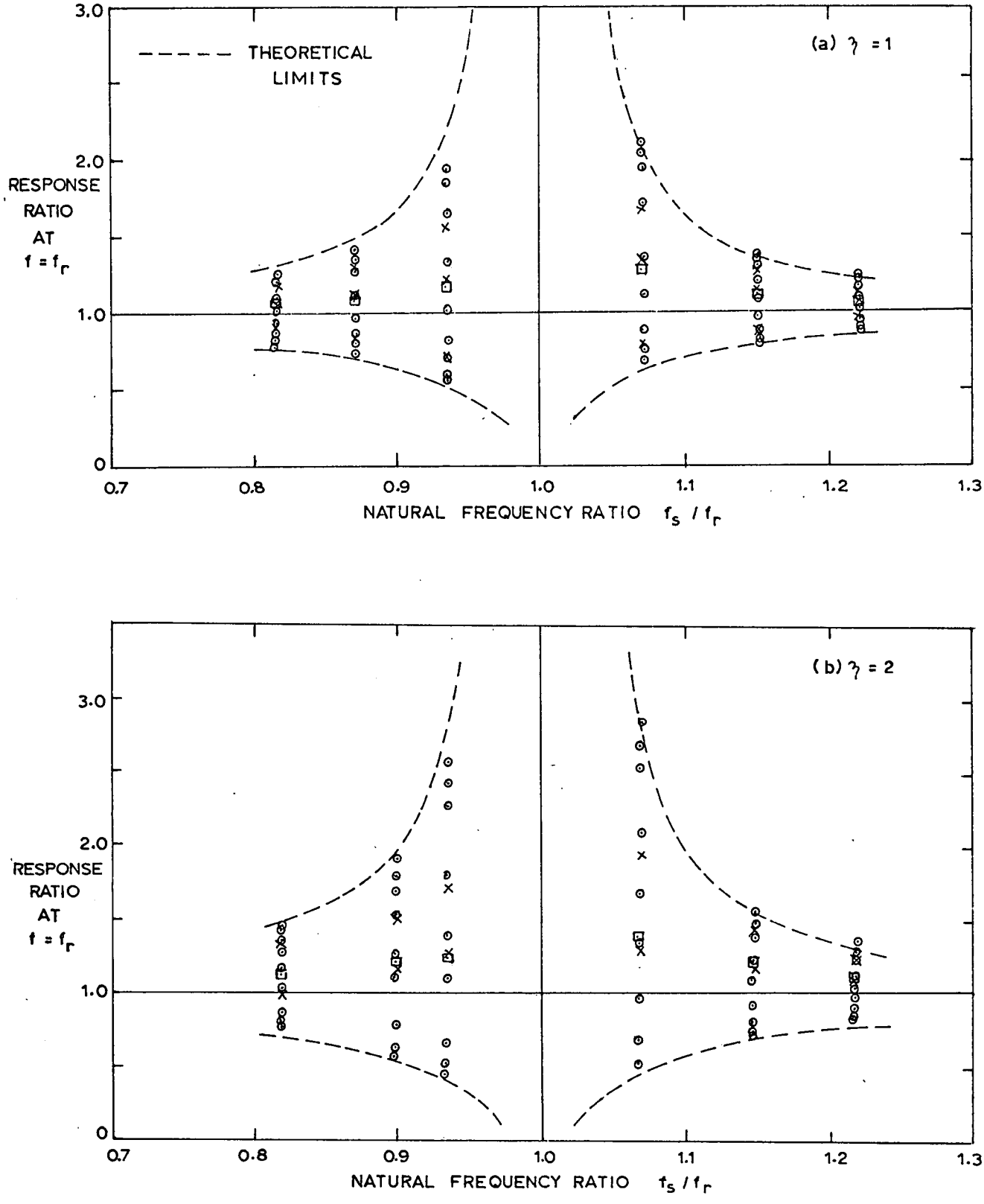

Fig. 4.6.8

Single Vibrator, Single Reference Simulation. Experimental results for the ratio of simulated to service response spectral density, measured at f_r, for a range of correlations between the generalized forces in the r^{th} and s^{th} modes.

unfavourable phasing. Two cases are shown, corresponding to $\gamma = 1$ and 2. Experimental results were obtained for a range of values of resonant frequency ratio and covering a wide range of correlations using the harmonic analogue. Careful scaling was necessary to obtain the requisite value of γ. The results are plotted with circles to show fully coherent cases, $|S^{z}_{rs}|^2 = S^{z}_{rr} . S^{z}_{ss}$, and crosses to show intermediate correlations, while squares indicate the uncorrelated case $S^{z}_{rs} = 0$. To achieve these service cases, a horizontal and a vertical vibrator were used to excite the H and V modes independently. In Figure 4.6.8 the existence of the limits is confirmed and the growth of the range of possible errors in the ratio $S^{q}_{ii(II)} / S^{q}_{ii(I)}$ as the frequency ratio approaches 1 is fairly accurately confirmed.

4.7 Conclusions

An experimental investigation of one and two vibrator simulation has been carried out using a harmonic analogue method. The results show that single vibrator simulation using a single reference response can give an accurate result over frequency intervals of approximately uni-modal response, but can lead to large errors if two natural frequencies are close together. Over such frequency intervals, a two vibrator simulation, using two reference responses can achieve satisfactory simulation. The single vibrator simulation experiments have also shown that large errors can occur at frequencies between resonant peaks because of anti-resonance effects. Such effects are characterized by sharp minima in the receptance between the simulating force and the reference response, with a corresponding increase in the force required to maintain the reference spectral density. This is only to be expected since the uni-modal representation is no longer valid at such frequencies. There is

some danger that such errors could occur in practical applications of single vibrator simulation, even although accurate simulation of the resonant peaks is obtained. A simple remedy is to take due notice of such receptance minima, and avoid compensating the vibrator force for them. Strictly simulation errors will still occur, but they will not be in the form of undesirable large peaks, comparable with resonant peaks.

CHAPTER 5

SIMULATION BASED ON BROAD BAND SPECTRAL DENSITIES

5.1 Introduction

The discussion of simulation in chapters 3 and 4 has been based on the concept of spectral densities as continuous functions of frequency, and simulation has implied a point by point matching of spectral densities. This means in practice that the bandwidth of spectral density estimates must be chosen to be small enough to resolve accurately the fluctuations of response spectral density, and this entails bandwidths of the order of $\frac{1}{4}$ of the 3db bandwidth of the resonant peaks. Such small bandwidths make long sample records necessary and require a massive amount of data processing. The associated problem of adjusting force levels in correspondingly narrow contiguous bands seems likely to cause practical difficulties. There is therefore some interest in seeking simplifications of the procedure.

A major simplification is possible over frequency intervals containing a single resonant peak, i.e. where a single degree of freedom representation is valid, provided that the service excitation is such that the generalized force spectral density of the resonant mode is a relatively smooth function compared with the fluctuations of the modal receptance. In this case, a single value of average response spectral density for the frequency interval may be used as a reference for simulation, and its reproduction ensures an accurate reproduction of the actual narrow band spectral densities and cross spectral densities of the whole structure over the frequency band. This is the main result of the chapter. The result is not valid if there is more than one resonant frequency within the band. In this case simulation using an arrangement of forces with a multiplicity of reference responses is possible in theory and this is discussed briefly. Finally some experimental results are reported.

5.2 Simulation using a Single Broad-Band Reference Response

Consider a frequency interval B containing a single resonant frequency, ω_r . B is considered to be much wider than the bandwidth of the resonant peak associated with the mode. For the case of low damping, the assumption is made that any significant response at any frequency within B is caused by the resonant mode, so that a single degree of freedom approximation may be used to represent the cross spectral density between any pair of response co-ordinates q_i , q_j :

$$S^q_{ij} = C^*_{ri} C_{rj} S^f_{rr} = C^*_{ri} C_{rj} \alpha^*_r \alpha_r S^z_{rr} \qquad 5.2.1$$

In 5.2.1, C_{ri} is the previously defined influence coefficient, and α_r , α_s are modal receptances. The assumption is made that $S^z_{rr}(\omega)$ is a smooth function of frequency within the interval B.

The direct spectral density of a reference response co-ordinate is similarly obtained:

$$S^q_{aa} = |C_{ra}|^2 |\alpha_r|^2 S^z_{rr} \qquad 5.2.2$$

Introduce the broad band average spectral density of the reference response:

$$\langle S^q_{aa} \rangle \equiv \frac{1}{B} \int_B S^q_{aa} \, d\omega \qquad 5.2.3$$

This is essentially the spectral density measured using an ideal rectangular filter of band width B.

From 5.2.2 :

$$\langle S^q_{aa} \rangle = \frac{1}{B} \int_B |C_{ra}|^2 |\alpha_r|^2 S^z_{rr} \, d\omega$$

$$= \frac{S^z_{rr}}{B} \int_B |C_{ra}|^2 |\alpha_r|^2 \, d\omega \qquad 5.2.4$$

In 5.2.4 C_{ra} may be frequency dependent, if for example q_a is a velocity or an acceleration. But for low modal damping, α_r is

in the form of a function having a single prominent peak at ω_+

In 5.2.4 $|\alpha_+|^2$ will act in the nature of an impulse function, so that $|C_{+a}(\omega_+)|^2$ can be taken outside the integral. Further, since the area under the curve of $|\alpha_+|^2$ is concentrated near ω_+, integration of $|\alpha_+|^2$ over the interval B can be conveniently replaced by integration over the semi-infinite interval provided B is much greater than the 3db bandwidth of $|\alpha_+|$. This integral has a simple closed form for the case where α_+ has the representation:

$$\alpha_+(\omega) = \frac{1}{M_+ \left[\omega_+^2 - \omega^2 + i2\delta_+\omega_+\omega\right]}$$

That is, $$\int_B |\alpha_+|^2 d\omega \doteq \int_0^\infty |\alpha_+|^2 d\omega = I_{++} \qquad 5.2.5$$

where: $$I_{++} = \frac{\pi}{4M_+^2\omega_+^3\delta_+}$$

5.2.4 becomes:

$$\langle S^q_{aa}\rangle = \frac{S^z_{++}}{B} |C_{+a}(\omega_+)|^2 \int_B |\alpha_+|^2 d\omega$$

$$= \frac{S^z_{++}}{B} |C_{+a}(\omega_+)|^2 I_{++} \qquad 5.2.6$$

In 5.2.6, I_{++} is always positive, and provided that $C_{+a} \neq 0$, then 5.2.6 has a unique inverse. If $\langle S^q_{aa}\rangle_{II} = \langle S^q_{aa}\rangle_I$, then $S^z_{++(II)} = S^z_{++(I)}$, and by 5.2.1, narrow band simulation will be obtained for any q_i, q_j.

$$S^q_{ij}(\omega)_{II} = S^q_{ij}(\omega)_I \quad ; \omega \in B. \qquad 5.2.7$$

A single vibrator, having an adjustable spectral density S^p_{KK} (constant over B) may be used to reproduce the broad band spectral density at the reference transducer.

For such an excitation:

$$S^q_{aa} = |\alpha_{aK}|^2 S^p_{KK}$$

Hence: $$\langle S^q_{aa}\rangle = \frac{S^p_{KK}}{B} \int_B |\alpha_{aK}|^2 d\omega \qquad 5.2.8$$

In 5.2.8, the integral is non negative. Provided the force causes some generalized force in the rth mode, then a value of S^{p}_{KK} can be obtained which will reproduce a prescribed value of $\langle S^{q}_{aa} \rangle$ and this force will achieve narrow band spectral density simulation of the whole structure.

While this result has a highly approximate basis, namely the assumption of uni-modal response in the band, its inherent simplicity makes it highly attractive as a practical basis for simulation. Clearly, the amount of data processing is reduced, and adjustment of the force spectral density is achieved by setting up the required levels in broad contiguous bands. The choice of B need not reflect the fluctuations of the response spectral densities. As long as the band B contains only one resonant frequency the assumptions would seem to be reasonably valid. The reproduction of the reference level could well be achieved by means other than a vibrator, e.g. a controllable acoustic field.

If the band B contains two natural frequencies, the simple single vibrator approach will not be valid. In this case, a two degree of freedom representation of the structure is necessary over the band B:

$$S^{q}_{ij} = \sum_{r,s=1}^{2} C^{*}_{ri}\, C_{sj}\, S^{f}_{rs} = \sum_{r,s=1}^{2} C^{*}_{ri}\, C_{sj}\, \alpha^{*}_{r}\, \alpha_{s}\, S^{z}_{rs} \qquad 5.2.9$$

and

$$S^{q}_{aa} = \sum_{r,s=1}^{2} C^{*}_{ra}\, C_{sa}\, \alpha^{*}_{r}\, \alpha_{s}\, S^{z}_{rs} \qquad 5.2.10$$

Taking the band average of S^{q}_{aa} :

$$\langle S^{q}_{aa} \rangle = \frac{1}{B} \sum_{r,s=1}^{2} S^{z}_{rs} \int_{B} C^{*}_{ra}\, C_{sa}\, \alpha^{*}_{r}\, \alpha_{s}\, d\omega \qquad 5.2.11$$

The influence coefficients may be frequency dependent if the response q_a is a velocity or acceleration, but if $B << f_o$ where f_o is the band centre, then C_{ra} and C_{sa} may be taken outside the integral and evaluated at the band centre frequency. Then:

$$\langle S^q_{aa} \rangle = \frac{1}{B} \sum C^*_{ra} C_{sa} S^z_{rs} \left\{ \int_B \alpha^*_r \alpha_s \, d\omega \right\} \qquad 5.2.12$$

$$= \frac{1}{B} \left[\sum_{r=1}^{2} |C_{ra}|^2 S^z_{rr} I_{rr} + \sum_{r \neq s} C^*_{ra} C_{sa} S^z_{rs} \int_B \alpha^*_r \alpha_s \, d\omega \right] \qquad 5.2.13$$

In 5.2.13 the integral: $\int_B |\alpha_r|^2 d\omega$ has been replaced by its corresponding closed form: $I_{rr} = \int_o^\infty |\alpha_r|^2 d\omega$. Integrals involving modal receptance products may be likewise replaced by integrals denoted $I_{rs} = \int_o^\infty \alpha^*_r \alpha_s \, d\omega$; the assumption being that both modal receptances have no significant value outside the interval B so that the limits of integration may be extended without much error. Closed forms for integrals of the type I_{rs} have been given by Robson (1966) for the case where the damping in the modal receptances is assumed hysteretic. For the case of assumed viscous damping the integrals are evaluated in Appendix II. I_{rs} is of course complex, with $I_{sr} = I^*_{rs}$.
By the Cauchy-Schwarz inequality:

$$|I_{rs}|^2 \leqslant I_{rr} . I_{ss} \qquad 5.2.14$$

Computed values of $|I_{rs}|$ from the expression II.16 of Appendix II, are shown in Fig. 5.2.1 for two different values of viscous damping, assumed equal in both modes. These curves show that $|I_{rs}|$ is large if the modal receptances overlap, but falls off rapidly if the natural frequencies are separate.

Writing 5.2.13 as:

$$\langle S^q_{aa} \rangle = \frac{1}{B} \left[\sum_{r=1}^{2} |C_{ra}|^2 I_{rr} S^z_{rr} + \sum_{r \neq s}^{2} C^*_{ra} C_{sa} I_{rs} S^z_{rs} \right] \qquad 5.2.15$$

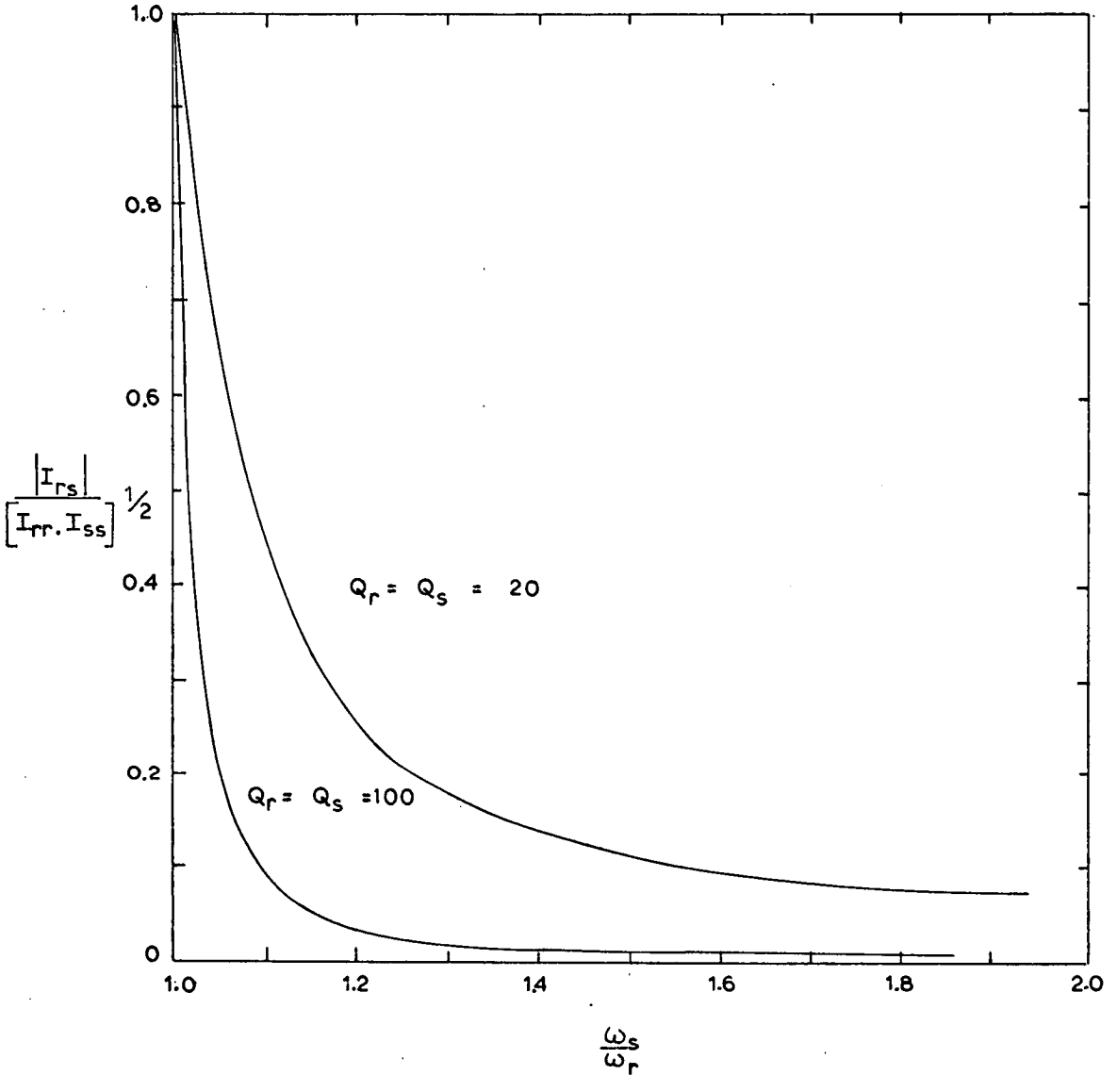

Fig. 5.2.1

The Effects of Overlapping of Modal Receptances on the Value of the Integral: $I_{rs} = \int_0^\infty \alpha_r^* \alpha_s \, d\omega$ for Two Values of Modal Damping.

and recalling the expression for the narrow band cross spectral density between any pair of structure responses:

$$S^{q}_{ij}(\omega) = \sum_{r,s=1}^{2} C^{*}_{ri} C_{sj} \alpha^{*}_{r} \alpha_{s} S^{z}_{rs} \quad ; \quad \omega \in B . \qquad 5.2.16$$

It is clear from 5.2.15 that reproduction of the single reference broad band spectral density, $\langle S^{q}_{aa} \rangle$, does not guarantee the reproduction of the individual values of the four service generalized force quantities, and does not lead in general to narrow band simulation of any response of the type 5.2.16.

5.3 Multi-Force Simulation using Broad-Band Observations

The result that narrow band simulation of the whole structure using a single broad band reference response breaks down when there are two resonant frequencies within the band suggests the possibility of achieving narrow band simulation using a more complicated system of simulating forces and broad band references. It is possible to theorize about this, but practical difficulties arise in implementing such solutions.

An initial result is that if there are N modes having resonant frequencies within the band, and the assumption still holds that the set of service generalized force spectral densities are smooth over B, then simulation can be achieved by a set of N forces having a particular spectral density matrix whose elements are constant over B.

Let $[S^{p}_{KL}]$ be the spectral density matrix of the simulating forces. Then the matrix of generalized force spectral densities is given by:

$$[S^{z}_{rs}] = [\phi][S^{p}_{kl}][\phi]' \qquad 5.3.1$$

where $[\phi]$ is the N square matrix of the mode shape components at the force locations. Assume $\det[\phi] \neq 0$. Then $[\phi]^{-1}$ exists and:

$$[S^{p}_{kl}] = [\phi]^{-1}[S^{z}_{rs}][\phi']^{-1} \qquad 5.3.2$$

By 5.3.2, there exists a set of N random forces which can reproduce a prescribed set of spectral densities of N generalised forces and can therefore simulate all the narrow band spectral densities of the structure. This proves the existence of a solution. The difficulty is that the elements of $[S^{z}_{rs}]$ are not observable, and the solution $[S^{p}_{kl}]$ must be inferred from observed spectral densities. This is illustrated by the case N = 2.

The concept of a broad band cross spectral density can be introduced, being the average over a broad frequency interval of a cross spectral density. For the case of two resonant frequencies within the band, it is shown that simulation of the broad band spectral densities and cross spectral densities of a pair of reference responses can achieve simulation of the narrow band spectral densities of the whole structure.

Recall the expression for the cross spectral density of any pair of response co-ordinates (5.2.9). This may be written using matrices:

$$S^{q}_{ij} = [c_i]^{\dagger}[S^{e}_{rs}][c_j] \qquad 5.3.3$$

$$= [c_i]^{\dagger}[\alpha_r]^{\dagger}[S^{z}_{rs}][\alpha_r][c_j] \qquad 5.3.4$$

Now consider a pair of reference responses, q_a , q_b . having spectral density matrix $[S^{q}_{ab}]$. Denote $[C] = [C_a , C_b]$, the 2 x 2 matrix of modal influence coefficients for the two references.

Then: $$[S^{q}_{ab}] = [C]^{\dagger}[S^{f}_{rs}][C] \qquad 5.3.5$$

$$= [C]^{\dagger}[\alpha_r]^{\dagger}[S^{z}_{rs}][\alpha_r][C] \qquad 5.3.6$$

Simulation of any narrow band response (5.3.3) requires that $[S^{z}_{rs}]$ be reproduced. Now in 5.3.5 take an average over the frequency band. Again, $[C]$ may be considered independent of frequency. Then:

$$[\langle S^{q}_{ab}\rangle] = [C]^{\dagger}[\langle S^{q}_{rs}\rangle][C] \qquad 5.3.7$$

where :

$$\langle S^{q}_{rs}\rangle = \frac{1}{B}\int_{B} \alpha^{*}_{r}\alpha_s S^{z}_{rs}\, d\omega$$

$$= \frac{S^{z}_{rs}}{B}\int_{B} \alpha^{*}_{r}\alpha_s\, d\omega$$

$$\doteq \frac{I_{rs}}{B} S^{z}_{rs} \qquad 5.3.8$$

Hence: $$[\langle S^{q}_{rs}\rangle] = \frac{1}{B}[I_{rs}.S^{z}_{rs}] \qquad 5.3.9$$

Now, provided that the transducer locations are such that $\det[C] \neq 0$, then $[C]^{-1}$ exists and from 5.3.7 :

$$[\langle S^{q}_{rs}\rangle] = [C^{-1}]^{\dagger}[\langle S^{q}_{ab}\rangle][C^{-1}] \qquad 5.3.10$$

5.3.10 shows that a set of broad band reference spectral densities $[\langle S^{q}_{ab}\rangle]$ implies a unique set of broad band spectral densities of the two generalized co-ordinates $[\langle S^{q}_{rs}\rangle]$. By reproducing $[\langle S^{q}_{ab}\rangle]$, the set $[\langle S^{q}_{rs}\rangle]$ are reproduced. From 5.3.8 this implies that $[S^{z}_{rs}]$ is reproduced provided $I_{rs} \neq 0$, and finally 5.3.4 implies simulation of the narrow band spectral densities of the whole structure. The necessary condition that the I_{rs} quantities be non zero must be examined. While I_{rr} and I_{ss} are non-zero (5.2.5), I_{rs} is complex, and $|I_{rs}|$ depends on the degree of overlapping of the modal receptances. Fig. 5.2.1 shows that $|I_{rs}|$ will tend to be small compared with I_{rr}

and I_{ss} if the modal receptances do not overlap significantly. Strictly $|I_{rs}|$ will be non zero but the relation 5.3.9 will be poorly conditioned, with an adverse effect upon the accuracy of simulation.

Ideally, if the modal receptances do not overlap significantly, then the interval B may be sub-divided into a pair of intervals each containing a single resonant frequency and hence the unimodal representation would be valid in each band. This may not be possible if bandwidths are pre-determined by test equipment. In such a case a simplification occurs in that narrow band simulation requires that only S^{z}_{rr} and S^{z}_{ss} be reproduced, with no constraint on S^{z}_{rs} . This is seen from 5.2.9. where cross products of modal receptances may be considered to be second order at any frequency in B. Studies of this situation show that it is possible to achieve narrow band simulation over B by reproducing only a pair of broad band direct spectral densities. There is then no unique solution for the system of forces required to achieve this. It is not, however, always possible to achieve this using a pair of independent forces.

There is clearly a marked increase in the complexity of the simulation test in progressing from the uni-modal to the bi-modal case. In the uni-modal case, the test can be set up by adjusting a single excitation gain control in each band to achieve a prescribed response of a single reference response. In the bi-modal case, the direct and cross spectral densities of a pair of simulating forces must be set up to obtain a prescribed set of responses at a pair of reference transducers. This would seem to be difficult. The required excitation may be calculated from the service reference responses and measured receptances, but this is extremely tedious. Writing down the corres-

ponding relationships for narrow band spectra:

$$[S^q_{ab}] = \overline{[\alpha]}\,[S^p_{KL}]\,[\alpha]' \qquad 5.3.11$$

Taking a frequency average of both sides:

$$[\langle S^q_{ab}\rangle] = \langle \overline{[\alpha]}\,[S^p_{KL}]\,[\alpha]' \rangle \qquad 5.3.12$$

By assumption $[S^p_{KL}]$ is not frequency dependent, but the receptance elements are. It is necessary to invert this relationship to calculate $[S^p_{KL}]$ from $[\langle S^q_{ab}\rangle]$, and this can only be achieved by expanding the right hand side and taking a frequency average of the coefficients of S^p_{KL}. These involve products of receptances. Then the relation 5.3.12 may be inverted. In principle it is possible, but it involves the calculation of frequency averages of receptance products, of the form: $\frac{1}{B}\int_B \alpha^*_{aK}\,\alpha_{bL}\,d\omega$, from measured receptances.

5.4 Experimental Verification of Broad Band Simulation

Some experiments were carried out to demonstrate the validity of Broad-Band Simulation. The tests were limited in scope but were sufficient to demonstrate that (a) if there is a single resonant frequency within a particular broad band, then accurate simulation of narrow band direct spectral densities is obtained if a single reference broad band spectral density is reproduced, and (b) if there is more than one resonant frequency within the band, then reproduction of only a single broad band spectral density can give rise to large errors in the simulated narrow band spectral densities.

The cantilever model was used, and the service environment was produced by an arrangement of small vibrators. Simulation was then attempted using a further vibrator, adjusting the gain to reproduce the broad band spectral density of a reference accelerometer. In each case, the broad band spectral densities of a further three accelerometers were measured and sample records of the accelerometer outputs were stored on magnetic tape so that narrow band spectral densities could be obtained by digital computation. Comparisons of the service and simulated cases were then made.

5.5 Apparatus and Method of Test

The tests were originally carried out using two Peekel noise generators to obtain a pair of statistically independent forces for the service case. One was found to have a troublesome intermittent fault, while the output of the second was found to fluctuate, making accurate response measurements very difficult. The tests were subsequently carried out with the addition of a Hewlett Packard Noise Generator which proved to have a very stable output and had an additional facility of variable noise bandwidth.

To obtain the broad band spectral densities, the accelerometers were connected through a switch to the Bruel and Kjaer 2107 analyser which was adjusted to have a $\frac{1}{3}$ octave pass-band. The output of the analyser was taken to the Bruel and Kjaer type 2417 random noise voltmeter. This instrument has a variable time constant of up to 100 secs and was used to measure the r.m.s. value of the analyser output. This reading was proportional to the square root of the broad band spectral density over the $\frac{1}{3}$ octave band.

Narrow band spectral densities were obtained using a conventional data processing scheme. The accelerometers outputs were recorded using an Elliot-Tandberg tape recorder on the F.M. channel, after passing through the $\frac{1}{3}$ octave filter. A PDP8 computer was used to convert the recordings into 8 bit samples on punched tape which was finally used as data for an Atlas Autocode program to obtain the spectral densities. The programs were developed jointly by the author and by G. R. Campbell (Campbell, 1968) and only a brief description is given here.

The PDP8 program gave control of the sampling interval as a multiple of $30\mu s$, and the number of samples stored. The store capacity was 3830 samples. On completion of the sampling, the samples were transferred to eight track paper tape, together with a tape identifier. The Atlas Autocode program was then used with the KDF9 computer to compute the autocorrelations of each record from the lagged products, and then to compute the spectral density estimates by the standard Fourier Series Transformation (Bendat and Piersol, 1967). For this part of the program, a fast Harmonic Analysis library routine was used in a modified form. The bandwidth of the spectral density estimates is of course determined by the sampling interval and the maximum lag number of the autocorrelations. This was originally arranged to be 1 Hz with a sampling interval of 2.5 mS and a maximum lag number of 200. Early trials of the program gave rise to negative spectral densities and although this was subsequently found to be due to a programming fault, a triangular lag window was introduced into the program to avoid the effects of negative side lobes on spectral windows. This meant that the effective bandwidth was increased to 2 Hz. The standard error of the estimates was of the order of 0.2. This was considered adequately small.

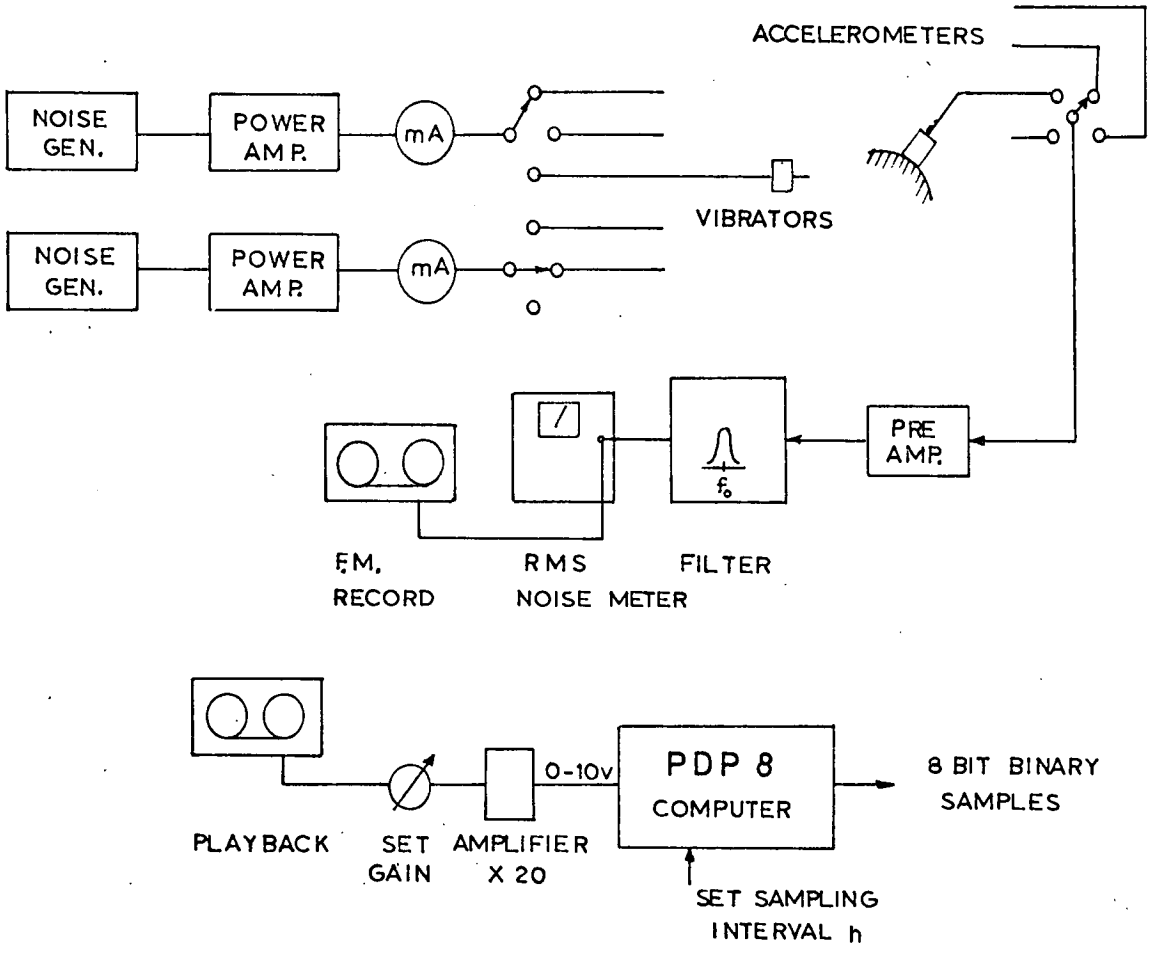

KDF 9 PROGRAM

(1) Correct samples to zero mean.

(2) Compute Autocorrelation Function from lagged products at $\tau = rh$, $r = 1,2,..m$.

(3) Normalize Autocorrelation Function.

(4) Weight Autocorrelation Function by Triangular Lag Window:

$$R'(rh) = R(rh)(1 - r/m).$$

(5) Compute Spectral Density Estimates by Finite Fourier Series Cosine Transformation.

Fig. 5.5.1

Apparatus and Processing Scheme for Wide Band Simulation Tests.

Figure 5.5.1 shows diagrammatically the equipment used in the tests. During the sampling, the signals were monitored on an oscilloscope and the tape recorder play back gain was adjusted for each record to make full use of the PDP8 input range (0 to -10 Volts). A -5 volts bias was required and was obtained by using the zero control of the Rochar amplifier to off-set its output to -5 v. In view of these gain adjustments, the computer program was designed to normalize all autocorrelation functions, and the final narrow band spectral densities were scaled in proportion to their corresponding broad band values.

5.6 Test 1

This was a test of broad band simulation for the case of a single resonant frequency within the band. The second horizontal mode of the model was used, having a resonant frequency of 134.4 Hz. The analyser was tuned to 135 Hz and set to have a 3db bandwidth of $\frac{1}{3}$ octave. All vibrators were confined to the horizontal plane so that the adjacent vertical mode was not excited. Fig. 5.6.1 shows the positions of the two service vibrators and the simulating vibrator. Table 5.6.1 shows the mode shape components at the accelerometer locations. Accelerometer (1) was used as reference.

Table 5.6.1

Accelerometer	1 (ref)	2	3	4
Mode Component	+0.726	-0.83	-0.32	-0.485

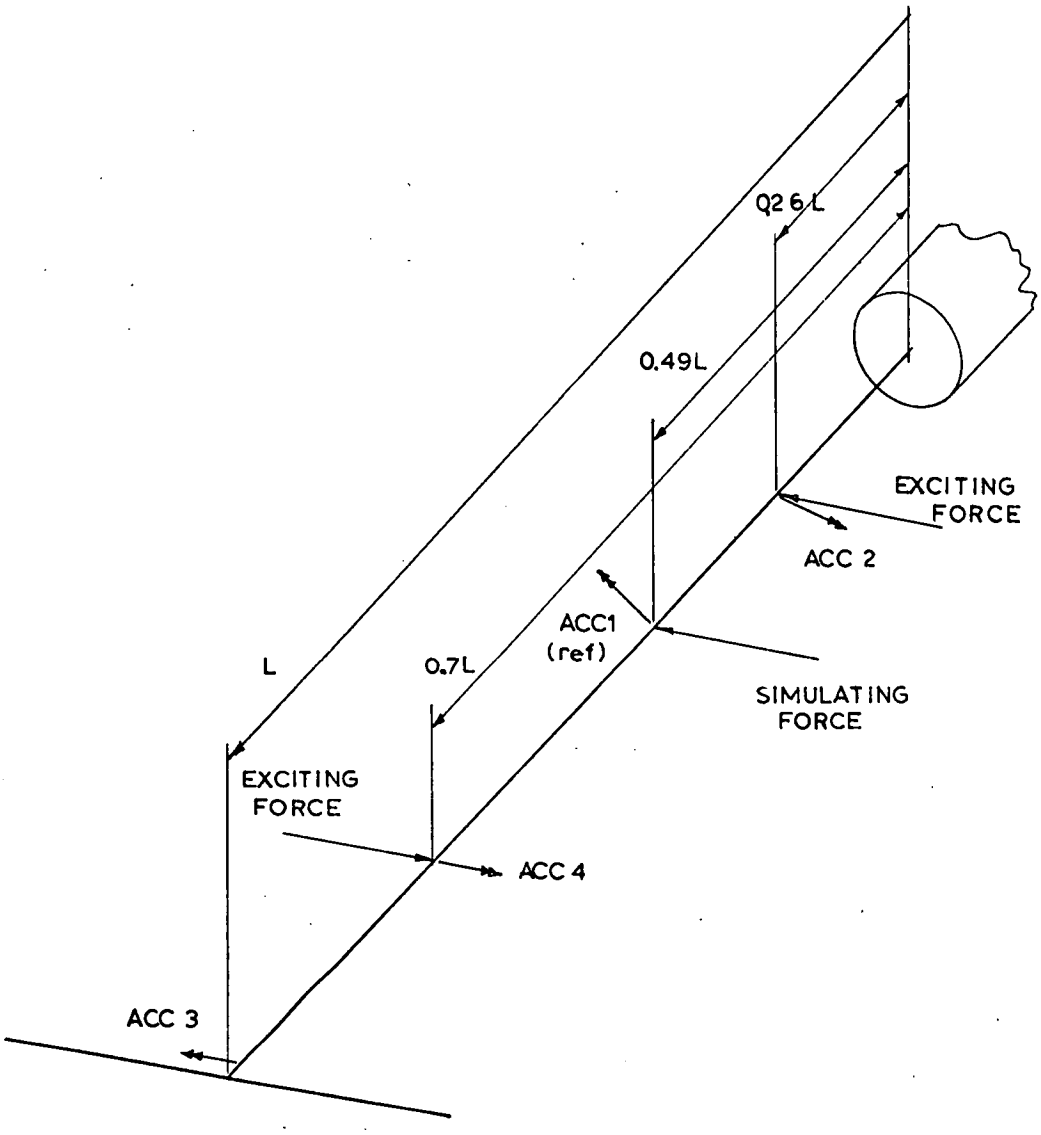

Fig. 5.6.1

Wide Band Simulation Test 1.
Locations of Vibrators and Accelerometers.

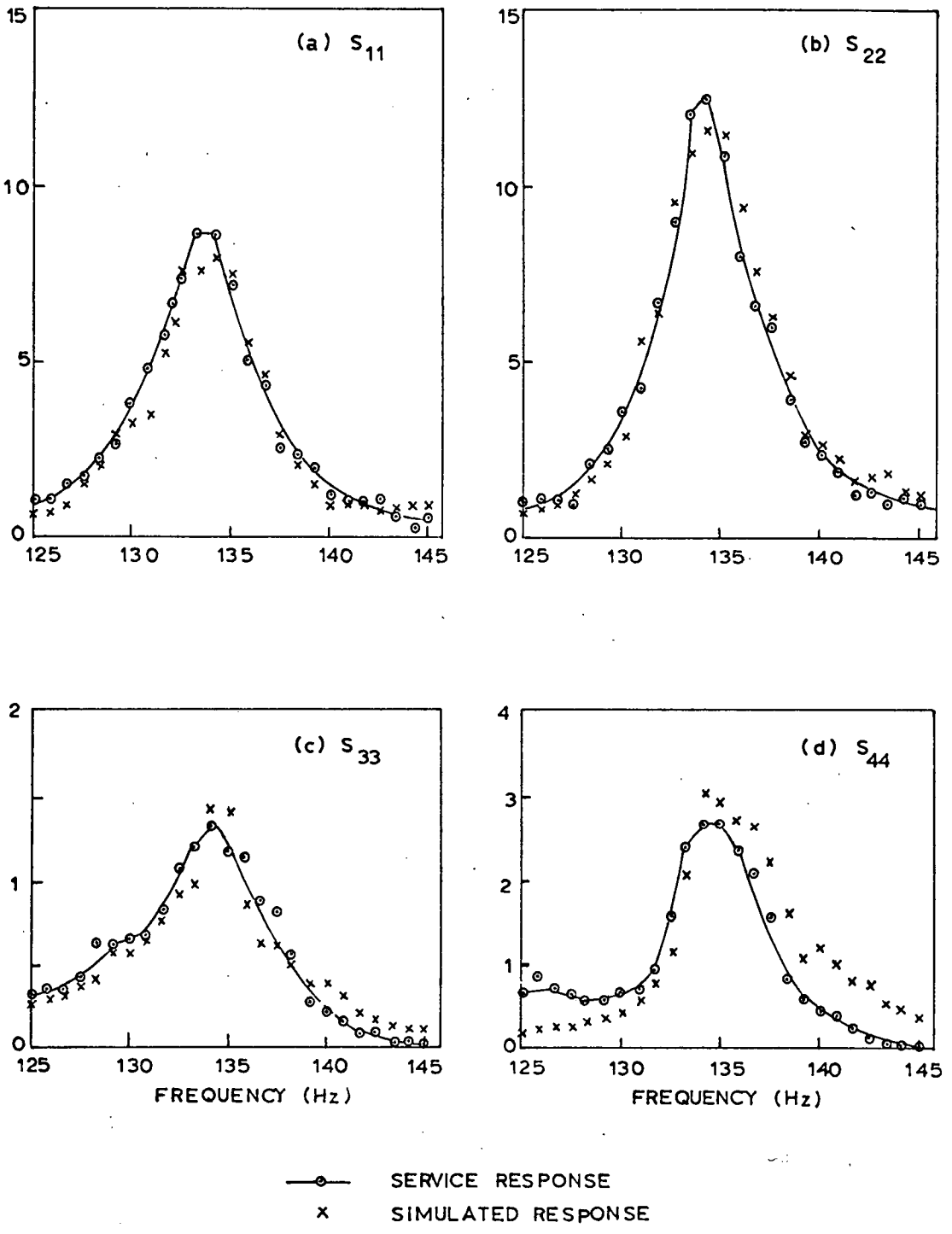

Fig. 5.6.2

Wide Band Simulation Test 1.
Narrow Band Spectral Densities of Service
and Simulated Responses.

In the trial case (A), vibrators 1 and 2 were driven independently with 85 mA r.m.s. and in the simulation case (B), the current of vibrator 3 was adjusted until the same broad band spectral density was achieved at the reference accelerometer. Table 5.6.2 compares the results for the measured broad-band spectral densities of the four accelerometers in the two cases.

Table 5.6.2 Comparison of Broad-Band Spectral Densities

Accelerometer	1 (ref)	2	3	4
Case (A)	344	442	84.3	125
Case (B)	344	466	79.5	112
Ratio B/A	1.0	1.05	0.94	0.91

The corresponding narrow band spectral density estimates are shown in Figure 5.6.2.

The values of Table 5.6.2 show a high degree of correspondence between the two cases, showing that simulation of the broad band spectral densities was achieved. The graphs of Fig. 5.6.2 show that simulation of the narrow band spectral densities for all four positions was reasonably well achieved, bearing in mind the inevitable scatter of results due to sampling.

5.7 Test 2

Broad band simulation with a single vibrator will produce errors in general if there is more than one resonant frequency within the

band. This experiment demonstrates these errors. The model was set up so that the second horizontal and vertical modes had natural frequencies of 148.5 and 164.0 Hz respectively. With the 2107 Analyser tuned to 155 Hz with a $\frac{1}{3}$ octave bandwidth, the two frequencies were well within the 3db band. The service excitation was represented by a horizontal and a vertical vibrator, each driven from an independent noise generator. The simulating vibrator was coupled at 45^{o} to the horizontal so as to excite both modes. Table 5.7.1 shows the components of the mode shapes at the accelerometer positions, and Fig. 5.7.1 shows the arrangement of vibrators.

Table 5.7.1

Accelerometer	1 (ref)	2	3	4	Frequency
Horizontal Mode	.698	.715	.368	.064	148.5
Vertical Mode	.687	-.732	.023	-.946	164.0

Simulation of the response was attempted by reproducing the broad band spectral density of accelerometer 1. Table 5.7.2 lists the measured values of broad band spectral density for the four accelerometers. Case A is the service case and case B the simulated case.

Table 5.7.2 Comparison of Broad-Band Spectral Densities

Accelerometer	1 (ref)	2	3	4
Case A	164	180	36	97
Case B	164	236	24	187
Ratio B/A	1.0	1.31	0.67	1.93

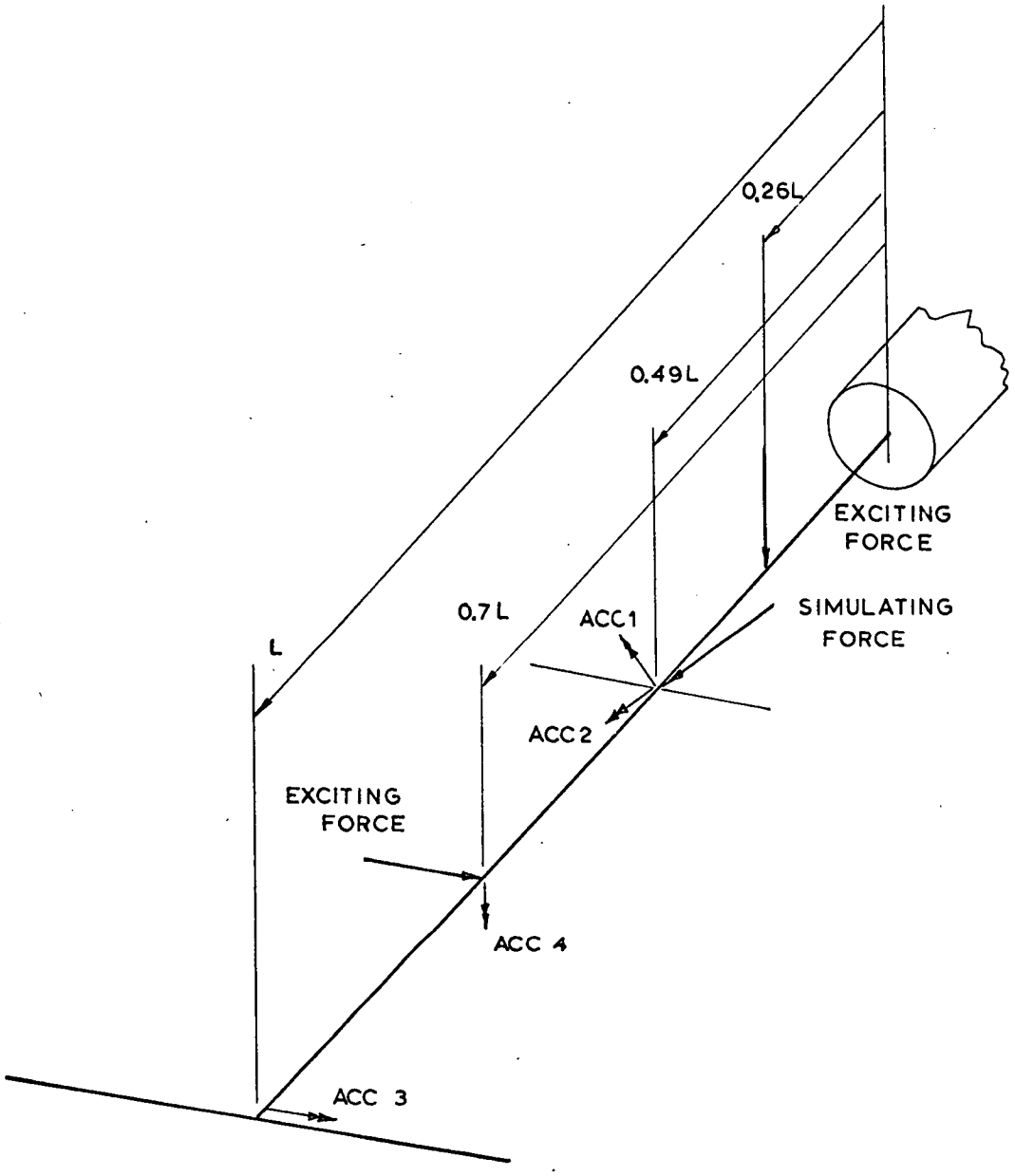

Fig. 5.7.1

Wide Band Simulation Test 2.
Locations of Vibrators and Accelerometers.

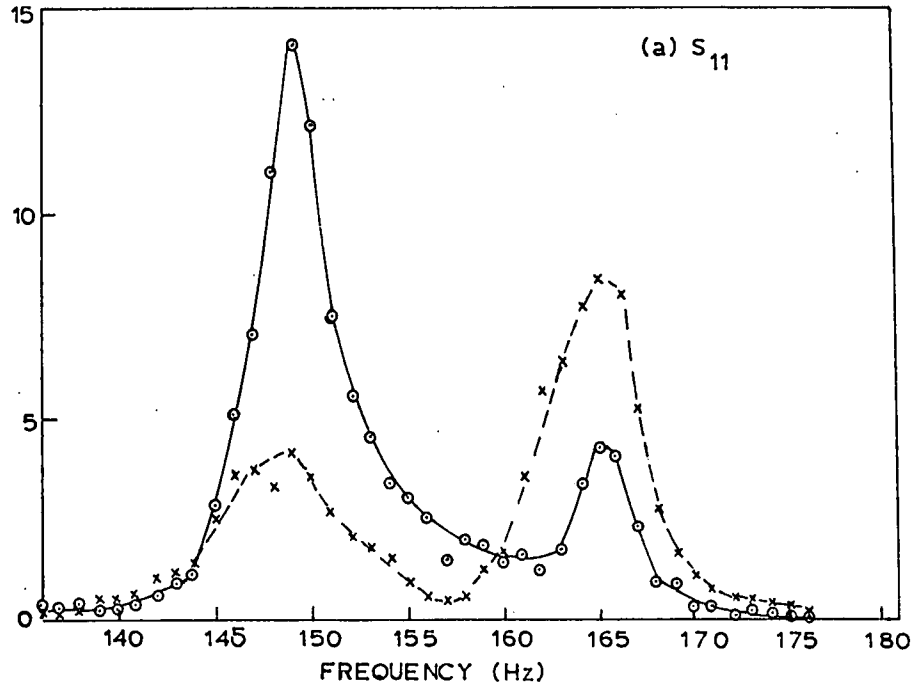

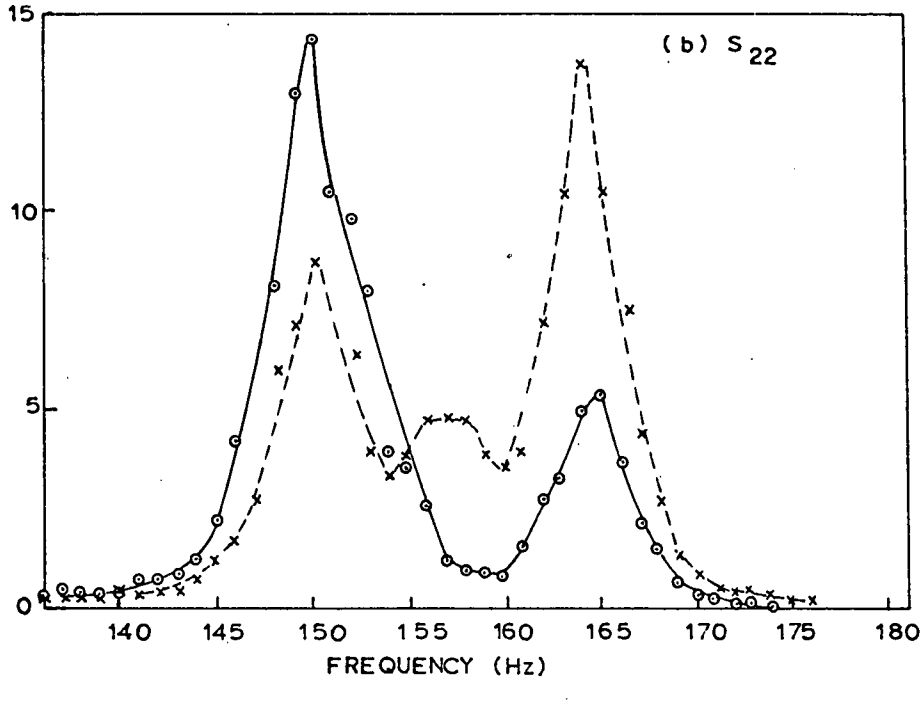

—o— SERVICE RESPONSE

--x-- SIMULATED RESPONSE

Fig. 5.7.2

Wide Band Simulation Test 2

Narrow Band Spectral Densities of Service and Simulated Responses.

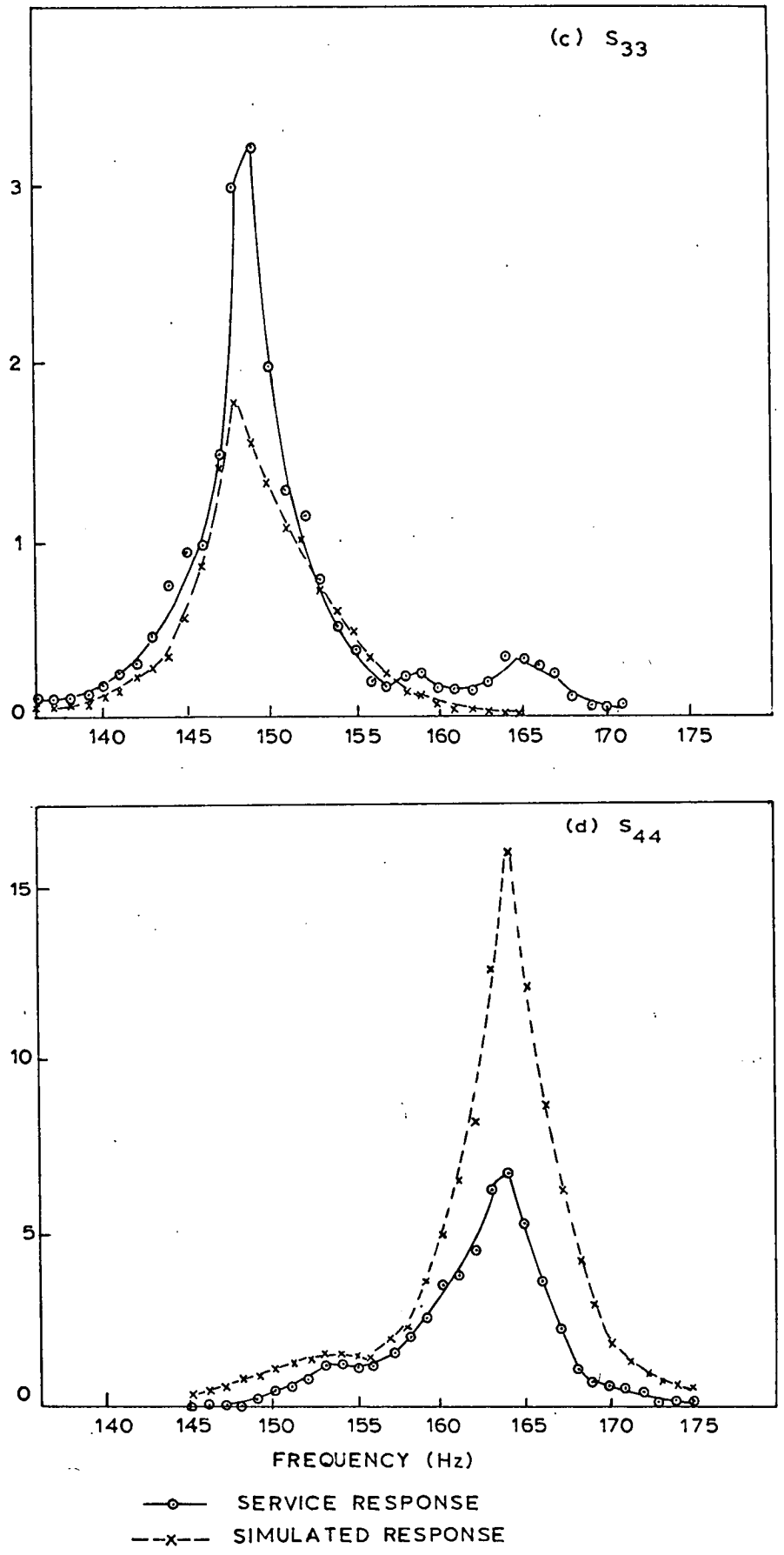

Fig. 5.7.2 (continued).

Wide Band Simulation Test 2.

The corresponding narrow band spectral density estimates are shown in Figure 5.7.2. In this case there are large discrepancies between the broad band spectral densities in the two cases and in the magnitudes and shapes of the narrow band spectral densities, showing that very poor simulation was achieved.

5.8 Conclusion

A modification of spectral density simulation using wide band average spectral densities has been discussed. In the case of a single resonant frequency within each observation band, a major simplification occurs in that reproduction of a single average value of reference spectral density over the band can lead to simulation of the actual (narrow band) spectral densities of the whole structure over the band. If two or more resonant frequencies occur within a particular band, then the procedure can lead to inaccurate simulation. These statements have been verified experimentally. A multi-force simulation is theoretically possible for the case of more than one resonant frequency per band, but there would seem to be practical difficulties in applying it.

CHAPTER 6

STATISTICAL APPROACH TO SIMULATION

6.1 Introduction

It is clear that severe practical difficulties will arise in attempting to use the basic theory of simulation at high frequencies in complex multi-modal structures. While simulation, in theory, can always be attained, its realization must be considered to be beyond the scope of practical test capability when control of more than a few vibrators is required. In such cases there are prospects for meaningful simulation using an approximate approach which makes reasonable demands on test facilities. In similar circumstances, the problem of the prediction of response has been approached using the statistical energy method (Lyon, 1967). This method attempts to predict only averages over space and frequency bands of response spectral densities for structures containing numbers of homogeneous modes in each band. It is assumed that sample responses are well represented by space averages and these may be predicted from the average properties of the environment. (Dyer, 1963)

Noiseux (1964) has investigated the simulation of a reverberant acoustic field by vibrators, using results from the statistical energy approach. His method was based upon the expression for the nett power flow from the acoustic field to the structure in a frequency band:

$$P_{IN} = \frac{n_s}{M_s} \cdot R_{RAD} \cdot \frac{2\pi^2 c}{\omega^2 \rho} \cdot \bar{p}^2 \qquad 6.1.1$$

where n_s is the modal density of the structure, Ms is the structure mass, c and ρ are ambient speed of sound and density in the fluid, ω is the band centre and $\bar{p}^2$ the mean square acoustic pressure.

The quantity R_{RAD} is the average radiation resistance of the modes in the band such that with a mean square velocity over the structure of $\bar{v}^2$, the radiated power P_o is given by:

$$P_o = \bar{v}^2 R_{RAD} \qquad 6.1.2$$

Using 6.1.1, the power input in each frequency band can be estimated for the structure. In Noiseux's approach, the power inputs of vibrators are monitored and adjusted to achieve the predicted levels in each band. The input power per band is also the power dissipated per band by radiation and by internal friction, and may be written:

$$P_{IN} = \bar{v}^2 \left[R_{RAD} + R_{MECH} \right] \qquad 6.1.3$$

R_{MECH} is a resistance term, such that $\bar{v}^2 R_{MECH}$ is the internally dissipated power. $\bar{v}^2$ represents the space average mean square velocity for a single filtered band - effectively the broad band velocity spectral density. By 6.1.3, it is this latter quantity which is simulated.

The attractions of this approach are the simplicity of its parameters, and the absence of any need for reference responses from a dynamically similar structure in the service environment. The approach is limited to the simulation of acoustic fields, but there are prospects for a related approach for environments in general. Implicit in the Noiseux approach is the idea that sample responses at different points on the structure will be adequately reproduced if their space average is reproduced, and that this condition is satisfied by observing only broad band average spectral densities. The band encompasses a number of modal frequencies so that in theory, averaging over a number of modal contributions irons out the fluctuations in response spectral density from point to point. If such a condition holds then simulation can be envisaged in the following way:

For any frequency band, a single broad band reference response, or an average over a few sample responses, will give a good indication of the space average response in the band. This may be reproduced by a single vibrator or some other controllable test environment, requiring a single level adjustment in each band. By the initial assumption the broad band average responses of every point on the structure will be reasonably well reproduced.

However this projected form of simulation must be examined carefully to establish a basic legitimacy. It is clear that a broad observation band for spectraldensity measurements brings about only an apparent reduction in the complexity of the response. Broad band measurements are practical expedients which mask the finely scaled variations of response spectral density. Simulation of broad band responses will not in general lead to simulation of the actual spectral densities within the band, and therefore does not represent a simulation in probability of the sample function behaviour of any response as discussed in Chapter 3. However a justification of this degree of simulation can be formulated on the basis of a distribution of peaks and level crossings in sample functions. It is also important to establish the accuracy of the approach. This is too general a question, but the relevant parameters are deduced, and a considerable insight is gained from digital computer calculations and from experimental work on a large rectangular plate.

6.2 Basis for Simulation

Broad band direct spectral densities, where the band width is much wider than the band width of a resonant peak of a structure mode, are convenient measures of the response of complex multi - modal structures to random environments, and they play a central role in the statistical energy approach.

It remains to show that the simulation of broad band average spectral densities at every point of the structure is a reasonable goal of simulation. The approximate broad band approach cannot guarantee a point by point simulation of the narrow band spectral densities within each band and so cannot achieve simulation in distribution of the response processes. It can be justified in the following way.

Consider a process $\{q(t)\}$, being stationary and gaussian. At any time t_k, the probability distribution of the amplitude $q(t_k)$ is determined only by the variance $\sigma^2(t_k)$ which is independent of t_k and is given by:

$$\sigma^2 = 2\int_0^\infty S^q(\omega)\,d\omega \qquad 6.2.1$$

where $S^q(\omega)$ is the spectral density of $q(t)$. In 6.2.1 the integral may be replaced exactly by the sum of broad band spectral densities in contiguous bands:

$$\sigma^2 = 2\sum_{\omega_i}\int_{\omega_i-\frac{B_i}{2}}^{\omega_i+\frac{B_i}{2}} S^q(\omega)\,d\omega = 2\sum_i B_i\langle S^q(\omega)\rangle_{B_i} \qquad 6.2.2$$

In 6.2.2 B_i represents a set of contiguous bands, having band centre frequency ω_i. Further, consider Rice's result (Rice, 1945) for the probability of a peak in the $q(t)$ process in a specified interval $(\delta x, \delta t)$, as modified by Robson (1963). With $R \equiv R^q(o)$

and $R'' \equiv \frac{d^2}{d\tau^2}\left[R^q(\tau)\right]_{\tau=0}$ etc.

$$\text{Prob}\left[\text{peak in } \delta x, \delta t\right] = \delta x\,\delta t\left[\frac{-R''}{2\pi R}\right]^{\frac{1}{2}}\frac{x}{[2R]^{\frac{1}{2}}}\exp\left[\frac{-x^2}{2R}\right] \qquad 6.2.3$$

Now: $$R = 2\int_0^\infty S^q(\omega)\,d\omega \qquad 6.2.4$$

and : $$R'' = 2\int_0^\infty \omega^2\, S^q(\omega)\,d\omega \qquad 6.2.5$$

6.2.4 has already been related to broad band spectral densities. 6.2.5 may be approximated by a sum of broad band spectral densities weighted by the square of the band centre frequency provided thatthe band width B_i is much less than the band centre ω_i :

$$R'' \doteq 2 \sum_i \omega_i^2 B_i \langle S^q(\omega) \rangle_{B_i} \qquad 6.2.6.$$

It follows from 6.2.2 and 6.2.6 that two independent processes having the same broad band spectral densities will have the same probability distributions of amplitudes and of peaks. Consequently in a long record the total number of crossings of any specified amplitude level and the total number of peaks in a prescribed amplitude interval will be similar for both processes. This would seem to constitute a valuable basis for approximate simulation. It is approximate in the sense that higher order probabilities e.g. Prob[peak in $(\delta x_1, \delta t_1)$ and peak in $(\delta x_2, \delta t_2)$] are not reproduced, nor are joint probabilities of the occurence of simultaneous peaks in two distinct responses reproduced. (The basic theory of simulation in distribution does take care of all these higher order probabilities).

6.3 Application to Complex Multi - Modal Structures

The approximate basis for simulation is that broad band spectral densities are reproduced for all responses of the structure in contiguous bands over the frequency range of interest. In the introduction the possibility arose of achieving this with simple facilities by virtue of the averaging effect of a number of modal contributions in each band. This is now examined.

Consider a band B containing N resonant frequencies. The direct spectral density of any response co-ordinate q_i still has form:

$$S^q_{ii}(\omega) = \sum_{r,s=1}^{\infty} C^*_{ri} C_{si} S^f_{rs}(\omega) = \sum_{r,s=1}^{\infty} C^*_{ri} C_{si} \alpha^*_r \alpha_s S^z_{rs}(\omega) \qquad 6.3.1$$

This is valid for any environment, represented by the values of generalized force spectral density in the various modes. The summation is strictly over all the modes. In taking a band average of 6.3.1 it will be assumed that the spectral densities of the environment, represented by S^{z}_{rs} , are slowly varying functions over B. The modal influence coefficients c_{ri} etc. may be frequency dependent (e.g. for velocity response) but may be evaluated at the band centre frequency.

Then:

$$\langle S^{q}_{ii} \rangle_B = \sum_{r,s=1}^{\infty} c^{*}_{ri} c_{si} \langle S^{f}_{rs} \rangle_B = \sum_{r,s=1}^{\infty} c^{*}_{ri} c_{si} \langle \alpha^{*}_{r} \alpha_s \rangle_B S^{z}_{rs} \qquad 6.3.2$$

The angular brackets denote band average. This expression may be approximated in the following way. Band averages of modal receptance products like $\langle \alpha^{*}_{r} \alpha_s \rangle$ will be considered significant only if both modes have resonant frequency within the band. The summation need only be taken over the N modes within the band denoted $r = 1,2,.. N$.
It is convenient to replace integrals of receptance products by integrals over the infinite interval as in Chapter 5.

$$\langle \alpha^{*}_{r} \alpha_s \rangle = \frac{1}{B} \int_B \alpha^{*}_{r} \alpha_s \, d\omega \doteq \frac{1}{B} \int_0^{\infty} \alpha^{*}_{r} \alpha_s \, d\omega = \frac{I_{rs}}{B} \qquad 6.3.3$$

Note that: $$\langle S^{f}_{rr} \rangle = S^{z}_{rr} \langle |\alpha_r|^2 \rangle \doteq \frac{S^{z}_{rr}}{B} \int_0^{\infty} |\alpha_r|^2 d\omega = \frac{\bar{f}^2_r}{2B} \qquad 6.3.4$$

where the overbar denotes time average. Finally a further simplification is possible if correlations between the modes are neglected. The basis for this is that $|I_{rs}|^2 \ll I_{rr} . I_{ss}$ if the peaks of the modal receptances do not overlap within B. To this degree of approximation, the broad band response spectral density may be expressed as:

$$\langle S^{q}_{ii} \rangle = \frac{1}{B} \sum_{r=1}^{N} |c_{ri}|^2 I_{rr} S^{z}_{rr} \qquad 6.3.5$$

It can be seen from 6.3.5 that even in the case of uncorrelated motion in the modes, accurate simulation of all broad band responses of the structure requires that the set of N generalized force spectral densities, S^{z}_{rr}, r = 1,2,.. N, be reproduced. This is not to be considered feasible for large N.

The alternative is to consider the average properties of the series expression, 6.3.5, treating the individual terms in a statistical sense in the spirit of the statistical energy approach. For any given environment, represented by a set of values of S^{z}_{rr}, r = 1,2,... N, the modal influence coefficients at any location will not be known. So the expression 6.3.5 may be regarded as a weighted sum of non-negative random numbers at any location. A parallel may then be drawn between such a series and sums of independent non-negative random variables. (e.g. a chi-square random variable with N degrees of freedom) A general result for such sums is that the fluctuations about the mean decrease with increasing N, so that it may be expected that the fluctuations about the space mean of the broad band spectral density from point to point will decrease with increasing N for a given environment. This relies on the mode shapes being distributed through the structure in a fairly homogeneous fashion. A further complication is that the S^{z}_{rr} terms themselves arise from the interaction of the mode shapes with the environment, so these must be considered to be indeterminate in detail. In examining the possibilities for accurate simulation, one method would be to use a mathematical model of a specific environment, together with a specific structure having a defined set of modes, and carry out sample calculations. It was considered that only a limited picture could be obtained by this method. Results of greater generality are possible using a probabilistic treatment of the environment, in which a set of values of S^{z}_{rr}, r = 1,2,... N, is regarded as a random sample drawn from a suitable population.

There then exists an ensemble of possible responses which characterizes the indeterminacy of the practical situation.

It is convenient to take the particular case of a plate or shell like system, so that the modal influence coefficient for displacement at (x_i, y_i) for the r^{th} mode may be written:

$$C_{ri} = \phi_r(x_i, y_i) \qquad 6.3.6$$

where $\phi_r(x,y)$ is the r^{th} mode shape. It is convenient now to use S to represent broad band spectral density. The displacement spectral density at (x_i, y_i) becomes:

$$S^w_{ii} = \frac{1}{B}\sum_{r=1}^{N} \phi_r^2(x_i, y_i)\, \bar{\xi}_r^2 = \frac{1}{B}\sum_{r=1}^{N} \phi_r^2(x_i, y_i) I_{rr} S^{\ddot{z}}_{rr} \qquad 6.3.7$$

The simulation approach can be conceived as replacing one sample set of values of $S^{\ddot{z}}_{rr}$ by another set drawn from a similar, or a different population. Each sample set generates a response 'surface' for displacement $S^w(x,y)$ according to 6.3.7 and for other response types e.g. velocity, acceleration, strain, there is a corresponding response surface S^q_{ii} according to 6.3.5. The response surface corresponding to the simulating environment, denoted $S^q_{ii(II)}$ is required to be a close match to $S^q_{ii(I)}$ generated by the service environment after amplitude scaling has taken place. Scaling of the simulated response may be based on matching the service response at a single reference:

$$S^q(x_a, y_a)_{II} = S^q(x_a, y_a)_I \qquad 6.3.8$$

or it may be possible to reproduce the space mean response:

$$\langle S^q(x,y)\rangle_{A(II)} = \langle S^q(x,y)\rangle_{A(I)} \qquad 6.3.9$$

The angular brackets now denote space average over structure area A.

The effects of amplitude scaling are indirectly included in the analysis by requiring that the 'shapes' of the unscaled response surfaces are similar. This means that the service and simulated responses at every point must correspond after some form of normalization. A convenient form of normalization is to divide by the space average displacement response. This is embodied in the following condition for simulation:

$$\frac{S^{q}_{ii\,(II)}}{\langle S^{w}_{II} \rangle_A} \doteq \frac{S^{q}_{ii\,(I)}}{\langle S^{w}_{I} \rangle_A} \quad ; \text{for all } q_i . \qquad 6.3.10$$

The quantities $S^{q}_{ii\,(I)}$, $S^{q}_{ii\,(II)}$ and the corresponding space averages in 6.3.10 are not to be regarded as deterministic, but as random samples. Condition 6.3.10 may be expected to hold with high probability in a single trial if, for all x_i, y_i:

$$E\{ S^{q\prime}_{ii\,(II)} \} = E\{ S^{q\prime}_{ii\,(I)} \} \qquad 6.3.11$$

$$\left.\begin{aligned} \varepsilon^2_I &= \frac{var\{ S^{q\prime}_{ii\,(I)} \}}{E^2\{ S^{q\prime}_{ii\,(I)} \}} << 1 \\ \varepsilon^2_{II} &= \frac{var\{ S^{q\prime}_{ii\,(II)} \}}{E^2\{ S^{q\prime}_{ii\,(II)} \}} << 1 \end{aligned}\right\} \qquad 6.3.12$$

The prime on S^{q}_{ii} denotes normalization as in 6.3.10. $E\{\ \}$ and $var\{\ \}$ denote expectation and variance of the corresponding random variables over an ensemble of possible environments. ε is the normalized standard deviation, or coefficient of variation.

The validity and accuracy of the method both depend on adequately satisfying conditions 6.3.11 and 6.3.12, and to examine these it is necessary to introduce a probabilistic description of the range of possible environments. Referring to 6.3.5 this would seem to require that distributions of the S^{Σ}_{++} quantities be specified.

In fact it is convenient to include the I_{rr} terms within the probabilistic model so that an environment may be represented by a sample set of values of $(I_{rr}.\ S^{z}_{rr}) \equiv \overline{p^2}_r$, $r = 1,2,..\ N$. (These may be conveniently referred to as modal energies).

Denote the k^{th} sample set of modal energies drawn from a population by:

$$\overline{p^2}_{r(k)} = H_{r(k)}\ ,\ r = 1,2,..\ N \qquad 6.3.13$$

For any type of environment, assume that H_r is a random variable with the representation:

$$H_r = G.h_r\ ;\ r = 1,2,..\ N \qquad 6.3.14$$

where G is an arbitrary multiplier, and h_r is a random variable with:

$$E\{h_r\} = m\ ;\ r = 1,2,..\ N \qquad 6.3.15$$

$$\text{var}\{h_r\} = \sigma^2;\ r = 1,2,..\ N \qquad 6.3.16$$

$$E\{h_r.\ h_s\} = m^2;\ r \neq s\ ;\ r,s = 1,2,..\ N \qquad 6.3.17$$

The modal energies are assumed to be equally and independently distributed, having effectively a single parameter, namely the normalized standard deviation σ/m. The actual distribution of H_r is not specified. This model is justified by its simplicity and its generality. It is certainly relevant to the case of point forces located at random on the structure. In the case of distributed pressure fields, it is conceivable that in some cases the assumption of independence of modal energies will not be strictly valid since correlations will certainly exist between the responses of modes close together in wavenumber within the band.

Now for the k^{th} sample set of modal energies from the hypothetical population, the broad band spectral density of any response q_i may be written from 6.3.5:

$$S^{q}_{ii\,(k)} = \frac{1}{B}\sum_{r=1}^{N} |C_{ri}|^2 H_{r(k)} = \frac{G_{(k)}}{B}\sum_{1}^{N} |C_{ri}|^2 h_{r(k)} \qquad 6.3.18$$

and the spectral density of displacement at (x_i, y_i) is given by:

$$S^{w}_{ii\,(k)} = \frac{1}{B}\sum_{1}^{N} \phi^2_r(x_i,y_i) H_{r(k)} = \frac{G_{(k)}}{B}\sum_{1}^{N} \phi^2_{ri}\, h_{r(k)} \qquad 6.3.19$$

Taking the space average of 6.3.19:

$$\langle S^{w}_{(k)} \rangle = \frac{G_{(k)}}{B}\sum_{r=1}^{N} \langle \phi^2_{ri} \rangle h_{r(k)} = \frac{G_{(k)}}{B}\langle \phi^2 \rangle \sum_{1}^{N} h_{r(k)}$$

$$= \frac{G_{(k)}}{B}.\langle \phi^2 \rangle . N . m_{(k)} \qquad 6.3.20$$

$m_{(k)}$ is the sample mean of modal energies for the k^{th} sample. In 6.3.20 all mode shapes are assumed to be normalized to have the same mean square. From 6.3.18 and 6.3.20 follows the normalized response for the k^{th} sample:

$$S^{q'}_{ii\,(k)} = \frac{S^{q}_{ii\,(k)}}{\langle S^{w}_{(k)} \rangle} = \frac{1}{N\langle \phi^2 \rangle}\sum_{r=1}^{N} |C_{ri}|^2 \frac{h_{r(k)}}{m_{(k)}} \qquad 6.3.21$$

Taking the expectation of this over the sample space of environments:

$$E\{ S^{q'}_{ii} \} = \frac{1}{N\langle \phi^2 \rangle}\sum_{r=1}^{N} |C_{ri}|^2 E\left\{ \frac{h_{r(k)}}{m_{(k)}} \right\} \qquad 6.3.22$$

The expected values of the quotients in 6.3.22 are difficult to evaluate even if the distribution of h_r is specified. But for large N, $m_{(k)}$ will be close to m for any sample set, and:

$$E\left\{ \frac{h_{r(k)}}{m_{(k)}} \right\} \doteq \frac{E\{ h_{r(k)} \}}{m} = 1 \qquad 6.3.23$$

Hence:

$$E\{S_{ii}^{q'}\} = \frac{1}{N\langle\phi^2\rangle}\sum_{i}^{N}|C_{ri}|^2 \qquad 6.3.24$$

Since 6.3.24 is independent of the environment parameters, it follows that condition 6.3.11 is satisfied for all broad band responses, even if the service case (I) and simulated case (II) are represented by different populations.

Now consider the coefficient of variation for the sample space of environments, through the variance of $S_{ii(k)}^{q'}$. From 6.3.21 and 6.3.22 this may be written:

$$\text{var}\{S_{ii}^{q'}\} = E\{(S_{ii}^{q'})^2\} - E^2\{S_{ii}^{q'}\}$$

$$= \frac{1}{N^2\langle\phi^2\rangle^2}\left[\sum_{r,s}^{N}|C_{ri}|^2|C_{si}|^2 E\left\{\frac{h_{r(k)}h_{s(k)}}{m_{(k)}^2}\right\} - \sum_{r,s}^{N}|C_{ri}|^2|C_{si}|^2 E\left\{\frac{h_{r(k)}}{m_{(k)}}\right\}E\left\{\frac{h_{s(k)}}{m_{(k)}}\right\}\right] \qquad 6.3.25$$

The expectations in 6.3.25 are not amenable to exact analysis, but for large N , the following approximation is valid:

$$E\left\{\frac{h_{r(k)}^2}{m_{(k)}^2}\right\} \doteq E\left\{\frac{h_{r(k)}^2}{m^2}\right\} = 1 + \frac{\sigma^2}{m^2}$$

Also the random variables $\frac{h_{r(k)}}{m_{(k)}}$ and $\frac{h_{s(k)}}{m_{(k)}}$ are not strictly independent since $m_{(k)} = \frac{1}{N}\sum_{r=1}^{N} h_{r(k)}$, but the correlation will be small for large N , and will be neglected. 6.3.25 reduces to:

$$\text{var}\{S_{ii}^{q'}\} = \frac{(\sigma/m)^2\sum_{r}^{N}|C_{ri}|^4}{N^2\langle\phi^2\rangle^2} \qquad 6.3.26$$

Hence the coefficient of variation is given by:

$$\varepsilon_i^2 = \frac{\text{var}\{S_{ii}^{q'}\}}{E^2\{S_{ii}^{q'}\}} = \frac{(\sigma/m)^2\sum_{r}^{N}|C_{ri}|^4}{\sum_{r,s}^{N}|C_{ri}|^2|C_{si}|^2} \qquad 6.3.27$$

6.3.27 shows that the coefficient of variation for any response is proportional to the dispersion of the modal energies arising from the environment, (σ/m).

It will also vary from point to point on the structure. There is a general indication in 6.3.27 of the convergence of ε_i^2 to zero with increasing N from the fact that there are N terms in the numerator and N^2 terms in the denominator. On this basis condition 6.3.12 will be adequately satisfied at some ultimate value of N, so that in principle, the validity of the statistical approach is established.

It is desirable to obtain a quantitative estimate of the requisite number of modes per band. This is possible for displacement response, in which case 6.3.27 takes the form:

$$\varepsilon_i^2 = \frac{\mathrm{var}\{S_{ii}^{w'}\}}{E^2\{S_{ii}^{w'}\}} = \frac{(\sigma_m)^2 \sum \phi_{+i}^4}{\sum \phi_{+i}^2 \phi_{si}^2} \qquad 6.3.28$$

Following Bolotin (1964), the plate or shell modes in the interior region may be represented by:

$$\phi_+(x,y) = \sin k_{+x}(x - x_{+o}) \sin k_{+y}(y - y_{+o}) \qquad 6.3.29$$

In 6.3.29, k_{+x} and k_{+y} are wavenumbers in the X and Y directions and x_{+o}, y_{+o} are phase constants. 6.3.28 cannot be evaluated easily at any particular position, but its space average over the structure area may be estimated:

$$\langle \varepsilon_i^2 \rangle = (\sigma_m)^2 \left\langle \frac{\sum \phi_{+i}^4}{\sum \phi_{+i}^2 \phi_{si}^2} \right\rangle \qquad 6.3.30$$

If the modes are distributed throughout the structure, then at large N the denominator in 6.3.25 will not vary much from point to point and may be replaced by its space average. Hence:

$$\langle \varepsilon_i^2 \rangle \doteq (\sigma_m)^2 \frac{\langle \sum \phi_{+i}^4 \rangle}{\langle \sum \phi_{+i}^2 \phi_{si}^2 \rangle} \qquad 6.3.31$$

Substituting from 6.3.29, the space averages may be obtained by integration.

For the numerator terms, integration of ϕ_{+}^{4} over a single wavelength in the X and Y directions is required. The integral is independent of wavenumber and may be evaluated in terms of Gamma Functions. (Dwight, 1961). Hence $\langle \phi_{+i}^{4} \rangle = 0.140$. The space average of the denominator terms may be estimated by integration. If the wavenumbers are not the same, $k_{+x} \neq k_{sx}$ and $k_{+y} \neq k_{sy}$, then by integrating over several wavelengths of one mode shape and neglecting small end effects, $\langle \phi_{+i}^{2} \phi_{si}^{2} \rangle = 0.0625$. For many mode pairs in the same band, the mode shapes in the X or Y direction will be similar and the above estimate will be poor for such pairs. This effect cannot be easily included, so the estimate will be used for all pairs.

Finally:

$$\langle \varepsilon_i^2 \rangle = \frac{2.24}{N} \left(\frac{\sigma}{m}\right)^2 \qquad 6.3.32$$

This is an approximate but useful guide to the accuracy of the statistical approach with a given number of modes per band. The space average of ε_i^2 for displacement response is inversely proportional to N , and at any given N its value depends directly on the dispersion of modal energies for the particular environment. The problem of estimating this latter quantity has not been investigated in detail, but presumably suitable values can be arrived at on the basis of experimental results or analytical models of the environment.

The case of excitation of a plate by single or multiple point forces is easily treated. This case is relevant to simulation conditions, and may be used to gain some insight into the area of validity of the statistical approach. For the case of a single force with spectral density S_{kk}^{p} positioned at random on the structure, σ/m is 1.12, assuming equal generalized masses and damping for the modes.

With a set of K independent forces having equal spectral densities, σ/m is proportional to $K^{-\frac{1}{2}}$. Returning to the single force case, expression 6.3.32 shows that the space average of ε_i will be 0.1 or 10% with 280 modes in the band. By appeal to the Central Limit Theorem, $S_{ii}^{\omega\prime}$ will be more or less Gaussian irrespective of the actual distribution of the modal energies, so that in a single trial, $S_{ii}^{\omega\prime}$ will be within 20% of the expected value with 0.95 probability.

The accuracy of the simulation process as a whole must be considered. This consists of replacing one sample response surface by another, scaled to reproduce the space mean or alternatively scaled to reproduce the response at a single reference location or the average response of a multiple set of references. In terms of the statistical approach each surface is considered to be a random function, so that the accuracy to be expected in a single trial can only be inferred from probabilistic statements. An exact treatment of this problem, that is seeking to establish a variance for $S_{ii\,(II)}^{q}/S_{ii\,(I)}^{q}$ or even for its space average, subject to amplitude scaling, would seem prohibitive.

Let $S_{ii\,(I)}^{q}$ and $S_{ii\,(II)}^{q}$ represent the response at any point of the structure in the service and simulated cases respectively, and let $S_{ii\,(I)}^{q\prime}$ and $S_{ii\,(II)}^{q\prime}$ denote the normalized responses.

$$S_{ii}^{q\prime} = \frac{S_{ii}^{q}}{\langle S^{\omega} \rangle}$$

Suppose that a representative value of coefficient of variation ε_i is known. This of course depends on the particular environment and is a function of position. For convenience a single value will be assumed to be valid for both service and simulated environments.

The ratio $S_{ii\,(II)}^{q}/S_{ii\,(I)}^{q}$ is a random variable in any simulation test. Writing this:

$$\frac{S_{ii\,(II)}^{q}}{S_{ii\,(I)}^{q}} = \frac{S_{ii\,(II)}^{q\prime}}{S_{ii\,(I)}^{q\prime}} \frac{\langle S_{ii\,(II)}^{\omega} \rangle}{\langle S_{ii\,(I)}^{\omega} \rangle} \qquad 6.3.33$$

If the simulation achieves reproduction of the space average displacement response, then:

$$\frac{S^{q}_{ii\,(m)}}{S^{q}_{ii\,(x)}} = \frac{S^{q'}_{ii\,(m)}}{S^{q'}_{ii\,(x)}} \qquad 6.3.34$$

For any structure response q_i, the numerator and denominator in 6.3.34 take the form of a sum of N positive random numbers. A well known procedure for obtaining approximate distribution functions for such sums is to represent them by chi-square distributions having an appropriate number of degrees of freedom. (Crandall, 1963, Chapter 2). The equivalent number of degrees of freedom, n, is obtained from:

$$\varepsilon_i^2 = \frac{2}{n} \qquad 6.3.35$$

Carrying the analogy a stage further, the ratio 6.3.34 may be regarded as the ratio of two independent chi-square random variables and its distribution will be well represented by Fisher's F-distribution (Kendall and Stuart, 1958), in which case the expectation of the response ratio is given by:

$$E\left\{\frac{S^{q}_{ii\,(m)}}{S^{q}_{ii\,(x)}}\right\} = \frac{n}{n-2} \doteqdot 1 \quad ; \text{ for large n.} \qquad 6.3.36$$

and the variance by:

$$\text{var}\left\{\frac{S^{q}_{ii\,(m)}}{S^{q}_{ii\,(x)}}\right\} = \frac{2n^2(2n-2)}{n(n-2)^2(n-4)} \doteqdot \frac{4}{n} \qquad 6.3.37$$

In 6.3.36 and 37, the results for the F-distribution with equal degrees of freedom in the numerator and denominator have been used.

In the case of simulation of a single reference response a similar prediction of the variance of the response ratio may be made.

Let $S^{q}_{aa(x)}$ represent the service response at the reference:

Then $$S^{q}_{aa(m)} = S^{q}_{aa(x)} \qquad 6.3.38$$

This does not in general achieve simulation of the space mean. By 6.3.38:

$$\langle S^{w}_{(m)} \rangle = \frac{S^{q'}_{aa(x)}}{S^{q'}_{aa(m)}} \cdot \langle S^{w}_{(x)} \rangle \qquad 6.3.39$$

Hence, the response ratio in the simulation test for any response co-ordinate q_i is given by:

$$\frac{S^{q}_{ii(m)}}{S^{q}_{ii(x)}} = \frac{S^{q'}_{ii(m)} \langle S^{w}_{(m)} \rangle}{S^{q'}_{ii(x)} \langle S^{w}_{(x)} \rangle} = \frac{S^{q'}_{ii(m)}}{S^{q'}_{ii(x)}} \frac{S^{q'}_{aa(x)}}{S^{q'}_{aa(m)}} \qquad 6.3.40$$

In this case, the response ratio may be regarded as the product of two F-distributed random variables, assumed independent for responses at points not too close to the reference.

Then:

$$E\left\{\frac{S^{q}_{ii(m)}}{S^{q}_{ii(x)}}\right\} \doteq 1 \quad ; \text{ for n large.} \qquad 6.3.41$$

$$\text{var}\left\{\frac{S^{q}_{ii(m)}}{S^{q}_{ii(x)}}\right\} \doteq \text{var}\left\{\frac{S^{q'}_{ii(m)}}{S^{q'}_{ii(x)}}\right\} E^{2}\left\{\frac{S^{q'}_{aa(x)}}{S^{q'}_{aa(m)}}\right\} + \text{var}\left\{\frac{S^{q'}_{aa(x)}}{S^{q'}_{aa(m)}}\right\} E^{2}\left\{\frac{S^{q'}_{ii(m)}}{S^{q'}_{ii(x)}}\right\} \doteq \frac{8}{n} \qquad 6.3.42$$

The results 6.3.37 or 6.3.42 in conjunction with the estimated number of degrees of freedom 6.3.35 make possible simple predictions of the variance or standard deviation of the response ratio at any point, and together with the result that the F-distribution tends to normality at large n, allow estimates to be made of the simulation accuracy to be expected in a single trial. By 6.3.35, the coefficient of variation of normalized response ε_i plays a central role in the estimation of simulation accuracy, and must be known. For displacement response, ε_i may be estimated from its space average 6.3.32 provided the dispersion of the modal energies can be estimated.

The question of the accuracy of simulation of other kinds of response will be considered in the next section.

Returning to the case of a single random force on the structure, it is possible to simulate the response with a second force located at random on the structure, whose spectral density is adjusted to match the broad band response at a single reference. With 280 modes in the band, ε was estimated to be 0.1 By 6.3.35, the equivalent number of degrees of freedom is estimated to be 200. By 6.3.42 the variance of the response ratio is .04, i.e. a standard deviation of 0.2. The analysis predicts that errors in the response ratio of 20% are quite possible, and errors of 40% not impossible. While the general validity of the statistical approach has been established it would seem from the illustrative case considered that a distressingly large number of modes per band are required to obtain a nominal degree of accuracy.

6.4 Further Considerations of the Statistical Approach

From the results of the previous section it is possible to estimate the accuracy of simulation of displacement responses. The accuracy of simulation of other responses e.g. velocity and acceleration, may be important. Also accurate stress or strain simulation will be obviously important in endurance tests. The formal expression (6.3.27) for the coefficient of variation is relevant to all such responses and is the key factor in considering simulation accuracy.

For velocity and acceleration responses, it follows immediately that the results for displacement simulation accuracy can be used. The influence coefficients for displacement have only to be multiplied by $(i\omega)$ or $(-\omega^2)$ to represent velocity or acceleration.

ω may be replaced by the band centre frequency in taking the band average, and the frequency factor cancels out in 6.3.27.

In the cases of stress and strain responses, a complication arises in that the modal influence coefficients contain space derivatives of the mode shapes, and will contain wavenumbers explicitly. Further, for a plate or shell structure, a frequency band will usually contain a wide range of wavenumbers so that a wider distribution in the values of influence coefficients might be expected for any response. This can only result in a reduction in the simulation accuracy of such responses. There is little hope of obtaining general results for this aspect of simulation, but the rectangular plate case has been studied to obtain insight into the problem.

Consider a rectangular plate, having side lengths a and b, thickness h, plate rigidity D, and material density ρ . For simply supported edges, the natural frequencies are given by:

$$\omega = [k_x^2 + k_y^2][\frac{D}{\rho h}]^{\frac{1}{2}} \qquad 6.4.1$$

with:

$$k_x = \frac{m\pi}{a} \; ; \; k_y = \frac{n\pi}{b} \; ; \; m,n = 1,2, \ldots \infty \qquad 6.4.2$$

The solutions 6.4.1 and 6.4.2 are good approximations for other edge conditions at frequencies well above the fundamental. (Bolotin, 1964). For points away from the boundaries, the representation of the r^{th} mode shape:

$$\phi_r(x,y) = \sin k_{rx}(x - x_{ro}) \sin k_{ry}(y - y_{ro}) \qquad 6.4.3$$

is valid for all boundary conditions. x_{ro} and y_{ro} are phase constants.

The modes may be usefully represented as points of intersection of a grid in wavenumber space, as in Fig. 6.4.1.

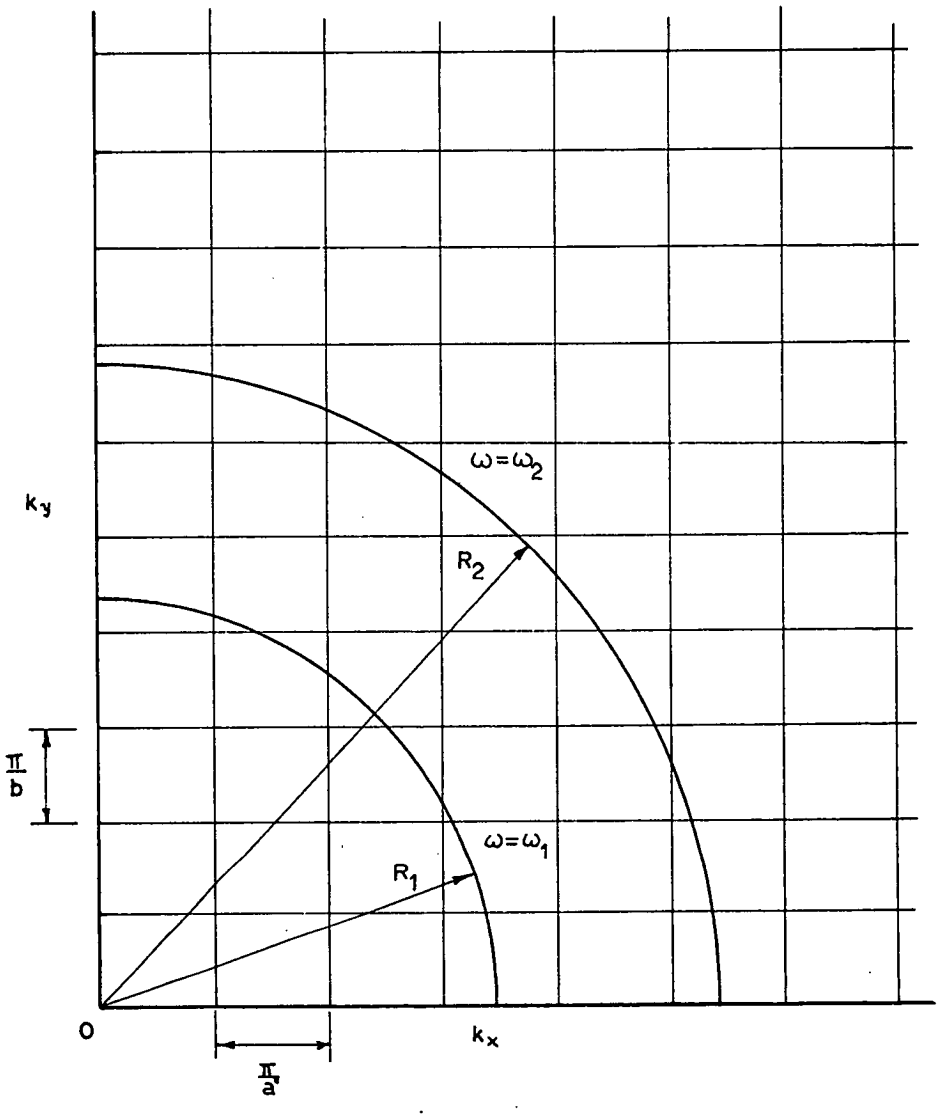

Fig. 6.4.1

Modes of a Simply-Supported Rectangular Plate as Points of Intersection of a Grid in Wavenumber Space.

From equation 6.4.1 it is seen that a line of constant frequency in wavenumber space is a circular arc, so that the modes having resonant frequency within a prescribed frequency band bounded by ω_1 and ω_2 are represented by the intersections of the grid between two circular arcs of radius $R_1 = (\omega_1^2 \frac{\rho h}{D})^{1/4}$ and $R_2 = (\omega_2^2 \frac{\rho h}{D})^{1/4}$. From this it is seen that a band of frequencies contains modes having a wide range of wavenumbers.

From Fig. 6.4.1 Bolotin's result for the sumber of modes having frequency less than Ω may be derived:

$$N(\Omega) = \frac{ab}{4\pi}\left[\frac{\rho h}{D}\right]^{\frac{1}{2}} \Omega \qquad 6.4.4$$

and hence the modal density (number of modal frequencies/radian/sec):

$$\frac{dN}{d\Omega} = \frac{ab}{4\pi}\left[\frac{\rho h}{D}\right]^{\frac{1}{2}} \qquad 6.4.5$$

Only flexural strains will be considered, so it is convenient to use curvature to represent direct strain. From 6.4.3 the modal influence coefficient for the curvature at (x_i, y_i) in a direction making an angle ψ_i with the X axis may be obtained by differentiation: (Curvatures are assumed small)

$$C_t(x_i, y_i, \psi_i) = k_{tx} k_{ty} \sin 2\psi_i \left[\cos k_{tx}(x_i - x_{to}) \cos k_{ty}(y_i - y_{to})\right] - \left[k_{tx}^2 \cos^2\psi_i + k_{ty}^2 \sin^2\psi_i\right]\left[\sin k_{tx}(x_i - x_{to}) \sin k_{ty}(y_i - y_{to})\right] \qquad 6.4.6$$

The expression for the corresponding broad band spectral density follows by substituting from 6.4.6 into 6.3.5. The general complexity of the influence coefficients and their dependence upon wavenumbers makes it impossible to obtain even a space average guide to the magnitude of the coefficient of variation (6.3.27.)

Bolotin (1964) has shown that the mean square stress at a clamped edge may be four times higher than the values in the interior. This sets additional importance on the accuracy of simulation of strains near a clamped or stiffened boundary. The modal influence coefficient for curvature in a direction normal to a clamped edge may be obtained from Bolotin's edge effect representation. (Bolotin, 1964).

For a clamped edge at $x = 0$, the r^{th} mode has the approximate form:

$$\phi_r(x,y) = \frac{\left[k_{rx}^2 + 2k_{ry}^2\right]^{\frac{1}{2}}}{\left[2(k_{rx}^2+k_{ry}^2)\right]^{\frac{1}{2}}} \left\{ \sin k_{rx} - \frac{k_{rx}\cos k_{rx} x}{\left[k_{rx}^2 + 2k_{ry}^2\right]^{\frac{1}{2}}} - \frac{k_{rx}\exp\left[-x(k_{rx}^2+2k_{ry}^2)^{\frac{1}{2}}\right]}{\left[k_{rx}^2 + 2k_{ry}^2\right]^{\frac{1}{2}}} \right\}$$

$$\times \left\{ \sin k_{ry}(y - y_{ro}) \right\} \qquad 6.4.7$$

For large x this tends to the expression 6.4.3 for the interior region. The influence coefficient for curvature at $x = 0$, normal to the boundary follows:

$$C_r(o, y_i) = \frac{\partial^2 \phi_r(o, y_i)}{\partial x^2}$$

which yields after simplification:

$$C_r(o,y_i) = 2^{\frac{1}{2}} k_{rx}\left[k_{rx}^2 + k_{ry}^2\right]^{\frac{1}{2}} \sin k_{ry}(y_i - y_{ro}) \qquad 6.4.8$$

In this case observe that $|C_{ri}|^2$ has the form:

$$C_r^2(o,y_i) = 2k_{rx}^2\left[k_{rx}^2 + k_{ry}^2\right] \sin^2 k_{ry}(y_i - y_{ro}) \qquad 6.4.9$$

Let (k_{ro}, θ_r) be the polar co-ordinates of the r^{th} mode in wavenumber space defined as:

$$\left.\begin{aligned} k_{rx} &= k_{ro}\sin\theta_r \\ k_{ry} &= k_{ro}\cos\theta_r \\ k_{ro}^2 &= k_{rx}^2 + k_{ry}^2 \end{aligned}\right\} \qquad 6.4.10$$

6.4.9 may be written:

$$C_r^2(o,y_i) = 2k_{ro}^4 \sin^2\theta_r \sin^2 k_{ry}(y_i - y_{ro}) \qquad 6.4.11$$

Apart from the scale factor, $2k_{+o}^4$, C_{+i}^2 for clamped edge strains has the same form as the square of the influence coefficient for displacement in the plate interior viz:

$$C_+^2(x_i,y_i) \equiv \phi_+^2(x_i,y_i) = \sin^2 k_{+x}(x_i - x_{+o}) \sin^2 k_{+y}(y_i - y_{+o}) \qquad 6.4.12$$

Further, in considering the formal expression for the coefficient of variation (6.3.27) for clamped edge strain response, k_{+o} may be replaced in each term by its band centre value and may be cancelled out in 6.3.27. In both these cases, the terms in the expression for coefficient of variation can take on the same range of values, so it may be expected that the space mean and the dispersion of sample values of ε_i will be the same for clamped edge strain response as for displacement response, and the accuracy of simulation will be comparable in any band.

It is not clear how formal analysis can make any further contributions.

6.5 Digital Computer Studies of Broad Band Responses.

In problems of a probabilistic nature which are not amenable to analysis, recourse may be made to numerical experiments based on the use of random numbers. Such methods, generally classed as "Monte Carlo" methods, have an impressive history of successful application, (Hammersley and Handscomb, 1964) and have gained recent impetus from the advent of the high speed computer. In their most elementary form, Monte Carlo methods lead to estimates of distributions or expected values of functions of random variables by simulating a large number of trials using random numbers drawn from suitable populations.

A procedure of this type was used to investigate the behaviour of broad band spectral densities of displacement and strain for a rectangular plate. The specific quantities which were estimated were sample values of the coefficient of variation ε_i of the normalized broad band spectral densities for (a) displacement at a number of random location on the plate, (b) direct strain at a number of sample locations and in randomly sampled directions in the plate interior, and (c) direct strain normal to a clamped boundary at a number of locations. In each case the effect of increasing the number of modes per band was studied.

In the first place it was necessary to specify a suitable distribution for the modal energies. Initially it was planned that the distribution should be representative of practical situations, but by virtue of the Central Limit Theorem, responses with more than a dozen modes involved approach a normal distribution irrespective of the actual form of the modal energy distribution. This latter is only then required to have a representative ratio of standard deviation to mean. Since it has been shown that ε_i is always proportional to σ/m, the calculations were in fact carried out with $\sigma/m = 1$; results for other cases may be obtained by scaling.

The distribution finally selected to represent modal energies was the normalized χ^2 distribution:

$$\frac{\chi^2}{n} = \frac{1}{n}\sum_{j=1}^{n} Z_j^2 \qquad 6.5.1$$

where Z_j ; $j = 1, 2 \ldots n$ are independent normal random variables having zero mean and unit variance. The random variable $\left(\frac{\chi^2}{n}\right)$ has unit mean and variance:

$$\mathrm{var}\left\{\frac{\chi^2}{n}\right\} = \frac{2}{n} \qquad 6.5.2$$

So the ratio of standard deviation to mean is:

$$\frac{\sigma}{m} = \left[\frac{2}{n}\right]^{\frac{1}{2}} \qquad 6.5.3$$

This can be easily adjusted by changing the number of terms in 6.5.1. For $n > 2$ the distribution is unimodal. For $n \leqslant 2$, it is J shaped. Since $\frac{\chi^2}{n}$ samples are positive with unit mean and adjustable variance they were regarded as a suitable choice to represent modal energies. Furthermore they may be easily generated on a computer. Starting with the basic routine RandomK , which generated independent random numbers uniformly distributed between 0 and 1, gaussian samples with zero mean and unit variance were obtained from these by taking the sum of a sequence of twenty of them and re-scaling. Finally the gaussian samples were squared and combined according to 6.5.1 with $n = 2$ to achieve the correct dispersion, $\sigma/m = 1$. A program was written in Atlas Autocode to generate and store 5×10^5 samples on magnetic tape for subsequent use.

The next stage was concerned with specifying the characteristics of the plate model. It was highly convenient to specify the model dimensions at this stage, although there is a little loss of generality in doing this. The following sizes were used:

Side lengths $a = 48$ ins; $b = 37$ ins.

Thickness $h = 0.064$ ins.

Modulus of Elasticity $E = 12 \times 10^6$

Poisson's Ratio $\nu = 0.3$

Third octave frequency bands with standard centre frequencies were used. A program was developed which evaluated all the natural frequencies and corresponding mode shapes (characterized by a pair of wavenumbers) in each frequency band.

The calculations were based on the simply - supported edge case. The results were filed on magnetic tape.

Finally, the estimation program was developed and used for selected $\frac{1}{3}$ octave bands containing a range of numbers of modes. The quantity to be estimated in each case was the coefficient of variation:

$$\varepsilon_i = \left[\frac{\mathrm{var}\{S_{ii}^{q\prime}\}}{E^2\{S_{ii}^{q\prime}\}}\right]^{\frac{1}{2}} \qquad 6.5.4$$

where S_{ii}^{q} is the broad band response spectral density for displacement or strain, and the prime indicates normalization by dividing through by the space average displacement response:

$$S_{ii}^{q\prime} = \frac{S_{ii}^{q}}{\langle S_{ii}^{w} \rangle} \qquad 6.5.5$$

In each case ε_i was estimated from the results of $n = 10^3$ independent trials using the estimators:

$$E\{S_{ii}^{q\prime}\} \doteq \frac{1}{n}\sum_{k=1}^{n} S_{ii(k)}^{q\prime} \qquad 6.5.6$$

$$\mathrm{var}\{S_{ii}^{q\prime}\} \doteq \frac{1}{n-1}\left[\sum_{k=1}^{n}(S_{ii(k)}^{q\prime})^2 - nE^2\{S_{ii}^{q\prime}\}\right] \qquad 6.5.7$$

The actual program was elaborate in its organization, but the calculations themselves were straightforward. A detailed listing is not included in the report. Matrix operations were used where possible to reduce running time. In outline the program was arranged as follows. The random sample locations were first allocated using the RandomK routine. For a specific band and response type, the influence coefficient for each location and mode were evaluated using the filed data.

At this stage the phase constants of the mode shapes were assumed to be randomly distributed in (0, 2π). Independent trial calculations were then made of $S_{ii}^{q\prime}$ using sets of modal energy samples from the magnetic tape file. The difficulty of normalizing S_{ii}^{q} without computing the actual space mean displacement was solved in the following way:

From 6.3.18 and 6.3.20 $S_{ii}^{q\prime}$ may be expressed as:

$$S_{ii}^{q\prime} = \frac{1}{\langle\phi^2\rangle \sum_{r=1}^{N} H_{r(k)}} \sum_{r=1}^{N} |C_{ri}|^2 H_{r(k)} \qquad 6.5.8$$

$$= \frac{1}{N\langle\phi^2\rangle} \sum_{r=1}^{N} |C_{ri}|^2 H'_{r(k)} \qquad 6.5.9$$

In 6.5.8 and 6.5.9, $H_{r(k)}$ is the rth modal energy in the kth sample set, and:

$$H'_{r(k)} = \frac{H_{r(k)}}{\frac{1}{N}\sum_{1}^{N} H_{r(k)}} \qquad 6.5.10$$

In 6.5.9 the factor $N\langle\phi^2\rangle$ is constant for the band and will not affect the estimate of ε_i . 6.5.9 shows that normalization of S_{ii}^{q} is efficiently carried out by correcting each sample set of modal energies to have unit mean.

Sample values of $S_{ii}^{q\prime}$ and $(S_{ii}^{q\prime})^2$ were stored and finally ε_i was estimated through 6.5.6 and 6.5.7.

The first set of trials investigated displacement response at a set of 25 randomly chosen locations. Subsequent trials investigated direct strain (curvature) response at 25 locations in randomly chosen directions and clamped edge normal strain at 25 random edge locations.

On the question of accuracy of the estimates, the standard error of ε_i may be estimated to be of the order of 3% using results from Hammersley and Handscomb. The standard error is proportional to $n^{-\frac{1}{2}}$ where n is the number of trials. This was considered to be an acceptable order of accuracy.

It was originally intended to extend the Monte Carlo studies to investigate the distributions of actual simulation errors and to give confidence in the application of the F-distribution to this problem. This was not possible because of restrictions on computer usage.

6.6 Discussion of Results

The results for displacement response are shown in Fig. 6.6.1. Estimates of the coefficients of variation are given for the 25 sample locations and for 6 frequency bands containing from 12 to 190 modes per band. The mean of the results in any band may be taken to be an estimate of the space average value, and this obviously decreases with increasing modes per band in proportion to $N^{-\frac{1}{2}}$.

The results of Fig. 6.6.1 also show that in any band a sizeable variation of ε_i may occur from point to point on the plate. While 25 samples are not enough to accurately define the spatial distribution of ε_i , they do give an estimate of its extent. For N = 12 the samples occupy a range of 60% of the mean. For N = 190 they are contained in a range of 20% of the mean. This dispersion is caused by the dispersion of values of $|c_{+i}|^2$ over the individual modes at any location.

The approximate estimate for the space average of ε_i given by 6.3.32 is shown dashed in Fig. 6.6.1.

$$\langle \varepsilon_i^2 \rangle^{\frac{1}{2}} = \frac{g}{m} \left[\frac{2.24}{N}\right]^{\frac{1}{2}}$$

The approximation would seem to give a marked over-estimate of the space average of ε_i in any band, being of the order of 30% higher than the root mean square of the 25 samples in each band. This can only by the result of the approximations made in deriving 6.3.32. In particular,replacing the energy sample mean by the population mean in deriving 6.3.32 is equivalent to normalizing the k^{th} response by dividing through by the expected value of the space average instead of using the kth sample space average and can only lead to an over-estimate of the coefficient of variation.

Fig. 6.6.2 shows the results for the coefficient of variation of curvature responses for 25 random points on the plate. There is an obvious reduction of the band average value, proportional to $N^{-\frac{1}{2}}$ and the space average value is very close to the displacement response case. However the dispersion of sample values about the mean is extremely large, being spread over a range of about 75% of the mean in every band. It is further obvious from the scatter of results that there are insufficient points in each band to adequately define the limits of the distribution of values of ε_i for direct strain. It is clear that strain responses will cover a wider range of values than displacement responses for the same number of modes per band. This is the result of the complexity and wavenumber dependence of the modal influence coefficients for direct strain which therefore assume a wide range of values, a range which increases with increasing frequency due to the wavenumber range also increasing. This causes an increased variability of the terms of the series expression for S^q_{ii} and compensates for the variance reducing effect of the increasing number of terms.

The final set of results were obtained for the normal curvature at a clamped edge. Fig. 6.6.3 shows the results for 25 random points along a clamped boundary. The sample mean falls off with increasing N, in proportion to $N^{-\frac{1}{2}}$. The dispersion of samples in each band is much smaller than for strain in the plate interior and in fact the results for sample mean and dispersion about the mean for this case are almost identical to the results for displacement response. This is to be expected on the basis of the discussion of the previous section.

Results for the ratio of broad band strain spectral densities at a clamped edge and in the plate interior are shown in Fig. 6.6.4. The results represent the average values over the 25 sample locations in each case. The ratio reaches a fairly constant level of 5.7 for bands containing more than 24 modes, showing that higher strain response levels are to be expected in the vicinity of clamped or stiffened edges than in the plate interior.

In summary, the restricted number of results obtained in the Monte Carlo calculations clearly demonstrate the reduction in the fluctuations of the normalized broad band response surfaces with increasing modes per band. Representative values of the coefficient of variation are obtained and the variations from point to point on the plate for each band are illustrated. The similarity between the results for plate displacement and clamped edge strain is confirmed although the approximate theoretical estimate of the space average coefficient of variation for displacement is shown to give a poor prediction of the experimental values. It may be concluded that there will be comparable accuracy of simulation of displacement response and of clamped edge strain response for a given number of modes per band.

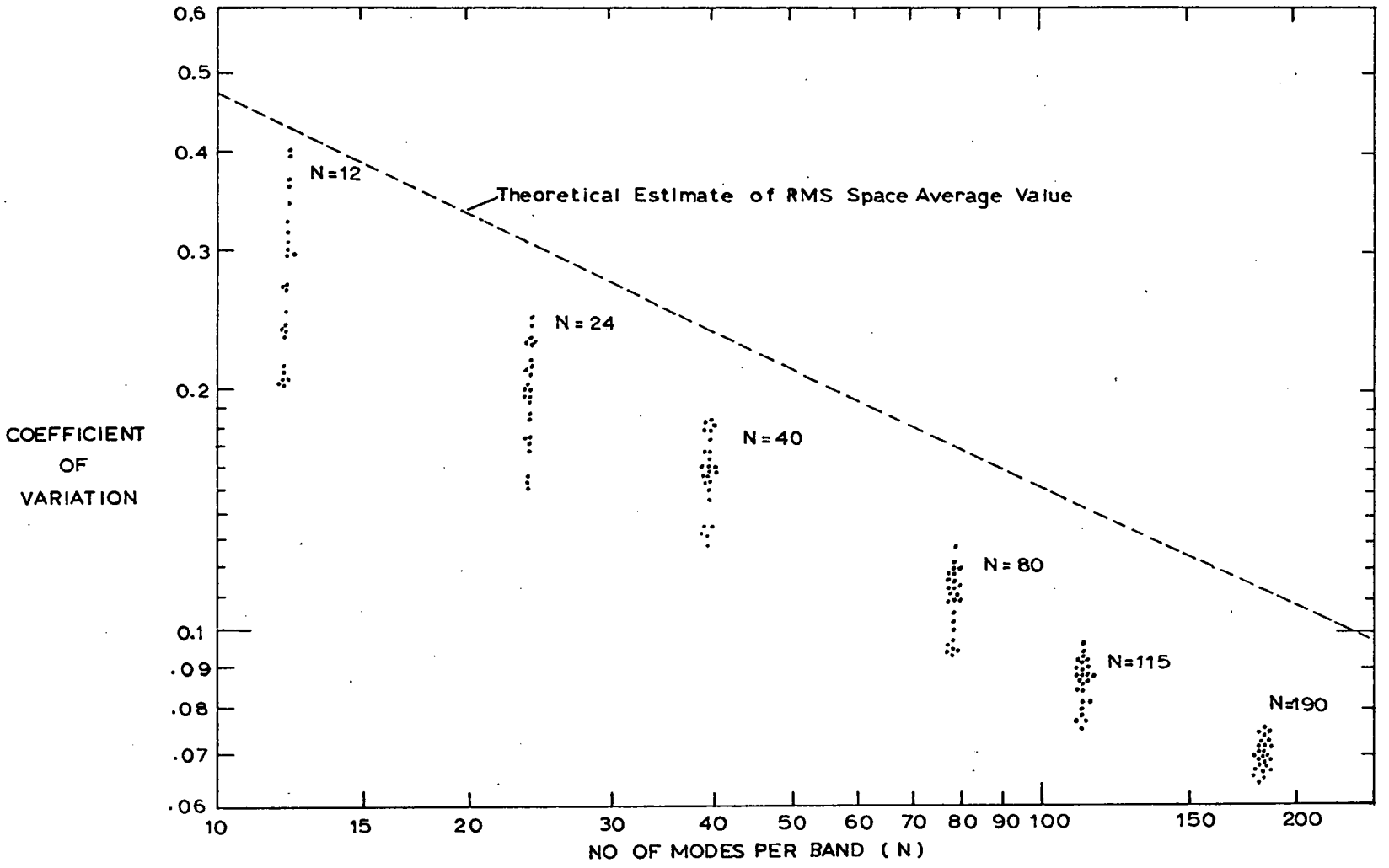

Fig. 6.6.1

Computed Samples of Coefficient of Variation for

Displacement Response of Rectangular Plate.

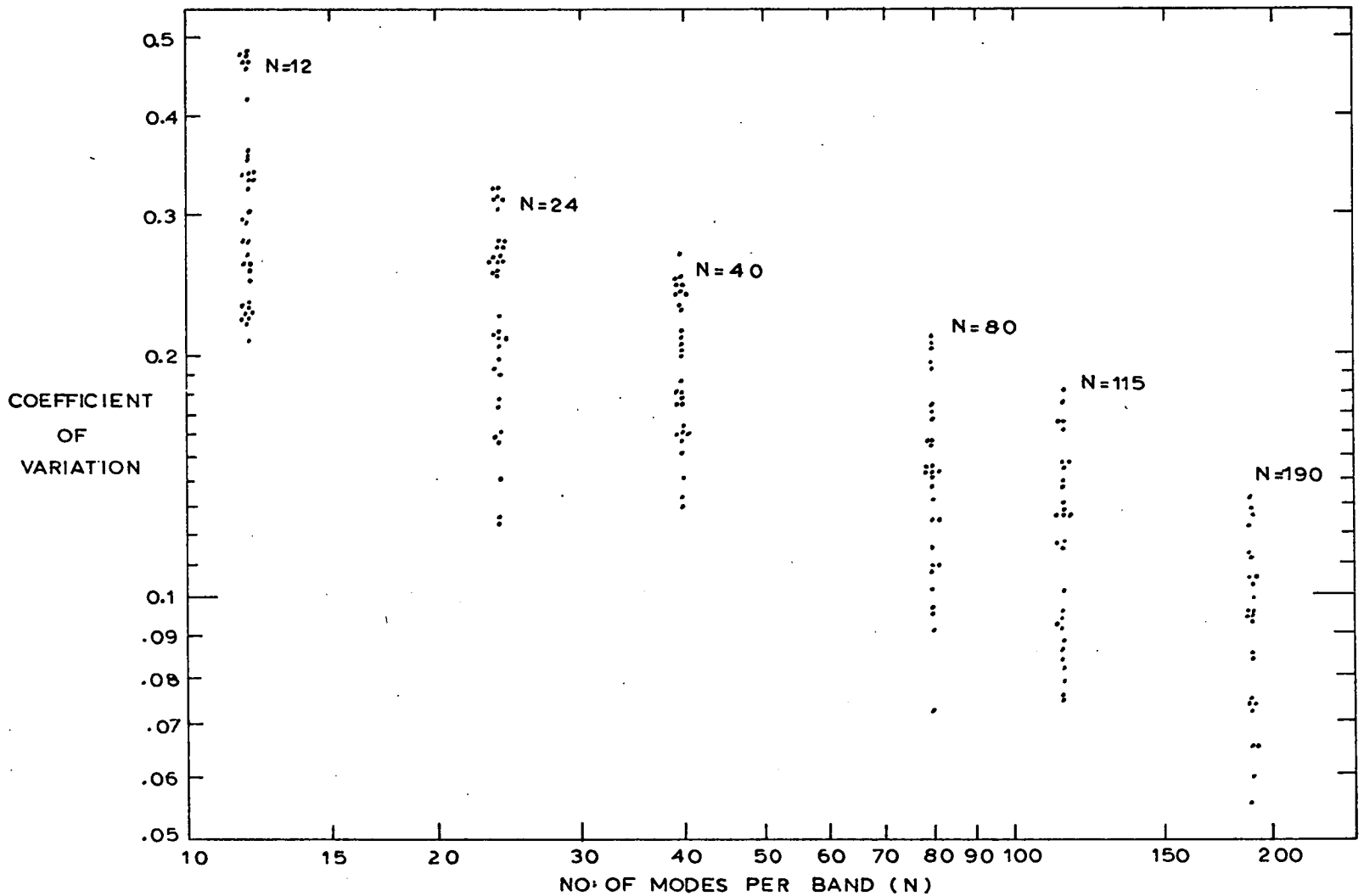

Fig. 6.6.2

Computed Samples of Coefficient of Variation for
Interior Strain Response of Rectangular Plate.

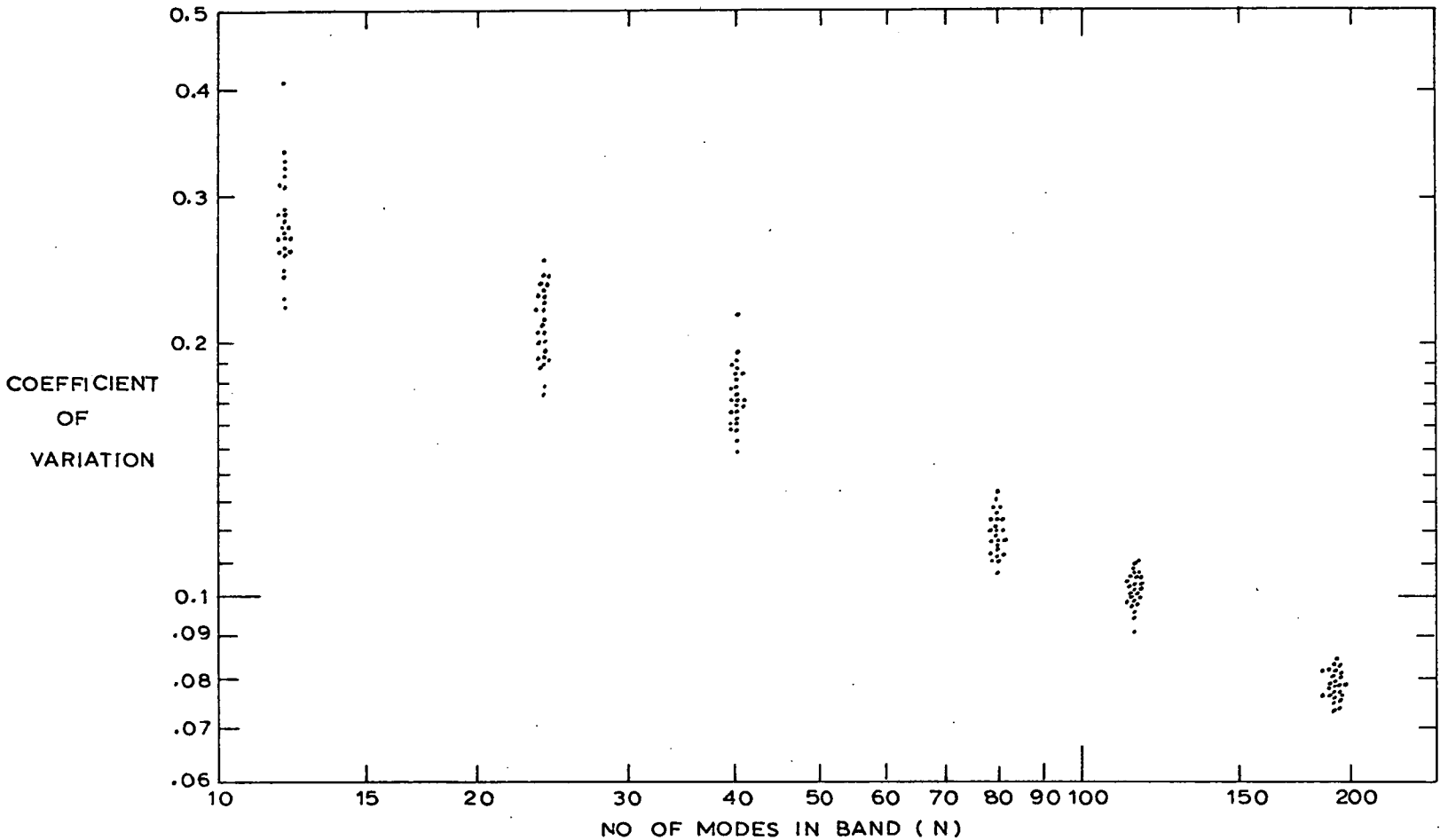

Fig. 6.6.3

Computed Samples of Coefficient of Variation for
Clamped-Edge Strain Response of Rectangular Plate.

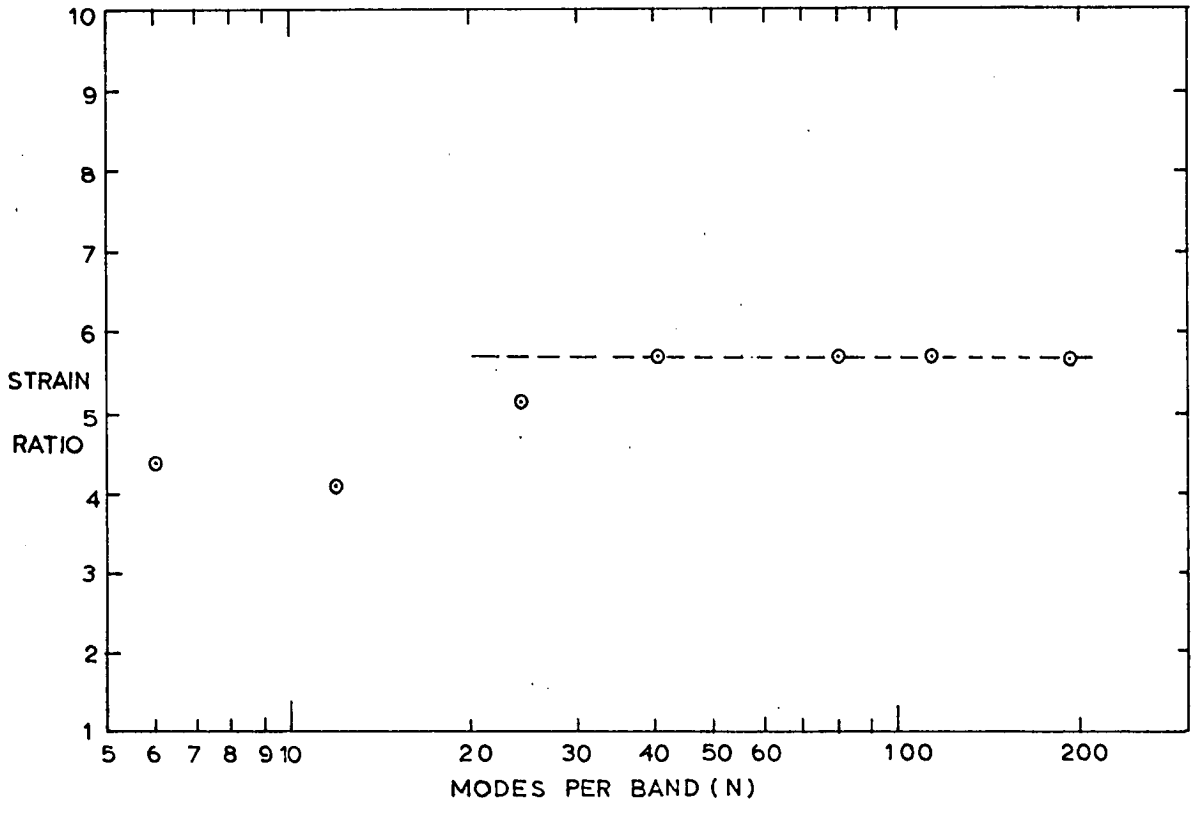

Fig. 6.6.4

Ratio of Average Values of Broad Band Strain Spectral Density for the Clamped Edge / Interior Region of the Rectangular Plate.

Many more modes per band will be required to obtain a comparable accuracy of simulation of interior strains but these will be less critical than the clamped edge strains.

6.7 Experimental Investigation

An experimental investigation of the statistical approach to simulation was carried out using a large rectangular plate model. An aluminium sheet, size 47 x 36 x 0.128 ins., was used and this was supported in a vertical position, being clamped along its longer edge to a lathe bed. Fig. 6.7.1 shows the arrangement.

Initial mode counting tests were carried out to check the estimated modal density of 0.109 modes/Hz . Modal frequencies were obtained by sweeping through the frequency range 0 to 1 kHz using a small vibrator and counting response peaks. This was repeated with the vibrator attached at two further locations. Fig. 6.7.2 shows the cumulative number of recorded modes compared with the theoretical estimate from Bolotin's result (6.4.4). Agreement is fairly good. The possibility of the response of a mode being masked by other modes cannot be avoided.

The investigation of simulation was based upon the representation of a service environment by a single vibrator sited at random on the plate surface. The broad band response spectral densities at a number of sample locations were recorded. Simulation of this response was attempted using a further vibrator located at random on the plate, the excitation level being adjusted in each band to repro-duce the broad band response at a designated reference point. The responses at the other sample points were recorded and from the response ratios in the two cases a measure of the accuracy of the simulation was obtained.

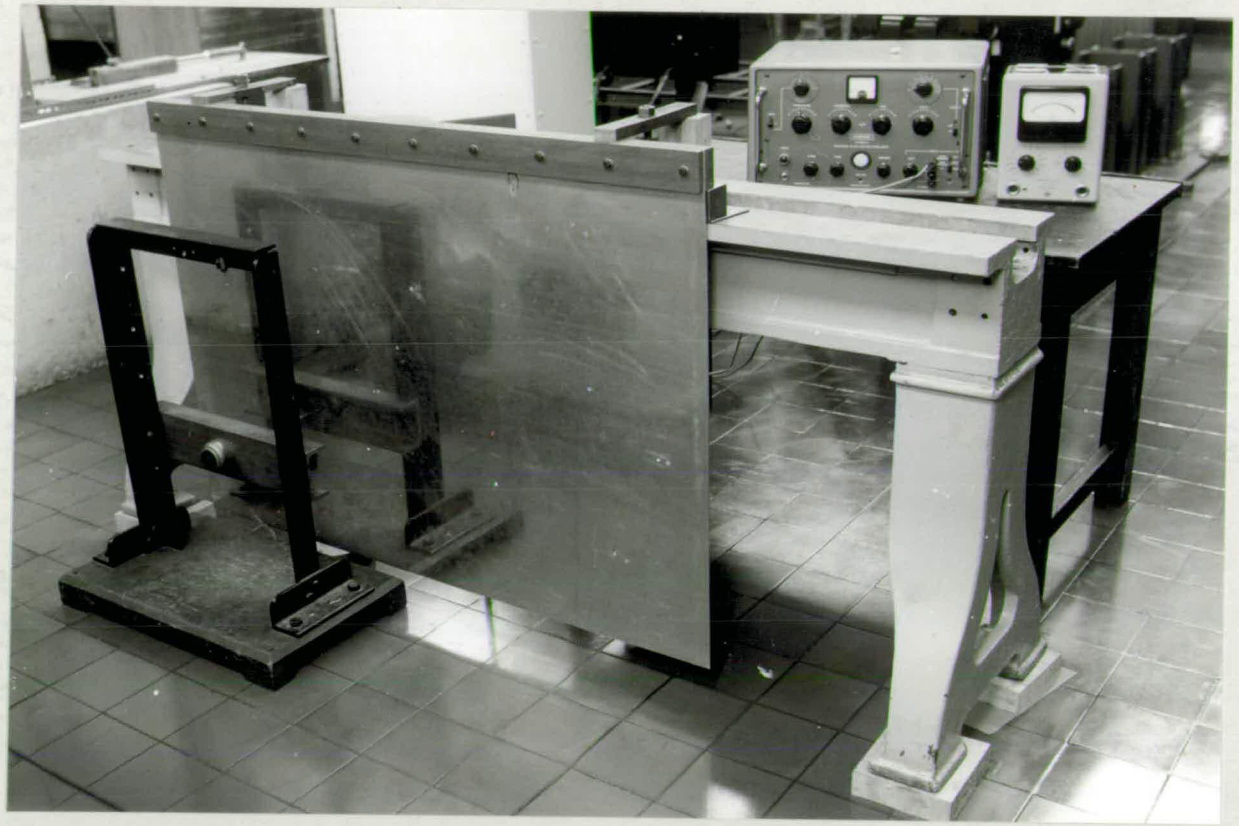

Fig. 6.7.1

Rectangular Plate Model.

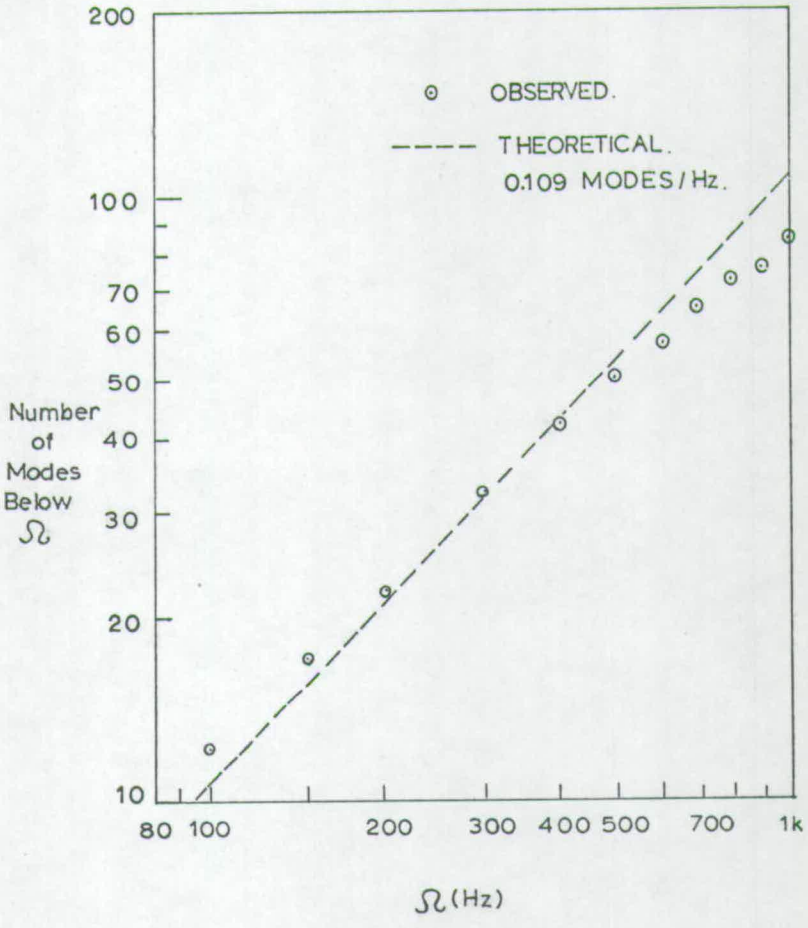

Fig. 6.7.2

Rectangular Plate: Cumulative Number of Observed Modes below any Frequency, compared with Theoretical Prediction.

Although the single vibrator service environment may seem far removed from the general case, it produces the essential feature of the general case, namely an indeterminate set of modal energies in any band. Furthermore in this case the dispersion of modal energies may be estimated on the basis of sinusoidal mode shapes.

In carrying out the tests, individual bands were examined in isolation, and a useful short cut was introduced. The process of adjustment of response levels at reference locations proved very time consuming. This was discarded in favour of recording responses at arbitrary excitation levels and scaling these up to simulate a matched response at the reference.

Fig. 6.7.3 shows the arrangement of apparatus for the tests. Filtering of the selected band was obtained using the Bruel and Kjaer Analyser Type 2107, set to have a 3db bandwidth of $\frac{1}{3}$ octave. Measurements were obtained for a number of bands containing a wide range of modes. The bandpass characteristic of the 2107 is not close to the ideal rectangular shape, so that it was never possible to state with precision the number of modes per band. At frequencies below 1 kHz, the filter was tuned to obvious clusters of modes, so that the number per band was reasonably well defined. At high frequencies this was not possible and the number per band was estimated from the product of modal density and 3db bandwidth.

The Hewlett Packard noise generator was used to provide the excitation. Note that the 2107 filter was inserted into the excitation system, following the noise generator and preceeding the power amplifier. In this way, all of the amplifier power was concentrated into a single band to obtain higher response levels, and also the problem of large low frequency motions being present when examining high frequency bands was avoided.

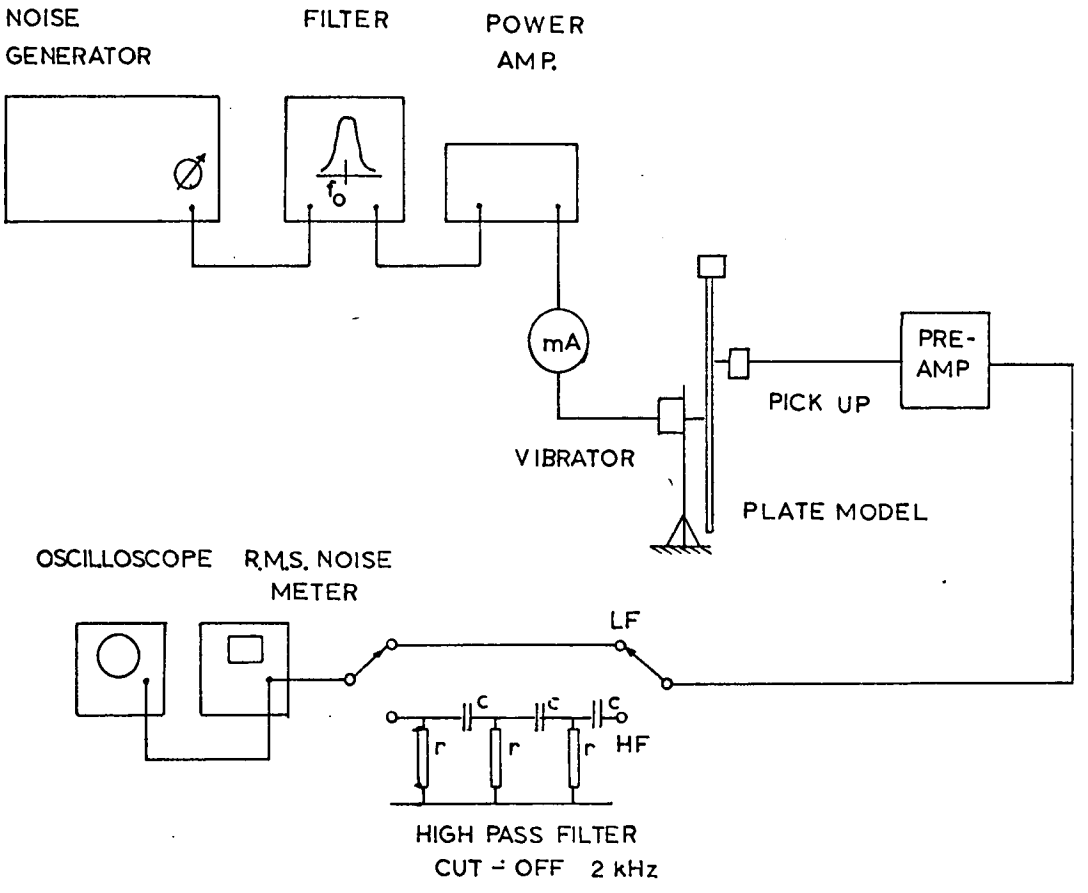

Fig. 6.7.3

Apparatus for Plate Tests.

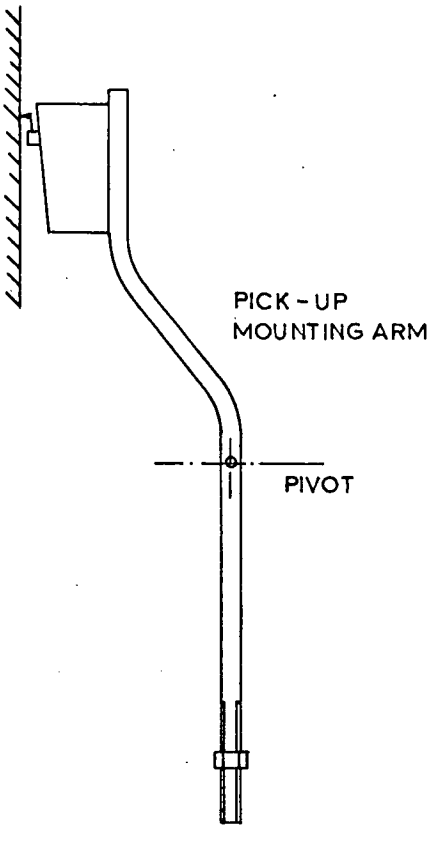

Fig. 6.7.4

Pick-Up Mounting Arrangement.

The vibrator was mounted in a heavy floor stand which permitted height adjustment and was coupled to the plate through 4BA screwed rod. Twelve excitation points distributed at random over the plate surface were used.

Several transducer systems were tried. The final choice was a stereo crystal cartridge (Acos Type GP-93) which gave a good output level proportional to displacement and was easily transferred from point to point. The cartridge was mounted on an inverted pendulum device as shown in Fig. 6.7.4. This was arranged to give the required stylus pressure of 6g against the vertical plate. The system was supported in a retort stand. The output from the pick-up was taken directly to the Bruel and Kjaer Random Noise Voltmeter, which measured the root mean square of the broad band signals (effectively the square root of the broad band spectral density). Some difficulty was experienced at high frequencies where it was found that a considerable amount of low frequency plate motion was present in the signal from the pick-up. This seemed to be due to noise leaking through the filter outside its passband. A further pre-amplifier was inserted after the pick-up, followed by a simple high pass filter having a cut-off frequency of 2 kHz and an attenuation of 18db/octave. This proved satisfactory, and enabled readings to be made up to band centre frequencies of 13 kHz.

The results were obtained for twelve frequency bands containing up to 170 modes per band. Twelve exciter positions were used and fourteen pick-up positions. By choosing each pick-up position in sequence as a reference and scaling up measured responses in the required ratio a large number of samples of response ratio were obtained. In fact 315 sample values together with their reciprocals were obtained in each band.

An Atlas Autocode program was used to scale the raw experimental levels to produce simulated response ratios.

6.8 Discussion of Experimental Results

The results are shown in Fig. 6.8.1. which is a graph of samples of Simulated Response Spectral Density/Service Response Spectral Density, with single point matching, against estimated modes per band. In Fig. 6.8.1, the extremes of the observed results are given together with the limits of the central 60% of observed results for each band. The results show that even with a sizeable number of modes per band a wide range of simulation errors is possible. The extreme values of response ratio show a reduction in spread with increasing modes per band although even with 170 modes per band the indicated range of possible error is large. The results for the 60% of distribution limits show a fairly obvious reduction in width with increasing modes per band for N greater then 50. Because of the relatively small sample size these cannot be taken to be accurate limits of the actual distribution of samples. A theoretical prediction of the 60% limits is shown by the dashed lines in Fig. 6.8.1. This was based upon an estimate for the coefficient of variation for the case of single force excitation. The space average of the Monte Carlo results was used, scaled up for $\sigma/m = 1.12$. The standard deviation of the response ratio at different numbers of modes per band was estimated using the F distribution approach of section 6.3 for single reference simulation. The 60% limits were obtained from tables of the normal distribution and the results are shown in Fig. 6.8.1. Bearing in mind the effects of a small sample size on the experimental results it is felt that the correspondence is fairly good between the theoretical and experimental limits.

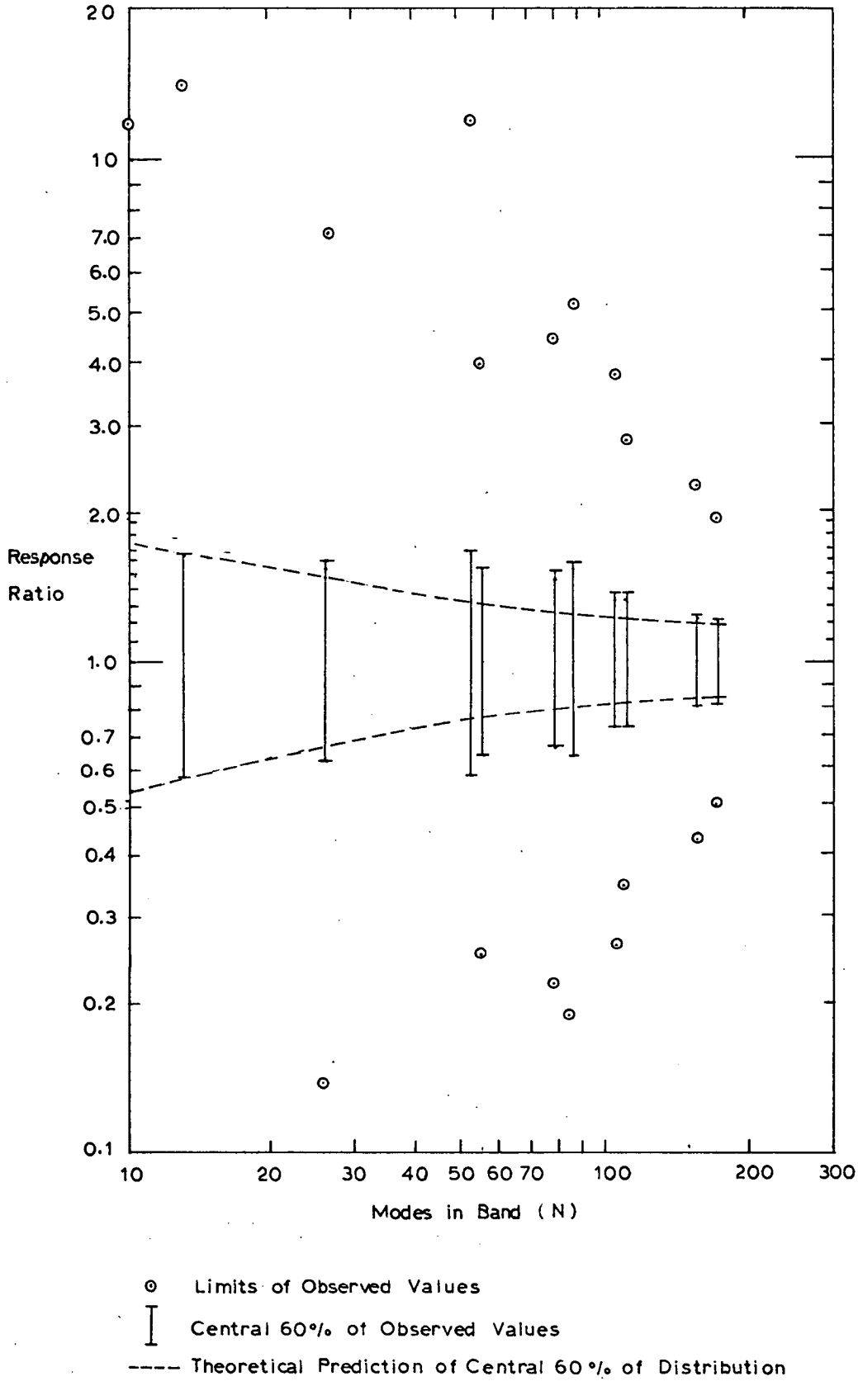

Fig. 6.8.1

Rectangular Plate: Samples of Broad Band Spectral Density Response Ratio for Single Vibrator, Single Reference Simulation in a range of Frequency Bands.

A final point is that while the effects of correlations between the modes have been neglected in the theoretical development they will certainly have occurred to some degree in the experimental responses, without producing any noticeable departures from the predicted behaviour.

6.9 Summary and Conclusion

A statistical approach to simulation has been examined for possible application to complex multi modal structures. The reproduction of broad band spectral densities at every point of the structure has been justified as a valuable goal of simulation and this may be adequately achieved using simple facilities due to the averaging effect of a large number of modal contributions in each band. The simulation test may be based upon reproducing a space average of several responses or a single reference response using substituted environment, which may be a single random force.

In analysing the response to service or simulating environments it has been assumed that the structure mode shapes cannot be precisely known and that the individual responses in each mode are not predictable in any particular case. In order to study the basis and the accuracy of this approach a probabilistic model of the environment was used so that hypothetical ensembles of possible responses were considered. Prediction of the accuracy of simulation in a single trial can only be based on a standard deviation of the response ratio over an ensemble of such trials.

It was shown that the coefficient of variation δ_i, of the normalized response surface was the key factor in the accuracy of the simulation.

While a general formulation for ε_i has been obtained in terms of the dispersion about the mean of the modal energies arising from an environment and its convergence to zero may be deduced for increasing modes per band, a numerical estimate of ε_i is not in general possible since it depends on the modal influence coefficients for the particular point. For displacement response, an approximate root mean square space average estimate of ε_i was derived for plate or shell structures having homogeneous sinusoidal mode shapes. The estimate is also valid for velocity and acceleration responses. Monte Carlo simulation trials on a digital computer were used to check this estimate and to give insight into the range of spatial variations of ε_i in frequency bands for displacement and strain responses. It was shown that the theoretical space average estimate gave a poor over-estimate of ε_i. Finally experimental results were obtained for the accuracy of simulation of a single random force on a large rectangular plate model. A fair measure of agreement was obtained between the experimental results and a theoretical prediction of their distribution.

Prospects for the statistical approach would seem to be diminished by the large number of modes per band apparently needed to achieve a nominal accuracy of say 20%. Even with a hundred modes per band, large errors were recorded in the cases studied. The question of what is an acceptable level of error is a difficult one and has not been established. There is no point in seeking greater accuracy than the order of measurement accuracy for spectral density estimates which might reasonably be of the order of 10% standard error. However further considerations would seem to give some hope that a much wider margin of error could be tolerated in each band.

The accuracy need only relate to the simulation of sample function behaviour as discussed in section 6.2. It may be shown for a random process with given mean square, that the expected number of peaks per second occurring in any amplitude interval is proportional to $\left[-R''/R\right]^{\frac{1}{2}}$, and this may be related to the broad band spectral densities as follows:

$$\left[\frac{-R''}{R}\right] \doteq \left[\frac{\sum \omega_o^2 \, B_o \, S_{ii}^q(\omega_o)}{\sum_{\omega_o} B_o \, S_{ii}^q(\omega_o)}\right]^{\frac{1}{2}} \qquad 6.9.1$$

The quantity $\left[-R''/R\right]^{\frac{1}{2}}$ is seen to be a characteristic frequency of the process, namely the radius of gyration of the spectral density curve about $\omega = 0$. Denote this Ω_o . It is seen from 6.9.1 that the cumulative effect of band errors on Ω_o is the important consideration rather than the magnitude of the simulation errors in individual bands, provided that the root mean square of the response is also adequately reproduced. Simulation accuracy for the statistical approach might well be defined as a tolerance of say 5% on the reproduction of the service value of Ω_o for every response of the structure. This improves the prospects for the statistical approach for three reasons. In the first place, errors in different bands will be positive or negative and statistically independent. This will reduce the overall errors in the series expressions in 6.9.1. Secondly, the square root operation in 6.9.1 means that error limits for any band should be referred to root spectral density rather than to spectral density. Thirdly, the radius of gyration analogue of 6.9.1 implies that large errors in the simulated spectrum in bands near Ω_o will have only a small effect upon the accuracy of simulation of Ω_o itself, while errors in the extreme upper and lower parts of the spectrum will have an accentuated effect.

Since Ω_o will generally lie in the mid-upper part of the frequency range, this means that large errors in broad band simulation can be tolerated in this region. At high frequencies, simulation errors will have a strong effect on Ω_o, but the accuracy will generally be improved in this region by the increased number of modes per band. Low frequency errors will also be significant, but this corresponds to frequency intervals where accurate uni-modal simulation will be possible. These effects remain to be established quantitatively but they would seem to hold some promise for an increased range of applicability of the statistical approach.

A final point is that the discussion of simulation accuracy contained in this chapter is equally relevant to the power flow simulation approach of Noiseux, (1964).

CHAPTER 7

CONCLUSIONS

7.1 Review of the Principal Results

The investigation has treated a highly idealized form of simulation, tests being based upon the availability of complete and accurate data from the responses of a dynamically similar structure in the service environment. This is justified since the intention has been to examine theoretical barriers to and theoretical possibilites for reasonably exact simulation by substitution, looking beyond current equipment limitations and the difficulties of basing tests upon inadequate information. Throughout the analysis the practical importance of simple results has been recognised and such results have been sought by introducing reasonable approximations. A consequence of the generality of the subject is the qualitative nature of the results.

In summary, the main results are as follows. Simulation in probability or in distribution is the fundamental basis for the tests as a consequence of the indeterministic nature of the environment, and simulation in spectral density of all structure responses at every frequency implies this. Exact simulation in spectral density at every frequency is not a practical possibility since it implies simulation of an infinite set of generalized force spectral densities at every frequency. By considering only resonant motion to be significant, a finite degree of freedom representation is justified for frequencies of interest. It then follows that simulation in spectral density of every response is achieved if the direct and cross spectral densities of a limited number of reference responses are reproduced;

the number corresponding to the number of modes having resonant frequency in the vicinity of the frequency under consideration. The simulation may be achieved using a set of the same number of force generators programmed to reproduce the reference spectral densities. The result is of extreme practical interest when the number of modes involved is only one, as will be the case if the structure has low damping and widely spaced natural frequencies. In this case a single direct spectral density is an adequate reference for the motions of the whole structure.

If two modes are contributing, the direct and cross spectral densities of a pair of reference responses characterize the structure motion and two programmed vibrators are required. For more than just a few contributing modes simulation is theoretically possible but obvious practical difficulties arise in dealing with a multitude of programmed vibrators.

In the case of frequency intervals of approximately unimodal response, the simulation can be simplified without loss of accuracy if broad observation bandwidth measurements of the reference response are used and the simulating force is adjusted in corresponding bands. The bandwidth may be arbitrarily wide provided it contains a single resonant frequency.

Finally, for complex multi-modal structures where the basic approach cannot lead to practical forms of simulation, an approach based upon reproducing the broad band spectral densities of the structure, where each band contains many modal frequencies, has been examined. This has been shown to be equivalent to reproducing the distributions of peaks and level crossings of the response sample functions.

There is possibility of achieving a close approximation to this degree of simulation using simple facilities e.g. a single vibrator, as a result of the averaging effects of a number of modal contributions within each band. While computer studies and experimental results indicate that a very large number of modes are required per band before the expected range of errors in the simulated broad band spectral densities is acceptably low, there is good reason to believe that the overall accuracy of the simulation can be much greater than the accuracy of simulation of the individual band responses, so that in fact a wider margin of error is tolerable in some bands. Further work remains to be done to establish the limits of applicability of this approach.

7.2 Application of the Results to Practical Environmental Testing

It is clear that a great deal of vibration testing is carried out on the basis of incomplete information and engineering judgement, with little pretence of accurately reproducing a service environment. Under such circumstances the results of the present work merely serve as a reference to demonstrate the minimal considerations that are necessary to achieve accurate simulation.

In circumstances where accurate simulation is desired and is economically feasible, the results of the present work are highly relevant. In applying the basic theory of simulation, two major practical difficulties emerge. In this approach there is first of all a need for a number (albeit a limited number) of accurate response measurements from a model in the service environment, and secondly there is a stringent requirement for dynamical similarity between the model used for field measurements and the environmental test model. The basic approach of Chapter 3 would lead to serious errors if the resonant frequencies did not precisely match in each case.

One would be trying to excite resonant amplitudes at non-resonant frequencies and vice versa. This difficulty is alleviated if the broad band approach of Chapter 5 is used. This approach is not susceptible to small variations of individual resonant frequencies from model to model and ensures that a resonant mode within a broad frequency band contributes its share of energy to the response irrespective of its precise position within the band. However the difficulties of dealing with the case of more than one resonant mode within each band have already been discussed in Chapter 5.

The question of the availability of service response information is an important one. It may be that the cost of obtaining this information is prohibitive, or that the structure is unique of its kind with no possibility of field response information for that particular model. Theoretically the possibility of simulating the environment still exists and may be conceived in the following way. (a) Estimate the generalized force spectral densities from an analytical model of the environment and knowledge of the natural modes of the structure. (b) Choose the important modes in any frequency range. (c) Estimate the system of vibrator forces required over each frequency interval containing resonant response to reproduce the service values of generalized force spectral densities, and apply these to the structure. The method requires accurate specification of the service environment, together with detailed knowledge of the structure modes. Consequently its usefulness would seem to be limited to well defined low frequency modes.

The statistical approach of Chapter 6 has obvious practical application to the testing of multi modal structures at high frequencies.

In this case the central problem is that of achieving a reasonable accuracy and while many aspects of this remain to be established, it is clear that the number of modal frequencies per band should be as high as possible, commensurate with the bandwidth being small compared with its centre frequency. There is no requirement for precise dynamical similarity between the field test and the environmental test models. In the complete absence of service reference responses, the scaling laws of the statistical energy approach may be used to compute spatial average responses for frequency bands which may be reproduced using vibrators.

PRINCIPAL NOTATION

a, b	Plate dimensions.
A	Area.
B	Width of frequency band.
C_{ri}	Modal influence coefficient.
D	Plate rigidity.
$E\{\ \}$	Expectation.
$f(\ )$	Probability density function.
$F(\ )$	Probability distribution function.
h	Plate thickness.
$h_{ik}(t)$	Impulse response at co-ordinate q_i.
$h_r(t)$	Impulse response of r^{th} mode.
H_r	Modal energy of r^{th} mode.
i	$\sqrt{-1}$.
I_{rs}	Integral of modal receptance product ($\equiv \int_0^\infty \alpha_r^* \alpha_s \, d\omega$)
k_{rx}	Wavenumber.
K_r	Generalized stiffness of r^{th} mode.
m	Mean of a random variable.
M_r	Generalized mass of r^{th} mode.
N	Number of modes in a frequency band.
p	Pressure.
P	Force.
q_i, q_j	Generalized co-ordinates.
Q	Magnification factor.

r, s	Subscripts referring to modes of vibration.
$R^{q}_{ij}(\tau)$	Cross-correlation function of $q_i(t)$, $q_j(t)$.
$S^{q}_{ij}(\omega)$	Cross spectral density of $q_i(t)$, $q_j(t)$.
t	Time.
$U(\ )$	Unit step function
var	Variance.
w	Plate deflection.
x, y	Spatial co-ordinates.
Z	Random variable.
$\alpha_{ik}(\omega)$	Cross receptance between q_i and P_k.
$\alpha_r(\omega)$	r^{th} modal receptance.
δ_r	Coefficient of viscous damping of r^{th} mode.
$\delta(\ )$	Delta function.
ε_i	Coefficient of variation. ($= \sqrt{\frac{\text{var}\{\ \}}{E^2\{\ \}}}$)
γ	Ratio of Generalized force spectral densities.
λ	Eigenvalue.
ν	Poisson's ratio.
ξ_r	r^{th} normal co-ordinate.
Ξ_r	Generalized force in r^{th} mode.
ρ	Density.
σ	Standard deviation.
τ	Time delay.
ϕ_r	r^{th} mode shape.
ψ	Phase angle.
ω	Circular frequency.
ω_r	Undamped natural frequency of r^{th} mode.

ω	Circular frequency.
$[A]$	Matrix.
$[A]'$	Transpose of $[A]$.
$[\bar{A}]$	Conjugate of $[A]$.
$[A]^{\dagger}$	Conjugate transpose of $[A]$.
$[A]^{-1}$	Inverse of $[A]$.
(A, B)	Inner product.
$\underset{\sim}{X}$	Vector.
$\underset{\sim}{X} \cdot \underset{\sim}{Y}$	Scalar product.
$\langle .. \rangle$	Averaging Operator.
Z^*	Complex conjugate of Z.

BIBLIOGRAPHY

BENDAT, J.S. and PIERSOL, A.G. — Measurement and Analysis of Random Data. John Wiley & Sons, New York, 1966.

BISHOP, R.E.D. and JOHNSON, D.C. — The Mechanics of Vibration. Cambridge University Press, 1960.

BLACKMAN, R.B. and — The Measurement of Power Spectra. Bell System Tech. Journal, Vol. 37 pp. 185-282, 485-569, 1958.

BOLOTIN, V.V. — On the Broadband Random Vibration of Elastic Systems. Proceedings of the 11th International Congress of Applied Mechanics, Munich 1964, Springer - Verlag, 1966.

BOOTH, G. — Vibration Generation. Chapter 9 in Random Vibration, Vol. 2. (Ed. Crandall) M.I.T. Press, 1963.

BOOTH, G.B. and BROCH, J.T. — Analog experiments compare improved sweep random tests with wide band random and sweep sine tests. Shock and Vibr. Bull. Vol. 34, 1965.

BROCH, J.T. — Some aspects of Sweep Random Vibration. Jour. Sound Vib. Vol. 3, 1966.

CAMPBELL, G.R. — The Measurement of Autocorrelation Functions using a Small Digital Computer. Honours Project Report, Dept. of Mech. Engineering, University of Edinburgh, 1968.

CHANDRASEKHAR, S. — Stochastic Problems in Physics and Astronomy. Reviews of Modern Physics Vol. 15 No. 1, Jan. 1943. (Also in Wax, 1954)

CRAMÉR, H. — On the Theory of Stationary Random Processes. Ann. of Maths. Vol. 41, 1940.

CRAMÉR, H. and LEADBETTER, M.R. — Stationary and Related Stochastic Processes. John Wiley & Sons, 1967.

CRANDALL, S.H. (ed.) — Random Vibration, Vol. 1 Technology Press, Cambridge, Mass., 1958.

CRANDALL, S.H. — Random Vibration. Applied Mechanics Review, Vol. 12 pp. 739-742, 1959.

CRANDALL, S.H. — The Measurement of Stationary Random Processes. Chapter 2 in Random Vibration, Vol. 2. M.I.T. Press, 1963.

CRANDALL, S.H. (Ed.) — Random Vibration, Vol. II. M.I.T. Press, 1963.

DOOB, J.L. — The Brownian Movement and Stochastic Equations. Annals of Mathematics, Vol. 43, No. 2, 1942.

DWIGHT, H.B. — Tables of Integrals and Other Mathematical Data. The Macmillan Co., 1961.

DYER, I. — Response of Plates to a Decaying and Convecting Random Pressure Field. Jour. Acoust. Soc. Amer., Vol. 31, 1959.

DYER, I. — Response of Space Vehicle Structures to Rocket Engine Noise. Chapter 7 in Random Vibration, Vol. 2. (S.H. Crandall, ed.), M.I.T. Press, 1963.

EICHLER, E. — Thermal Circuit Approach to Vibrations in Coupled Systems and the Noise Reduction of a Rectangular Box. Jour. Acoust. Soc. Amer., Vol. 37, 1965.

ERINGEN, A.C. — Response of Beams and Plates to Random Loads. Jour. Appl. Mech., Vol. 24, 1957.

FUNG, Y.C. — Statistical Aspects of Dynamic Loads. Jour. Aero. Sci., Vol. 20, 1953.

HAMMERSLEY, J.M. and HANDSCOMB, D.C. — Monte Carlo Methods. Methuen and Co. Ltd., 1964.

KENDALL, M.G. and STUART, A. — The Advanced Theory of Statistics, Vol. I. Griffin and Co., London, 1958.

KHINTCHINE, A. — Korrelations Theorie der Stationaren Stochastischen Progesse. Math. Ann., Vol. 109, pp. 604-615, 1934.

KOLMOGOROV, A.N. — Grundbegriffe der Wahrscheinlichkeits-rechnung. Erg. Mat. Vol. 2, No. 3, 1933.

LIEPMANN, H.W. — On the Application of Statistical Concepts to the Buffeting Problem. Jour. Aero. Sci, Vol. 19, 1952.

LIN, C.C. — On the Motion of a Pendulum in Turbulent Flow. Quart. Appl. Math. Vol. 1, pp. 43-48, 1943.

LIN, Y.K. — Probabilistic Theory of Structural Dynamics. McGraw-Hill, 1967.

LYON, R.H. — Response of Strings to Random Noise Fields. Jour. Acoust. Soc. Amer. Vol. 28, 1956.

LYON, R.H. and MAIDANIK, G. — Statistical Methods in Vibration Analysis. A.I.A.A. Jour. Vol. 2, 1964.

LYON, R.H. — Boundary Layer Noise Response Simulation with a Sound Field. Chapter 10 in "Acoustical Fatigue in Aerospace Structures" (W.J. Trapp and D.M. Forney, Jr., eds.) Syracuse Univ. Press, Binghampton, N.Y., 1965.

LYON, R.H. — Random Noise and Vibrations in Space Vehicles. The Shock and Vibration Information Genter, U.S. Department of Defence, 1967.

METZGAR, K.J. — The Basis for the Design of Simulation Equipment. Chapter 10 in "Random Vibration" Vol. 1 (S.H. Crandall, ed.) Technology Press, Cambridge, Mass., 1958.

MILES, J.W. — On Structural Fatigue under Random Loading. Jour. Aero. Sci., Vol. 21, 1954.

MORROW, C.T. — Applications to the development of Structure and Equipment for Space Missions. Chapter 10 in Random Vibrations, Vol. 2, (S.H. Crandall, ed.) M.I.T. Press, 1963.

MORROW, C.T. and MUCHMORE, R.B. — Shortcomings of Present Methods of Measuring and Simulating Vibration Environments. Jour. Appl. Mech., Vol. 22, Sept. 1955.

NOISEUX, D.U. — Simulation of Reverberant Acoustic Testing by a Vibration Shaker. Shock, Vibration and Associated Environments Bulletin No. 33, Pt. 3, March, 1964.

ORNSTEIN, L.S. — Verslag Acad. Amsterdam. Vol. 26, p. 1005, 1917.

ORNSTEIN, L.S. — Physik, Vol. 41, p. 848, 1927.

PAPOULIS, A. — Probability, Random Variables and Stochastic Processes. McGraw-Hill, 1965.

PENDERED, J.W. — Theoretical Investigation into the Effects of Close Natural Frequencies in Resonance Testing. Journ. Mech. Eng. Sci., Vol. 7, 1965.

PIERSOL, A.G. — The Development of Vibration Test Specifications for Flight Vehicle Components. Jour. Sound Vib. Vol. 4, 1966.

POWELL, A. — On the Fatigue Failure of Structures due to Vibrations excited by Random Pressure Fields. Jour. Acoust. Soc. Am. Vol. 28, 1956.

PRIEST, D.E. — Technical Characteristics of Simulation Equipment. Chapter 11 in "Random Vibration" Vol. 1, (S.H. Crandall, ed.) Technology Press, Cambridge, 1958.

RICE, S.O. — Mathematical Analysis of Random Noise. Bell System Technical Journal, Vol. 23, 1944 and Vol. 24, 1945. (Also Wax, 1954).

ROBSON, J.D. — An Introduction to Random Vibration. Edinburgh University Press, 1963.

ROBSON, J.D. — The Random Vibration Response of a System Having Many Degrees of Freedom. The Aero. Quart. Vol. 17, 1966.

ROBSON, J.D. and ROBERTS, J.W. — A Theoretical Basis for the Practical Simulation of Random Motions. Jour. Mech. Eng. Sci., Vol. 7, 1965.

TAYLOR, G.I. — Diffusion by Continuous Movements. Proc. London Math. Soc. (2) Vol. 20, 1920.

THOMSON, W.T. and BARTON, M.V. — The Response of Mechanical Systems to Random Excitation. Jour. Appl. Mech., Vol. 24, 1957.

UHLENBECK, G.E. and ORNSTEIN, L.S. — On the Theory of Brownian Motion. Physical Review, Vol. 36, Sept. 1930. (also in Wax, 1954.)

VIGNESS, I. — Field Measurements, Specifications and Testing. Chapter 8 in Random Vibration, Vol. 2. (S.H. Crandall, ed.) M.I.T. Press, 1963.

WANG, MING CHEN and UHLENBECK, G.E. — On the Theory of the Brownian Motion II. Reviews of Modern Physics, Vol. 17, April-July, 1945. (also in Wax, 1954)

WAX, N. (Ed.) — Selected Papers on Noise and Stocahstic Processes. Dover Publications, 1954.

WEINER, N. — Generalized Harmonic Analysis, Acta Math, Vol. 55, pp. 117-258, 1930.

A P P E N D I X I

SIMULATION TESTS USING THE HARMONIC ANALOGUE.

This Appendix contains the details of the locations of vibrators and accelerometers for the tests reported in chapter 4.

Test A:

System Natural Frequency: f_H = 133.7Hz.

System Damping: Q_H = 45

Vibrator and accelerometer Locations: Fig. I.1 shows the positions of the three vibrators used to represent the service environment and the simulating vibrator. The four accelerometers are also shown, and the mode shape components at the four accelerometer positions are given in Table I.1. These were obtained by exciting a uni-modal response. The maximum radial amplitude of vibration was measured at a designated reference axial plane (at x = 0.4L, measured from the clamp) using a pair of orthogonal accelerometers, and this was scaled to be unity.

Table I.1 Mode Shape Components at Accelerometers.

Accelerometer	1	2	3	4
Mode Component	0.75	0.67	0.20	0.57

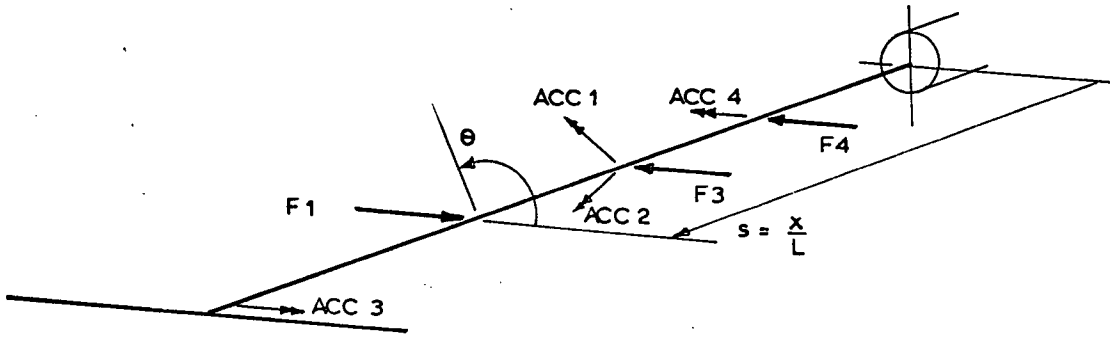

Fig. I.1

Test A: Locations of Vibrators and Accelerometers.

Table I.2 : Details of Locations in Fig. I.1.

	s	θ^o		s	θ^o
Accelerometer (1)	0.4	140	Exciting Vibrator F1	0.70	180
(2)	0.4	230	F4	0.26	0
(3)	1.0	0	Simulating Vibrator F3	0.49	0
(4)	0.25	180			

Test B:

System Natural Frequencies: $f_H = 134.8$ Hz; $f_V = 163.4$ Hz.

System Damping: $Q_H = 45$; $Q_V = 40$.

Table I.3 : Mode Shape Components at Accelerometers.

Accelerometer	1	2	3	4
H-Mode Component	0.72	0.71	0.02	0.62
V-Mode Component	0.64	-0.77	-0.33	-0.02

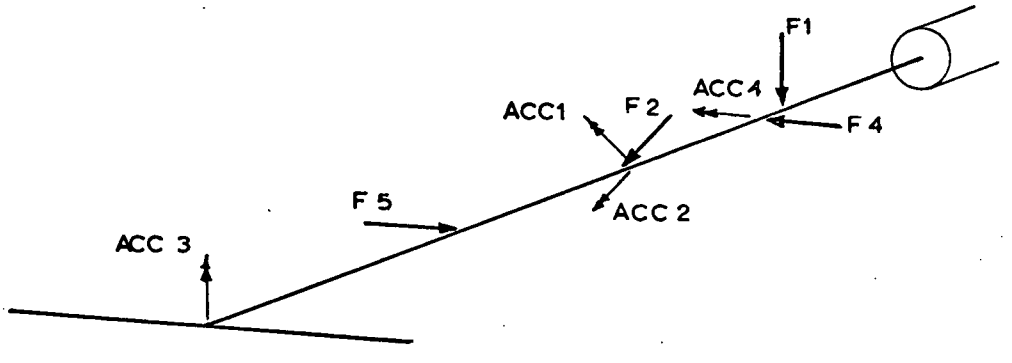

	s	θ		s	θ
Accelerometer(1)	0.4	135	Exciting Vibrator F1	0.21	90
(2)	0.4	225	F4	0.26	0
(3)	1.0	90	F5	0.70	180
(4)	0.25	180	Simulating Vibrator F2	0.44	45

Fig. I.2

Test B: Locations of Vibrators and Accelerometers.

Test C:

In Test C the locations of Vibrators and Accelerometers were the same as for Test B. (Fig. I.2). Accelerometer (1) was used as reference.

System Natural Frequencies: $f_H = 156.9$ Hz; $f_V = 165.0$ Hz.

System Damping: $Q_H = 42$; $Q_V = 45$.

Table I.4 : Mode Shape Components at Accelerometers.

Accelerometer	1	2	3	4
H-Mode Component	0.72	0.70	0.16	0.86
V-Mode Component	0.68	-0.74	-0.29	0.00

Test D:

In Test D, both the system and the exciting vibrators were identical to the Test C case. The mode shape components at the accelerometers are given by Table I.4. In this Test, accelerometers (1) and (2) were used as references and two vibrators (F2 and F3) were used to simulate the response.

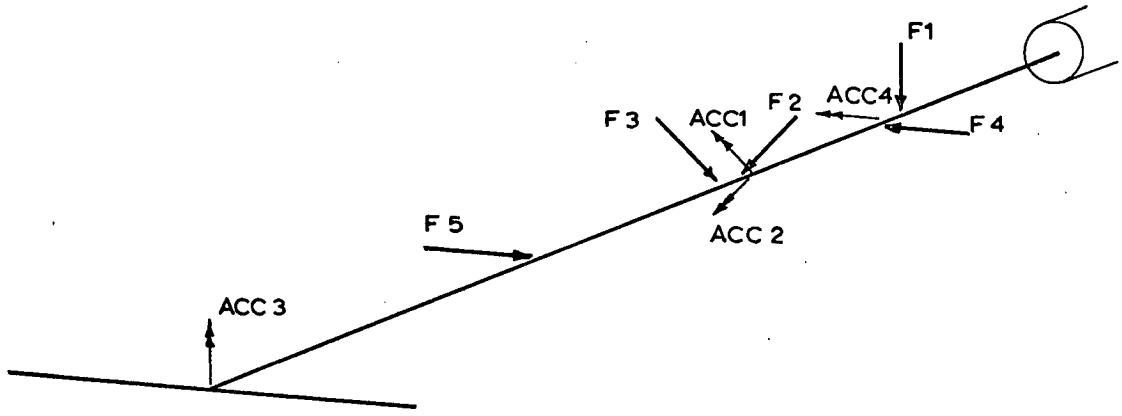

	s	θ		s	θ
Accelerometer(1)	0.4	135	Exciting Vibrator F1	0.21	90
(2)	0.4	225	F4	0.26	0
(3)	1.0	90	F5	0.7	180
(4)	0.25	180	Simulating Vibrator F2	0.44	45
			F3	0.49	135

Fig. I.3

Test D: Locations of Vibrators and Accelerometers.

Test E:

In this Test a plain cross-bar was used to give a frequency ratio f_{V/f_H} of 1.005. The oil damper was attached at an angle of 40^{o} to the vertical at x = 0.6 L to give some degree of damping coupling. The system natural frequencies and mode shapes were obtained before attaching the damper.

System Natural Frequencies : f_H = 176.4 Hz; f_V = 177.2 Hz.

Table I.5 : Mode Shape Components at Accelerometers:

Accelerometer	1	2	3	4
H-Mode Component	0.74	0.67	-0.06	0.64
V-Mode Component	0.77	-0.64	-0.81	-0.02

The locations of vibrators and accelerometers for Test E were identical to those for Test D. (Fig. I.3). For single vibrator simulation, accelerometer (1) and vibrator F2 were used. For two vibrator simulation, accelerometers (1) and (2) were used as references and vibrators F2 and F3 were used to simulate the response.

A P P E N D I X II

INTEGRATION OF MODAL RECEPTANCE PRODUCTS

The quantity $I_{rs} = \int_0^\infty \alpha_r^* \alpha_s \, d\omega$ is a complex valued integral, relevant to the broad-band response of elastic structures to random forces. α_r and α_s are modal receptances, and may be assumed to take the form:

$$\alpha_r(\omega) = \frac{1}{M_r[\omega_r^2 - \omega^2 + i\,2\delta_r\omega_r\omega]} \qquad \text{II.1}$$

when dissipation is represented by a coefficient of viscous damping, δ_r, in the mode.

An alternative representation of α_r is possible, where dissipation is represented by a coefficient of hysteretic or structural damping:

$$\alpha_r(\omega) = \frac{1}{M_r[\omega_r^2 - \omega^2 + i\,\gamma_r\omega_r^2]} \qquad \text{II.2}$$

where γ_r is a coefficient of structural damping. Strictly, by definition of structural damping, the representation II.2 is only valid for steady-state harmonic responses. Indeed, II.2 does not satisfy the condition for a real impulse response, $\alpha_r(-\omega) = \alpha_r^*(\omega)$. The integral I_{rs} with the representation II.2 has been evaluated by Robson (1966) by contour integration. It is more difficult to deal with the representation II.1, because the imaginary part of the integral is an odd function.

The integral has the form:

$$I_{rs} = \int_0^\infty \frac{d\omega}{M_r M_s\left[\omega_r^2 - \omega^2 - i\,2\delta_r\omega_r\omega\right]\left[\omega_s^2 - \omega^2 + i\,2\delta_s\omega_s\omega\right]} \qquad \text{II.3}$$

It is convenient to write I_{+s} as an integral over the infinite range using the unit sten function, $U(\omega)$:

$$I_{+s} = \int_{-\infty}^{\infty} U(\omega)\, \alpha_+^* \alpha_s \, d\omega \qquad \text{II.4}$$

Recalling that α_+, α_s are Fourier transforms of the modal impulse responses, denoted $h_+(t)$, $h_s(t)$, and using $U(\omega) = 1 - U(-\omega)$ and $\alpha(-\omega) = \alpha^*(\omega)$, then by Parseval's formula:

$$I_{+s} = 2\pi \int_{-\infty}^{\infty} h_+(t)\, h_s(t)\, dt \; - \; 2\pi \int_{-\infty}^{\infty} f(t)\, g(t)\, dt \qquad \text{II.5}$$

where $f(t)$ is the inverse Fourier transform of the quantity ($\alpha_+^* \alpha_s$), and $g(t)$ is the inverse Fourier transform of $U(\omega)$.

$h_+(t)$ is given by:

$$h_+(t) = \frac{U(t)}{M_+ \omega_+'} \, e^{-\delta_+ \omega_+ t} \sin \omega_+' t \; ; \quad \text{with} \quad \omega_+' = \omega_+ \left[1 - \delta_+^2\right]^{\frac{1}{2}} \qquad \text{II.6}$$

The first integral in II.5 may be evaluated using standard integrals.

$$2\pi \int_{-\infty}^{\infty} h_+ h_s \, dt = \frac{2\pi}{M_+ M_s \omega_+' \omega_s'} \int_0^{\infty} e^{-[\delta_+ \omega_+ \; \delta_s \omega_s] t} \sin \omega_+' t \, \sin \omega_s' t \; dt \qquad \text{II.7}$$

$$= \frac{4\pi\left[\delta_+ \omega_+ + \delta_s \omega_s\right]}{M_+ M_s \left[(\omega_+^2 - \omega_s^2)^2 + 4\, \omega_+ \omega_s (\delta_+ \omega_+ + \delta_s \omega_s)(\delta_+ \omega_s + \delta_s \omega_+)\right]} \qquad \text{II.8}$$

using Dwight, page 234.

The inverse transform of $U(\omega)$ is easily found:

$$g(t) = \frac{1}{2\pi} \int_{-\infty}^{\infty} U(\omega)\, e^{i\omega t} \, d\omega$$

Starting from the Fourier transform of $U(t)$:

$$\int_{-\infty}^{\infty} U(t)\, e^{-i\omega t} \, dt = \pi\, \delta(\omega) + \frac{1}{i\omega} \qquad \text{II.9}$$

Divide through by 2π and put $v = -\omega$ Hence:

$$g(t) = \frac{\delta(t)}{2} + \frac{i}{2\pi t} \qquad \text{II.10}$$

Next, $f(t) = \frac{1}{2\pi}\int_{-\infty}^{\infty} \alpha_+^* \alpha_s \, e^{i\omega t} d\omega$ is obtained. This has been found by the Convolution theorem and checked by contour integration. The former method is illustrated.

$f(t)$ may be written as a convolution:

$$f(t) = \int_{-\infty}^{\infty} h_+'(\tau)\, h_s(t-\tau)\, d\tau \qquad \text{II.11}$$

where $h_+'(\tau)$ is the inverse transform of $\alpha_+^*(\omega)$

Hence $h_+'(\tau) = h_+(-\tau)$

$$= -\frac{u(-\tau)}{M_+ \omega_+'} e^{\delta_+ \omega_+ \tau} \sin \omega_+' \tau$$

$$= \frac{[u(\tau) - 1]}{M_+ \omega_+'} e^{\delta_+ \omega_+ \tau} \sin \omega_+' \tau \qquad \text{II.12}$$

$h_s(t-\tau)$ is obtained from II.6 and the convolution can be evaluated after integration by parts:

$$f(t) = \frac{e^{\delta_+ \omega_+ t}}{M_+ M_s \omega_+'} \cdot \frac{2\omega_+'(\delta_+\omega_+ + \delta_s\omega_s)\cos\omega_+' t + [\omega_+^2 - \omega_s^2 - 2\omega_+\delta_+(\omega_+\delta_+ + \omega_s\delta_s)]\sin\omega_+' t}{[(\omega_+^2 - \omega_s^2)^2 + 4\omega_+\omega_s(\delta_+\omega_+ + \delta_s\omega_s)(\delta_+\omega_s + \delta_s\omega_+)]} \qquad \text{II.13}$$

for $t < 0$.

$$f(t) = \frac{e^{-\delta_s \omega_s t}}{M_+ M_s \omega_s'} \cdot \frac{2\omega_s'(\delta_+\omega_+ + \delta_s\omega_s)\cos\omega_s' t + [\omega_+^2 - \omega_s^2 + 2\omega_s\delta_s(\omega_+\delta_+ + \omega_s\delta_s)]\sin\omega_s' t}{[(\omega_+^2 - \omega_s^2)^2 + 4\omega_+\omega_s(\delta_+\omega_+ + \delta_s\omega_s)(\delta_+\omega_s + \delta_s\omega_+)]} \qquad \text{II.14}$$

for $t > 0$.

Observe that $f(t)$ is continuous at $t = 0$.

Finally, substituting in II.5

$$I_{+s} = 2\pi\int_{-\infty}^{\infty} h_+ h_s \, dt - 2\pi\int_{-\infty}^{\infty} f(t)\left[\frac{\delta(t)}{2} + \frac{i}{2\pi t}\right] dt$$

Hence:

$$I_{rs} = 2\pi\int_{-\infty}^{\infty} h_r h_s\,dt - \pi f(o) - i\int_{-\infty}^{\infty} \frac{f(t)}{2\pi t}\,dt \qquad \text{II.15}$$

The third term in II.15 may be evaluated after some manipulation, using standard integrals (Dwight, page 235).

$$I_{rs} = \frac{1}{M_r M_s\left[(\omega_r^2-\omega_s^2)^2+4\omega_r\omega_s(\delta_r\omega_r+\delta_s\omega_s)(\delta_r\omega_s+\delta_s\omega_r)\right]}\Bigg\{2\pi\left[\delta_r\omega_r+\delta_s\omega_s\right] -$$

$$-i\Bigg[2(\delta_r\omega_r+\delta_s\omega_s)\log\frac{\omega_r}{\omega_s} + \frac{\omega_r^2-\omega_s^2+2\delta_s\omega_s(\delta_r\omega_r+\delta_s\omega_s)}{\omega_s(1-\delta_s^2)^{\frac{1}{2}}}\tan^{-1}\frac{(1-\delta_s^2)^{\frac{1}{2}}}{\delta_s}$$

$$-\frac{\omega_s^2-\omega_r^2+2\delta_r\omega_r(\delta_r\omega_r+\delta_s\omega_s)}{\omega_r(1-\delta_r^2)^{\frac{1}{2}}}\tan^{-1}\frac{(1-\delta_r^2)^{\frac{1}{2}}}{\delta_r}\Bigg]\Bigg\} \qquad \text{II.16}$$

Observe that $I_{sr} = I_{rs}^*$ Also if $\omega_r = \omega_s$ and $\delta_r = \delta_s$ the imaginary part is zero and I_{rs} reduces to the well known result for a single degree of freedom.

$$I_{rr} = \frac{\pi}{4M_r^2\omega_r^3\delta_r} \qquad \text{II.17}$$

The quantity I_{rs} satisfies all the requirements as an inner product of the two modal receptances:

$$I_{rs} = (\alpha_r, \alpha_s) \equiv \int_0^{\infty} \alpha_r^*\,\alpha_s\,d\omega \qquad \text{II.18}$$

Applying the Cauchy-Schwarz inequality leads to:

$$|I_{rs}|^2 \leqslant I_{rr}.I_{ss} \qquad \text{II.19}$$